

A framework for generative design and drafting for the manufacture and assembly of windows

by

Omar Abdel-Jaber

A thesis submitted in partial fulfillment of the requirements for the degree of

Master of Science

in

Construction Engineering and Management

Department of Civil and Environmental Engineering
University of Alberta

© Omar Abdel-Jaber, 2022

Abstract

The process to fabricate windows for buildings begins with information provided through a web-based tool (also known as a Configure Price Quote), which includes window specifications and geometric information. The fabrication of the windows in the production line consists of the fabrication of the frame, the installation of the glass, the installation of hardware to allow for the operation of the window, the installation of the sealing product, packaging, and shipping to the construction site. This research aims to develop a framework to aid the web-based configuration tool (i.e., Configure Price Quote) to enable the sales representative or client to order and customize windows and improve the flow of information from the Configure Price Quote to the assembly line. As such, the proposed framework aims to automate the design and facilitate the drafting generation for the assembly and fabrication of windows and their sub-components. The proposed framework builds on similar tools developed for the manufacture of other types of products to enable the identification of the material and hardware used to build a window and to assess the business and design rules associated with the type and geometric location of the needed hardware. The research described in this thesis was conducted in collaboration with one of the largest window manufacturers in Canada at their facility in Edmonton, Alberta. The findings of this research are that the proposed framework reduces non-value-added activities in the design phase and improves the flow of information, thereby enabling window manufacturers to provide customized products in an efficient manner. Another notable contribution of this research is its focus on automating the design and facilitating the drafting generation of windows to support assemble-to-order products.

Acknowledgments

First of all, I would like to express my sincere gratitude to all the people who helped and guided me during my academic journey as this research could not have been accomplished without them. Special thanks to my supervisor Dr. Mohamed Al-Hussein for his supervision, feedback, patience, and support. Also, I would like to thank Anas Itani for his consistent support and guidance. Additionally, I would like to express my gratitude to Naan and Abdulrahman Abdeljaber for their academic support.

I also would like to thank my friends, Mu'taz Almomani and Ibrahim Alomari, for their personal support. Eight years of friendship and we are still close despite the distance between us. Moreover, I am deeply grateful to Mohammad Darwish, who supported me academically and as a friend. You are one of the few people that I feel lucky to have met here in Canada. Thank you for being there when I needed you. Also, I would like to express my sincere thanks to Abdallah Ajarmeh. For whenever life got hard, you were there for me; I feel so thankful that I met you. I could not ask for a better friend than you. Thanks for all that you do!

Lastly, I would like to thank my family for their support. Special thanks to my father, Khalid Abdel-Jaber. I am at a loss for words when I attempt to express what you mean to me. I could not have wished for a better friend and mentor. I would not be where I am today if not for you. Your love for me is forever engraved in my heart, forever lingering in my mind, and forever mine to cherish. Thank you for everything, Dad. I also would like to thank my mother, Aida Abu-Hishmeh, for her unmatched support to me and my family. Also, special thanks to my sisters, Layla and Yasmeen.

Table of Contents

Abstract.....	ii
Acknowledgments	iii
List of Tables	vii
List of Figures.....	viii
List of Abbreviations and Symbols	x
Chapter 1: Introduction	1
1.1 Background and motivation.....	1
1.2 Research objectives	3
1.3 Thesis organization	4
Chapter 2: Literature review.....	5
2.1 Overview	5
2.2 Manufacturing in construction	5
2.2.1 History of manufacturing in construction.....	6
2.2.2 Challenges facing manufacturing in construction.....	6
2.3 Mass customization	8
2.3.1 Development of mass customization	9
2.3.2 Customer order decoupling point.....	11
2.3.3 Mass customization in construction.....	14
2.4 Configuration systems.....	15
2.4.1 Structure of CPQ systems	17
2.4.2 CPQ in construction.....	18
Chapter 3: Methodology.....	20
3.1 Current practice for sales and design processes.....	20
3.2 Overview of the framework.....	23
3.3 Types of windows	24
3.4 Production line.....	25
3.4.1 Profile cutting and routing station (A/C)	27
3.4.2 Profile welding station for frame and sash (A/C).....	27
3.4.3 Automatic corner cleaning station (A/C).....	28
3.4.4 Sash hardware installation station (A/C)	29

3.4.5	Frame hardware installation and sash–frame joining station (A/C)	29
3.4.6	Profile cutting station (P/F).....	29
3.4.7	Profile welding station (P/F).....	29
3.4.8	Automatic corner cleaning station (P/F).....	30
3.4.9	Cleaning station (P/F).....	30
3.4.10	Final assembly station.....	30
3.4.11	Glazing station	30
3.4.12	Wrapping station.....	30
3.5	Window sub-components.....	32
3.6	Parametric design.....	33
3.7	Time study.....	36
Chapter 4: Implementation of the Proposed Methodology.....		42
4.1	Configuration logic.....	42
4.1.1	Dimensions and configuration	42
4.1.2	Window framing materials	48
4.1.3	Grilles.....	50
4.1.4	Glazing.....	51
4.1.5	Hardware colour.....	51
4.1.6	Miscellaneous	52
4.2	Window design	52
4.2.1	Locations of multi-lock handle cut-out and screws along frame (casement)	56
4.2.2	Operator selection and location (casement).....	58
4.2.3	Operator location on frame (casement).....	59
4.2.4	Operator track (casement).....	60
4.2.5	Hinge arm and screws on sash (casement)	63
4.3	Case study	67
4.3.1	Design and hardware geometric locations	69
4.3.2	Bill of materials (BOM).....	70
4.3.3	Quote.....	70
Chapter 5: Conclusion.....		72
5.1	Research Contributions	73
5.2	Research limitations.....	74

5.3	Recommendations for future studies.....	75
References		76
Appendix A: Hardware design for casement windows		82
1.	Tie-bar	82
1.1	Tie-bar rollers.....	83
1.2	Tie-bar guides.....	84
1.3	Tie-bar keepers.....	85
2.	Hinge selection	87
2.1.	Hinge track and screw locations	87
2.2.	Hinge track and screw locations	87
3.	Operator screws.....	89
4.	Operator bracket.....	90
5.	Snubber quantity and locations on frame.....	91
6.	Casement ramp on frame	93
7.	Limit device.....	94
Appendix B: Hardware design for Awning windows		97
1.	Awning operator selection	97
1.1	Operator cut-out location on frame	97
1.2	Operator screw location	98
1.3	Operator track	98
2.	Awning operator bracket	100
3.	Awning hinge track selection on frame	101
4.	Awning hinge arm on sash	102
5.	Awning Snubber.....	104
6.	Awning limit device.....	105

List of Tables

Table 3.1: Workstations and activities for A/C sub-line	30
Table 3.2: Workstations and activities for P/F sub-line	31
Table 3.3: Joint production line.....	31
Table 3.4: Labour required for the P/F sub-line.....	37
Table 3.5: Labour required for the A/C sub-line.....	37
Table 3.6: Labour required for the joining section	37
Table 3.7: Time study for A/C sub-line.....	38
Table 3.8: Time study for P/F sub-line.....	38
Table 3.9: Time study for the combined line.....	39
Table 4.1: Symbols for the multi-lock handle equations	58
Table 4.2: Symbols for the location of casement operators' equations.....	60
Table 4.3: Symbols for operator track equations (casement)	62
Table 4.4: Symbols for casement hinge arm equations	67
Table 4.5: Sample of the design output.....	69
Table 4.6: Sample BOM	70

List of Figures

Figure 2.1: Development of MC over time (Baranauskas et al., 2020)	10
Figure 2.2: CODP location in the process flow (Xu, 2007).....	12
Figure 2.3: Various positions for CODP (Olhager, 2010).	13
Figure 3.1: Sales current process.....	22
Figure 3.2: Overview of the framework.....	24
Figure 3.3: Types of windows: (a) fixed, (b) picture, (c) casement, and (d) awning (Note: the schemata above are drawn from Company ABC's 2017 product catalogue)	25
Figure 3.4: Overview of Line XYZ.....	26
Figure 3.5: Cutting station for A/C windows	27
Figure 3.6: Welding machine	28
Figure 3.7: Cleaning machine	29
Figure 3.8: Profiles available at Company ABC	32
Figure 3.9: SDL and Grilles (product information drawn from Company ABC's 2017 product catalogue)	33
Figure 3.10: Hardware for the windows	33
Figure 3.11: Reference points	35
Figure 3.12: General format for the equations	36
Figure 3.13: Overview of the simulation model	40
Figure 3.14: A/C sub-line	40
Figure 3.15: P/F sub-line	41
Figure 3.16: Total duration result with confidence interval.	41
Figure 4.1: Configuration process overview.....	43
Figure 4.2: Web interface.....	43
Figure 4.3: Web interface (merge and unit information table)	45
Figure 4.4: Window naming process.....	46
Figure 4.5: Configuration pattern	47
Figure 4.6: Window naming process (Decision Tree).....	47
Figure 4.7: Framing materials and exterior colours.....	48
Figure 4.8: Colour combinations available (product information drawn from Company ABC's 2017 product catalogue).....	49
Figure 4.9: Brickmould and Jamb extension (framing tab)	49
Figure 4.10: Grille patterns.....	50
Figure 4.11: Glazing tab	51
Figure 4.12: Operator colour	52
Figure 4.13: Miscellaneous tab in the interface.....	52
Figure 4.14: Hardware for casement windows.....	54
Figure 4.15: Hardware for awning windows.....	54
Figure 4.16: CAD details of a frame/sash cross-section	56
Figure 4.17: Multi-lock handle	57
Figure 4.18: Multi-lock handle cut-out details in RH casement window.....	58
Figure 4.19: Different types of operators.....	59

Figure 4.20: Casement operator cut-out details.....	60
Figure 4.21: CAD details for dual-arm operator track.....	62
Figure 4.22: Dual-arm operator track specifications	63
Figure 4.23: Hinge arm locations	63
Figure 4.24: Hinge arm and track.....	64
Figure 4.25: Standard 10" hinge.....	66
Figure 4.26: Standard 13" hinge.....	66
Figure 4.27: 10" egress standard hinge.....	67
Figure 4.28: Left side casement window	68
Figure 4.29: Sample quote output	71
Figure 5.1: Future state of window design by a CPQ tool	73
Figure A.1: Tie-bar rollers and guides CAD details.....	83
Figure A.2: Tie-bar rollers and guides CAD details.....	85
Figure A.3: Snubber details	92
Figure A.4: Snubber locations	93
Figure A.5: Location of the casement ramp	94
Figure A.6: Casement ramp details.....	94
Figure A.7: Limit device.....	96
Figure A.8: Limit track	96
Figure B.1: Awning operators	97
Figure B.2: Location of awning operator and its cut-out.....	98
Figure B.3: Awning operator track CAD details	100

List of Abbreviations and Symbols

Abbreviations

Abbreviation	Full description
A	Awning window
ATO	Assemble-to-order
C	Casement window
COPD	Customer order decoupling point
CPQ	Configure-price-quote
ETO	Engineer-to-order
LH	Left-hand side
MC	Mass customization
MTO	Make-to-order
MTS	Make-to-stock
OSC	Off-site construction
RH	Right-hand side

Symbols

Symbol	Description	Constant used in case study
δ_{xb}	Distance between the screw of the awning bracket and the center of the bracket	21.4
δ_{u2}	Distance between the second screw and center of the operator bracket	54
δ_{u1}	Distance between the first screw and center of the operator bracket	1.5
δ_{t3s13}	Distance between the first and third screw on the standard 13" hinge track	203.2
δ_{t3s10}	Distance between the first and third screw on the standard 10" hinge track	212.7
δ_{t3e}	Distance between the first and third screw on the egress hinge track	212.72
δ_{t3}	Distance between the first and fourth screw on the 13" hinge track	288.9
δ_{t2}	Distance between first and second screws on hinge track	101.6
δ_{t1}	Distance between first screw on hinge track and start of the hinge track	31.8
δ_{s2}	Distance between first snubber screw and snubber center	12.7

Symbol	Description	Constant used in case study
δ_{s1}	Distance between first snubber screw and snubber center	12.7
δ_{otscy}	Vertical distance between awning track's screws and bottom of frame	71
δ_{otsc2}	Distance between the center of the operator track and the nearest screw	61
δ_{otsc1}	Distance between edge screw and the nearest track's edge	15.875
δ_{ot}	Vertical distance between each screw center to the cut-out center of the lock handle	41.2
δ_{osc6}	Distance between the third and first screw	108
δ_{osc5}	Distance between the third and first screw	92.1
δ_{osc4}	Distance between the third and first screw	76.3
δ_{osc3}	Distance between the third and first screw	31.8
δ_{osc2}	Distance between the second and first screw	15.9
δ_{osc1}	Distance between the first screw (left side) to the edge of the cut-out of the awning operator	9
δ_{lt}	Distance between the two screws of the limit track	98
δ_{lb}	Distance between the two screws of the limit bracket	42
δ_{kl3}	Distance between the center of the tie-bar keeper and the third screw	11
δ_{kl2}	Distance between the center of the tie-bar keeper and the second screw	3
δ_{kl1}	Distance between the center of the tie-bar keeper and the first screw	9
δ_{cot3}	Distance between the first screw of the casement operator track and the hinge side of the sash (dual-arm operator)	144.6
δ_{cot2}	Distance between the first screw of the casement operator track and the hinge side of the sash (standard single arm operator)	107
δ_{cot1}	Distance between the first screw of the casement operator track and the hinge side of the sash (egress operators)	57
δ_{cosc3}	Distance between the first screw of the casement operator to the nearest outside edge of the window (dual-arm operator)	216
δ_{cosc2}	Distance between the first screw of the casement operator to the nearest outside edge of the window (standard single operator)	151
δ_{cosc1}	Distance between the first screw of the casement operator to the nearest outside edge of the window (Reverse and Egress operator)	101

Symbol	Description	Constant used in case study
δ_{cos5}	Distance between the sixth and first screw of the casement operator	108
δ_{cos4}	Distance between the fifth and first screw of the casement operator	92.1
δ_{cos3}	Distance between the fourth and first screw of the casement operator	76.3
δ_{cos2}	Distance between the third and first screw of the casement operator	31.8
δ_{cos1}	Distance between the second and first screw of the casement operator	15.9
δ_{cbsc}	Half the distance between each screw in a dyad bracket in a casement window	14.7
δ_{ca3}	Distance between the third and the first screw of the casement operators track	329.4
δ_{ca2}	Distance between the second and the first screw of the casement operators track	164.7
δ_{aha5}	Distance between the fifth screw to the first screw	102
δ_{aha44}	Distance between the fourth screw to the first screw (26" awning hinge)	71.5
δ_{aha43}	Distance between the fourth screw to the first screw (22" awning hinge)	228.6
δ_{aha42}	Distance between the fourth screw to the first screw (18" awning hinge)	177.8
δ_{aha41}	Distance between the fourth screw to the first screw (10", 14" awning hinge)	127
δ_{aha33}	Distance between the third screw to the first screw (26" awning hinge)	71.4
δ_{aha32}	Distance between the third screw to the first screw (18", 22" awning hinge)	127
δ_{aha31}	Distance between the third screw to the first screw (10", 14" awning hinge)	76.2
δ_{aha2}	Distance between the second screw to the first screw	34.9
δ_{aha1}	Distance between the first screw to the start of the awning hinge arm	31.8
δ_{ht3}	Distance between the last screw of the hinge track and the previous screw	111.1
δ_{ht2}	Distance between the screws of the awning hinge track (excluding the last screw)	101.6
δ_{ht1}	Distance between the first screw of the awning hinge track to the edge of the track	38.1
d_{tbc}	Width of tie-bar	13
d_s	Offset from the outer edge of the frame to the middle of the snubber	15

Symbol	Description	Constant used in case study
d_{rg2}	Distance between roller and guide	51
d_{rg1}	Distance between roller and guide	71
d_{oscy}	Distance between the third and first screw	33.7
d_{ld}	Distance from the limit bracket to the bottom inside frame	140
d_k	Distance between each roller center and the center of the tie-bar keeper	2.4
d_{go}	Distance between tie-bar center and center of tie-bar guide	3.9
d_{cr}	Distance from casement ramp center (screw location) to side frame inner edge	101.6
d_{cocy}	Vertical distance between the casement operator and the bottom of the frame	37.8
d_{coco1}	Distance between the center of the casement operator cut-out location and the outer edge of the window frame (Egress and reverse dyad)	158
d_{cob}	Distance between the center screw of the casement operator and the outside edge of the sash	14.2
d_{cdb}	Distance between the inner side of the frame to the center of the dyad bracket in casement windows	134
d_{aot}	Distance between the center of the operator track and the center of the awning operator	10.3
d_{aoby}	Vertical distance between the awning bracket and the bottom of the frame	68
d_{aob}	Distance between the center of the awning operator bracket and the center of the operator	9.8
d_{aco}	Distance between the cut-out center in awning and the bottom of the frame	41
d_{aha}	Distance between the start of the awning hinge arm and the bottom of the top frame	11
d_k	Distance between each roller center and the center of the tie-bar keeper	2.4
L_{lt}	Limit track length	114.3
L_{lb}	Limit bracket length	58
L_{coa}	Length of the awning operator cut-out	126
L_{aot}	Length of the awning operator track	406.4
M_c	Width of the mullion cover for box-to-box installation	3.175
P_w	Width of the frame's profile	60
r_{ts}	Distance between the first roller to the bottom of the tie-bar	20
r_{tf}	Distance between the last roller and the top of the tie-bar	80

Symbol	Description	Constant used in case study
T_s	Distance between the bottom of the tie-bar and the bottom of the profile	114

Chapter 1: Introduction

1.1 Background and motivation

Manufacturing has been integrated into the construction industry in recent decades to address productivity issues (McKinsey Global Institute, 2017). This trend has been most clear with respect to building products that are produced off site, such as windows. Gibb (2001) viewed them as part of the manufacturing in the construction industry. A window comprises a wide array of sub-components, such as profiles and hardware, and in this regard it can be considered an assemble-to-order (ATO) product. The process of manufacturing windows begins with the order, which formalizes the client's preferences and customization requests. Before the order proceeds to production, though, the typical practice is for each order of windows to be designed and drafted from scratch. This design method is strenuous, time-consuming, and repetitive, and includes many non-value-added activities. Moreover, it inhibits the flow of information and hinders the customization process. In these respects, the current practice for designing windows for assembly and manufacturing is highly inefficient, especially considering that construction projects are unique and require customized products, whereas most large manufacturers' organizational structures and work processes are based on mass production concepts (Choi & Jarboe, 1996). Moreover, the literature illustrates the need to improve product design and customization processes in off-site construction. For example, Monizza & Matt (2022) stated that greater flexibility in product customization and a novel approach to design are needed in order for off-site construction to realize its full potential.

There is a consensus within the literature regarding the need to adopt mass customization (MC) to improve the design and customization processes in off-site construction. MC, it should be noted, is a system that enables clients to customize their orders while allowing manufacturers to deliver

those products in high volumes at reasonable prices. However, there is still room for improvement in this area. For example, Wehlin (2021) stated that current practices for customized production are inefficient and that generating a bill of materials (BOM) for each customized product requires strenuous work.

In this context, this research proposes a framework based on MC to enhance the design phase of windows to aid the configure–price–quote (CPQ) tool in enabling the client to customize the windows. This is achieved by integrating the configuration process of standard sub-components into the design stage, as described by Larsen et al. (2019), enabling the production of customized products by different configurations of the sub-components by a design enabler (Bao et al., 2022). This framework automates the design of the windows and facilitates drafting for manufacturing. In specific, the framework identifies the windows' sub-components and captures their specifications and parameters. Accordingly, rule-based functions can be developed to govern the window design and geometric location of hardware by configuring the window's sub-components based upon the client inputs to the CPQ tool.

The rationale for incorporating the CPQ tool into the framework is that it is crucial for the sales process, as suggested by Poot et al. (2020), as the CPQ can improve communication between salesperson and client, as well as between the sales and planning departments (Poot et al., 2020).

The research gaps addressed can be summarized as follows:

- The current practice for customized production, including the design of customized windows, is inefficient (Wehlin et al., 2021).
- The design stage in window manufacturing is time consuming and suffers from non-value-added activities. Therefore, process waste increases with an increase in window customization.

- There is a lack of research on MC in the construction industry (Noergaard et al., 2020).
- The application of product configurators within the construction industry is relatively limited (Cao et al., 2021)
- There is a need to incorporate a visual representation of the product in configurators to improve the design stage to help in drafting the product to aid the shop floor and enhance the overall experience for the client (Poot et al., 2020)

1.2 Research objectives

In this research, a framework is developed for a web-based configuration tool (i.e., CPQ) to enable the client to order customized windows with an accurate quote for their order. Another contribution of the framework is that it enhances the sales process by reducing non-value-added activities and improves the flow of information between the company's departments. Furthermore, the framework automates the window design process to reduce waste and non-value-added activities in the design stage. Finally, the framework incorporates a geometric representation of the window sub-components, which is a cornerstone of automated drafting.

In specific, the research described herein is based on the following objectives:

- identify the sub-components of windows and develop rule-based functions to govern the configuration of windows;
- develop design-based rules to automate the design for manufacturing and assembly of windows;
- calculate the location of hardware to facilitate the automated drafting of the windows;
- develop an interface and process flow for the client; and
- develop a logic by which to calculate an accurate quote and BOM.

1.3 Thesis organization

This thesis consists of five chapters. Following the Introduction (Chapter 1), Chapter 2 (Literature Review) provides a detailed review of manufacturing in the construction industry. Moreover, it illustrates the gap in manufacturing that needs to be addressed regarding MC. Finally, it discusses the studies that have addressed MC by applying configuration tools. Chapter 3 (Methodology) sheds light on the types of windows produced by the case company and its current practice based on an analysis of the case company's production line. Moreover, a framework is proposed in this chapter for developing the configuration tool. Chapter 4 (Implementation of the Proposed Methodology) describes the process of developing the CPQ tool on a web-based interface, and also presents the results of the case study. Chapter 5 (Conclusion) summarizes the research findings and contributions, in addition to recommendations for future work.

Chapter 2: Literature review

2.1 Overview

This chapter reviews the existing literature in relation to the objectives of the research. The first part of the chapter, “manufacturing in construction”, discusses some of the drawbacks of the current manufacturing process, and illustrates how off-site construction in particular could be improved by addressing some of these deficiencies. The second part of this chapter, “mass customization” (MC), discusses the challenges that arise from enabling clients to customize their orders, and the solutions that have been proposed in the literature to solve these problems. Finally, the third part, “configuration systems”, sheds light on the latest advancements in configurators and their capability to address the abovementioned challenges.

2.2 Manufacturing in construction

The construction industry has performed poorly in recent decades relative to other industry sectors. For example, a recent study by McKinsey Global Institute (2017) showed that the labour productivity of the construction industry increased by only 1 percent in the past two decades, whereas there was a 3.6 percent increase in labour productivity in the manufacturing industry. Jang et al. (2021) concluded that this low productivity of construction results from many factors, such as the labour-intensive nature of the industry. Moreover, they argued that the environment is a crucial factor in productivity levels, i.e., construction activities are typically carried out on site in an uncontrolled environment where weather conditions, for example, can hinder the workflow or even pose a safety hazard. Meanwhile, a study conducted on the issues faced by Singaporean contractors suggested that high turnover rate is one of the most significant factors in the low productivity of construction (Lim & Alum, 1995).

2.2.1 History of manufacturing in construction

According to a review article by Jang et al. (2021), multiple terms have emerged to describe manufacturing in construction, including “prefabricated construction”, “modular construction”, and “off-site construction (OSC)”, the latter term being the most widely used. According to Jang et al., OSC is a construction approach in which components are fabricated in factories outside the construction site, then transported to the site for installation.

OSC is not a new approach to undertaking the delivery of construction projects (Gibb, 1999). Alazzaz & Whyte (2014) noted that OSC dates back to at least the 18th century. An early example of OSC is a portable colonial cottage constructed by John Manning, as OSC gained popularity during the colonial period. Additionally, Gibb (1999) points out that OSC was widely used in constructing hospitals during the Crimean War. Gibb (1999) has noted that the industrial revolution paved the way for OSC to emerge. The market conditions became particularly conducive to the growth of OSC after the Second World War with the rapid population growth seen during that period (Alazzaz & Whyte, 2014). Hosseini et al. (2018) concluded through an analysis of the ongoing increase in research, that there is increasing interest in OSC today, reporting that the level of interest in Western European countries has increased by around 40%. As further evidence of the growth of this paradigm, the OSC industry tripled in size in the UK between 2004 and 2006 (Hosseini et al., 2018). KPMG (2016) also stated that more than half of the housing projects planned by the largest companies in the UK incorporate off-site methods.

2.2.2 Challenges facing manufacturing in construction

As shown in the previous sections, integrating manufacturing into the construction industry has improved various aspects of the construction industry. Nonetheless, it is worth mentioning that, despite the advances that have occurred in the construction industry by this integration, it still faces

some challenges (Blismas et al., 2005). Especially, the construction industry's nature is drastically different from the manufacturing industry, as Blismas et al. (2005) explained. The International Council for Research and Innovation in Building and Construction (CIB) created a task group (TG74) to promote research on the constraints and challenges faced in OSC, studying the impacts of process, technology, and people on design, manufacturing, and construction (Arif et al., 2012). Accordingly, they identified nine major categories of challenges in OSC, and concluded that design-related challenges are among the most crucial to be addressed. They further noted that manufacturing a million products of the same car, for instance, is drastically different from manufacturing buildings or building components, arguing that this is due to the unique, non-uniform nature of construction projects.

Various other studies have drawn the same conclusion. For example, Elnaas et al. (2014) studied the key factors that decision-makers value most when choosing OSC as a construction method. Their results coincide with the previous findings that design-related issues (including the high cost of design) are a significant problem facing the OSC industry. Other studies have shown that choosing OSC as a delivery method after the project has already been designed can lead to negative impacts on plan and budget (Smith, 2014). In this regard, Gao et al. (2020) emphasized the importance of the concept of Design for Manufacturing and Assembly (DfMA), where designers focus on how to make the design conducive to manufacturing and assembly in order to reduce costs.

The second issue is that most large manufacturers' organizational structure and work processes are based on mass production concepts (Choi & Jarboe, 1996). In this manner, the OSC industry standardizes its products to reduce costs and time and achieve mass production (Popovic et al., 2018). On the other hand, Hu et al. (2019) noted that a "client-focused approach and

customization” are among the primary values of stakeholders, and that as such it is crucial for the manufacturer to be able to provide customized products that focus on the needs of clients. It is also for this reason that construction projects tend to follow a traditional on-site approach rather than utilizing OSC (Popovic et al., 2018).

To address these issues, MC can be utilized, along with a configuration tool—i.e., a configure–price–quote (CPQ) tool—to improve the design process and allow the OSC industry to produce affordable, customized products.

2.3 Mass customization

MC is a term was first coined by Davis (1987), in which he described the trend whereby manufacturers micro-divide markets to provide clients with customized products and services. Pine (1993) was one of the first authors to investigate the operational perspective of MC.. Tseng & Jiao (1996) gave a detailed definition that MC aims to enable clients to customize products without an increase in cost and lead time compared to mass-produced products. The concept was later further developed by MacCarthy et al. (2003), Rudberg & Wikner (2004), and Kaplan & Haenlein (2006), as described by (Fogliatto et al., 2012). Guo et al. (2019) explained that the development of MC arose from a desire on the part of manufacturers to gain a competitive edge. They noted that clients are increasingly demanding customized of products based on their requirements and preferences, thus increasing the competition among manufacturers to meet this demand for customization (2019). As Guo et al. argued, in today’s market, manufacturers must be responsive to emerging preferences and flexible to meet clients' changing requirements. McCarthy (2004) has identified a number of factors contributing to the current reality with respect to competition and client demands in the manufacturing sector. First, clients’ expectations and preferences have shifted towards niche products. Second, the life cycle of products has been

shortened significantly; (we can consider, for instance, the fashion industry). Third, a growing practice among manufacturers today is to develop product families for assembling to order in order to improve the performance of customized manufacturing by producing customized products in a similar time frame and cost compared to mass-produced products. Fourth, manufacturers seek to better understand clients' expectations and alter their own operations in order to meet those expectations. Finally, manufacturers endeavor to forecast market demand and identify potential areas of investment through effective communication with the client.

The topic of MC has received increasing attention in the literature in recent decades and has also been successfully implemented in practice. A notable example cited by Piller (2007) is American Power Conversion (APC). As Piller has noted, APC adopted MC to build complex infrastructure and components for a data center as customized modules configured by the client's requirements during the sales process, achieving a reduction in production costs and delivery time and an increased capacity to integrate new products and technology. As another example, Dell allows its clients to configure the laptop they want to buy (Suzić et al., 2018). Suzić et al. (2018) also showed that other major companies, such as IBM, Cisco, BMW, and Nike, have successfully utilized MC.

2.3.1 Development of mass customization

As shown in the previous section, MC is a relatively new paradigm that offers manufacturers a competitive edge in the market while better fulfilling clients' demands. Baranauskas et al. (2020) conducted a thorough analysis of the origins and evolution of MC, as shown in Figure 2.1

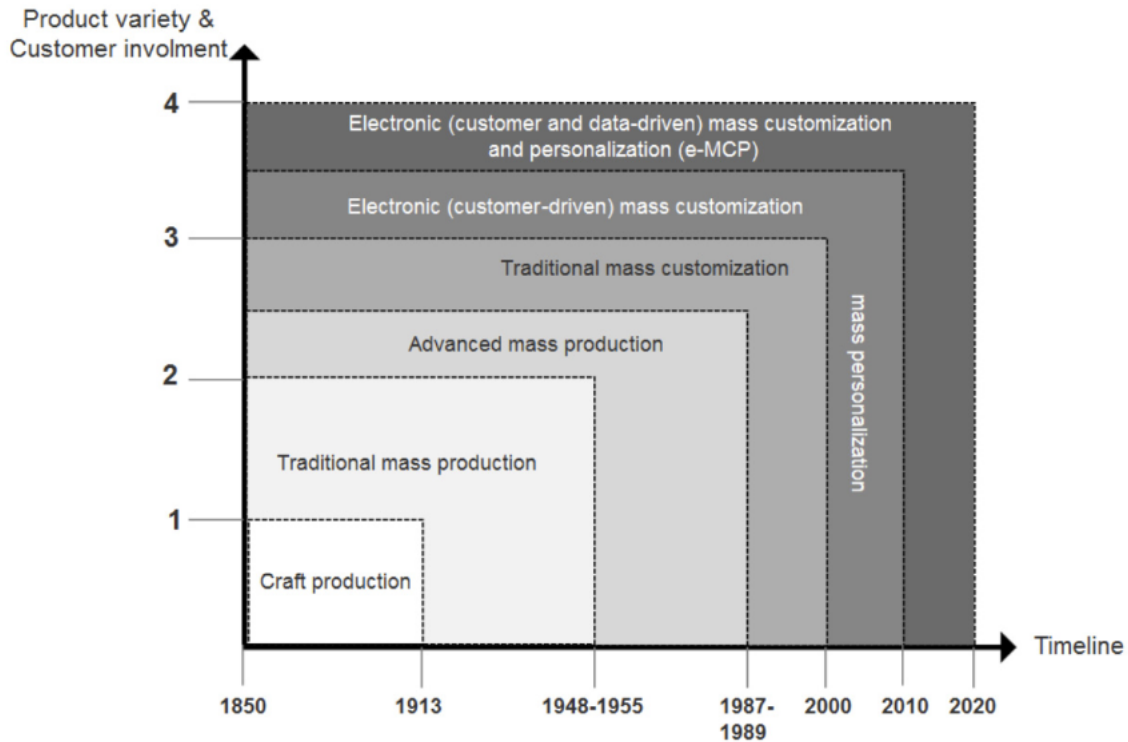


Figure 2.1: Development of MC over time (Baranauskas et al., 2020)

As shown in the figure above, the first stage in manufacturing was craft production, where the volume is low and primitive methods are employed. The second stage was driven by the emergence of the push concept and the mass production of a given product. New technologies and concepts such as lean manufacturing and mass personalization, then emerged to improve the manufacturing process, making it more flexible.

Roberts (2003) defined mass personalization as “The process of preparing an individualized communication for a specific person based on stated or implied preferences”, while he defined MC as “The process of producing a product, service, or communication to the exact specifications/desires of the purchaser or recipient.” On the other hand, Hu (2013) defined personalization of products as producing a product specifically to meet clients' demands based upon their design preferences. Electronic mass customization (e-MC), meanwhile, has been

defined by Yan et al. (2020) as delivering customized products at reasonable prices while allowing clients to engage in the design process through an online platform.

As shown in the figure above, the most recent trends in the development of MC have been electronic mass customization and personalization. Zhang et al. (2019) argued that, with the emergence of paradigms such as Internet of things (IoT) and cloud computing, the efficiency of information transfer has increased while miscommunication between departments has decreased. They also described a manufacturing company's infrastructure as having four modules: a data module, a design module, a manufacturing module, and a service module, asserting that the data module is the driver for the rest of the modules, as it is responsible for collecting and analyzing clients' and market data to facilitate the decision-making process in the MC environment.

2.3.2 Customer order decoupling point

As Rudberg & Wikner (2004) noted, in traditional mass production, everything throughout the product lifecycle is done in a make-to-stock (MTS) manner, including the design, gathering of raw materials, and assembly, in order to keep prices reasonable and competitive. This means, products are manufactured to be stocked, waiting for the customer order before being shipped. On the other hand, they note that consumers demand high flexibility to customize their orders (in addition to competitive pricing). However, manufacturing products in a make-to-order (MTO) fashion is expensive, so, as the authors go on to describe, clients usually have to compromise on either price or flexibility. They assert, though, that MC can achieve both flexibility and cost-competitiveness without a significant trade-off. In this regard, Guo et al. (2021) argued that, in order to gain flexibility in production while achieving mass production, MTS and MTO should be utilized together to reach the point at which MTS activities shift to value-added MTO activities. This point is called the client-order decoupling point (CODP) (Guo et al., 2021). James & Mondal (2021)

described CODP as “the point in the manufacturing process flow which differentiates the standardized production flow from the customized production flows”. As they went on to argue, this, in return, will efficiently satisfy clients' requirements in terms of customization without substantial compromise. Xu (2007) illustrated the concept of CODP using the process map that appears as Figure 2.2 below.

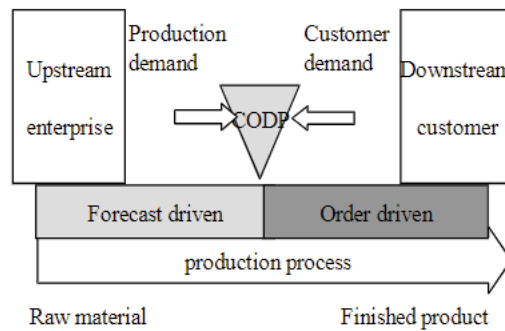


Figure 2.2: CODP location in the process flow (Xu, 2007).

For example, grocery products such as candy bars are made to stock, meaning that consumers cannot customize them because the CODP is downstream in the process. On the other hand, a product such as a home is made to order, meaning that the CODP is upstream, i.e., the design is not realized until after the client places the order. The location of the CODP, i.e., whether it is closer to downstream or upstream, determines the level of customization the client can expect, as explained by Xu (2007). Rudberg & Wikner (2004), similarly, explained that the further downstream the CODP is, the less customizability there will be and the more focus there will be on productivity in the process flow. On the other hand, if the CODP is further upstream, there will be more focus on customizability and less on productivity. In this context, as noted by Rudberg & Wikner (2004), the CODP can be thought of as the equilibrium point at which a reasonable degree of customizability can be realized without a significant compromise on productivity. The notion

underlying MC, then, is that this equilibrium point can be shifted upstream to increase flexibility while increasing productivity simultaneously, as explained by Rudberg & Wikner (2004).

Where precisely the CODP is in the production process determines the workflow for the product. It should be noted in this regard, though, that MTO and MTS are not the only two production strategies. Other notable ones include Assemble-To-Order (ATO) (also known as configure-to-order) and Engineer-To-Order (Olhager, 2010). The strategy employed depends on the location of the CODP, as illustrated by Olhager (2010) (see Figure 2.3). Mello et al. (2015) stated that ETO is usually adopted when the aim is to produce complex, low-volume products. Examples of products for which ETO is adopted include ships and heavy equipment (Elfving et al., 2002) and buildings (Gosling and Naim, 2009). In MTO, on the other hand, the engineering and/or design is already done before the client orders the product, and, in MTS, the product is produced and put in the inventory before the client demands it (Atan et al., 2017). In ATO, finally, the product is designed and its components manufactured in advance, but assembly of the end-product begins only after the client has placed the order (Atan et al., 2017).

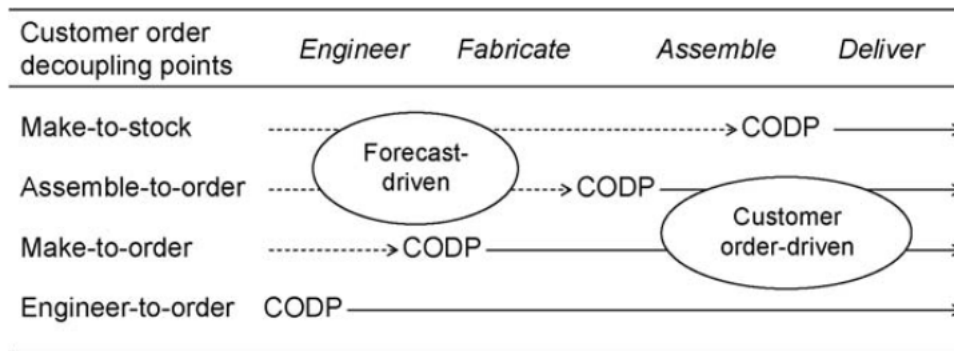


Figure 2.3: Various positions for CODP (Olhager, 2010).

2.3.3 Mass customization in construction

As previously mentioned, construction projects are distinct from other items that are traditionally manufactured in terms of the uniqueness of each product. They are typically designed and built based upon the client's order. If we think of a construction project as a product, it can be considered an ETO product based on Wortmann's (1983) categorization. Monizza & Matt (2022) noted that every ETO product must be engineered from scratch to fulfill the client's requirements, going on to explain that, due to this product uniqueness/variability and lack of standardization, construction tends to perform poorly relative to other industry sectors in terms of productivity, even with the introduction of manufacturing concepts and the rise of OSC (Larsen et al., (2019).

A review of the literature shows that the benefits of MC in construction have not yet been realized, with Noergaard et al. (2020) noting that further exploration is needed in this area in order for the potential benefits of MC to the construction industry to be realized. Most of the existing literature touches on one of two aspects (1) investigations of how the construction industry might adapt to MC, and (2) case studies of projects and construction enterprises that have utilized MC. Nevertheless, there is a consensus within the literature that adopting modularization and using a design enabler platform such as CPQ are effective strategies to enable MC in construction (Viana et al., 2017; Suzić et al., 2018). More specifically, Viana et al. (2017) concluded from their literature review that modularization could help to simplify the design stage and offer customization at a reasonable cost and time. Modularization, it should be noted, is the decomposition of a product into modules or sub-assemblies (Viana et al., 2017). Meanwhile, Viana et al. (2017) defined a platform as “a common set of components, modules, or parts in order to provide derivative products”.

Jensen et al. (2015) concluded that shifting construction from the traditional ETO paradigm toward CTO by adopting modularization and product families can enable MC in construction. To this end, they recommended that the components that make up a given product should be assigned a commonality index based upon which the designer could choose common components that can be utilized in various product variations. This is the thinking underlying the “product family” concept whereby various customizations are assembled with nearly the same components, but with different assembly processes.

Monizza & Matt (2022), like others mentioned above, argued that shifting to ATO or CTO manufacturing can simplify the construction manufacturing process, and they also asserted that the integration of technology in automating the design process can increase efficiency. In this regard, configurator tools/software (i.e., CPQ), along with product families, can bridge the gap to enable effective MC in construction. As noted by Wehlin et al. (2021), a configurator tool typically comprises two modules, one for the sales process and the second for the process of customizing the product. Nevertheless, the client’s interaction with the designer and/or manufacturer cannot be separated from the product development due to the nature of customization and client requirements. The sales process and the role of the configurator tool in facilitating client interactions will be discussed in the following section.

2.4 Configuration systems

Sorri et al. (2017) noted that the concept of product configurations emerged from the need to produce customized products, and that the ability to customize a product by modifying its sub-components to meet the client’s requirements is an efficient method for customization (2017). For successful customization, though, the manufacturer has to define the levels of customization available for the client to choose from, and the client’s choices need to be translated into

Parameters for the manufacturing process, hence the emergence of the concept of configurators (Trentin et al., 2014). As described by Trentin et al. (2014), the function of configurators is to facilitate the sales process and improve the client's interaction with salespeople. As further noted by Mourlas & Germanakos (2009), configurators allow manufacturers to come up with a suitable configuration of sub-components, thereby enhancing the sales process and boosting client satisfaction.

Configurators first appeared in the 1980s (Trentin et al., 2014). As described by Batchelor et al. (2012), they have evolved in three respects since that time. The first wave was a rule-based software utilizing If-Then conditional statements. This was followed in the 1990s by the development of constraint-based configurators encompassing If-Then statements, capacity, and compatibility constraints. As explained by Batchelor et al. (2012), the logic underlying this paradigm was that "you can have A and B and C, but you cannot have A with D or B with E, and you must have at least three of A, B, C, D, and E". The third wave, finally, was characterized by compilation-based configurators that use a compilation of steps in which all valid configurations are constructed to enhance maintenance and usability. In spite of this more recent evolution, as noted by Batchelor et al. (2012), the second wave is more dominant today.

Jordan et al. (2020) noted that the term CPQ, though it did not appear in the literature until relatively recently (the quotation process was introduced into the configuration system in 2006, and the term CPQ emerged around 2013), marks a demarcation point in the literature on this topic. They also noted that, since its introduction, most of the literature on this concept has tended to focus on the technical side of how to implement CPQ. Näsi (2020), meanwhile, noted that CPQ is primarily used in business-to-business settings.

2.4.1 Structure of CPQ systems

According to Bonev et al. (2015), an effective CPQ tool must be capable of configuring together predefined sub-components to form customized products according to rule-based functions. Xia & Wang (2008), similarly, emphasized the importance of the “product family” as a means of achieving more straightforward configurations and customizations. A product family (mentioned briefly in Section 2.3.3 above), it should be noted, is a “family” of variations on the same basic product, sharing all or most of the same sub-components, where the product variations to be realized depend on the configuration of those sub-components. These sub-components are typically pre-designed so that the manufacturing implications of any given configuration (i.e., product variant) can be evaluated prior to production (Sorokovaia, 2019). For this purpose, the constraints and parameters associated with the given sub-components must be identified (Sorokovaia, 2019). In this regard, rule-based functions can be developed to govern the logic of the configuration of sub-components, as Sorokovaia (2019) explained. Moreover, there should be no innovative or creative steps in the sales process; instead the product details should be determined in advance so that the design is automated through the CPQ (Sorokovaia, 2019).

Näsi (2020) also recommended that a CPQ tool be incorporated into the enterprise’s various systems, such as Client Resource Management (CRM), Enterprise Resource Planning (ERP), and Product Life-Cycle Management (PLM). CRM, it should be noted, enables the enterprise to manage and store information (e.g., sales data, client records) in order to ensure a smooth flow of information and to improve the efficiency of the sales process (Näsi, 2020). Näsi (2020) also explained that CRM makes it easier to access the company’s documents and acquire information to facilitate the sales process, noting that the CPQ configurator can detect available resources such as materials (and their prices) from the CRM and ERP before a quote is issued to the client. In

specific, the CPQ provides an interface to input the client's requirements. The CPQ then configures a product from the resources available in the company's database and generates a bill of materials (BOM) accordingly (Sorokovaia, 2019). Based on the BOM, the CPQ tool can calculate the cost automatically to provide the client with an accurate quote, thus mitigating the errors likely to be encountered if this process were to be performed manually.

2.4.2 CPQ in construction

Further study is needed with respect to the use of CPQ tools in construction. For example, Cao et al. (2021) stated that existing configurators "lack integration of knowledge from the downstream supply chain such as manufacturing". Farr et al. (2014) investigated the benefits of building information modelling (BIM) as a customization tool in the AEC industry, concluding it is not a common topic within the AEC industry and that there are benefits yet to be realized. That being said, the literature does include several case studies. For example, Kristianto et al. (2015) conducted a case study on a ship's engine to develop a configurator prototype. Moreover, Wehlin et al. (2021) developed a BIM-based configurator tool for a spiral staircase. The Wehlin et al. (2021) study is one of the few publications in this domain to have discussed the configurator as a sales tool for the client to use in the context of construction. However, all of these case studies have involved ETO products (as opposed to ATO construction products).

In summary, as noted above, the products used in construction projects are highly customized depending on the client requirements. The literature confirms that MC can be adopted by construction enterprises to aid in providing clients with customized, cost-effective products in an efficient manner. In the present research, to enable MC in construction, a configurator tool is developed to automate the design process. In specific, given the gap in the literature specifically with respect to ATO products in construction, a framework and a tool prototype are developed by

which to automate the configuration process and provide clients with customized ATO products that fulfill their requirements and preferences, all within a user-friendly interface. Since construction projects are unique, they require customized products. In this context, the developed framework aids the process of providing clients with customized products in an efficient manner by reducing non-value-adding activities in the design process and streamlining the sales process. Moreover, this framework enables the client to alter the design before the production begins without incurring the costs associated with redesign and/or with having to discard a finished product.

Chapter 3: Methodology

This research examines a window manufacturing production line. As per the categorization of Gibb (2001), window production is considered to be a form of manufacturing serving the construction industry. Windows are usually made of sub-components that are ready to be assembled and thus can be considered an assemble-to-order (ATO) product. Company ABC, which operates the production line under study, has a product family for line “XYZ”. This product family has several profiles and hardware components that are assembled together based on client orders. Thus, the client can customize the window within the constraints imposed by the particular materials and sub-components the company uses. However, as noted in the previous chapter, the window design process is not automated in the manner usually seen in configure–price–quote (CPQ) tools for other products. Therefore, for the purpose of this research it is necessary to first identify the types of windows available in the production line (product family). The sub-components of the window (profiles and hardware) that need to be assembled to produce the customized windows are then identified. Afterward, a parametric design is implemented linking the sub-components with a single reference point. Finally, the activities carried out at each station in the production line are broken down in order to calculate the labour hours, and a logic is developed to create a user interface through which the client can configure the window. As a benefit to the window manufacturer, the framework also generates in an automated manner the bill of materials (BOM) and geometric hardware locations, along with a logic by which to calculate the cost of the window in order to provide the client with an accurate quote.

3.1 Current practice for sales and design processes

The current practices underlying the sales process are examined by conducting interviews with personnel in the sales and planning departments at Company ABC, and the current practice is

characterized accordingly as shown in Figure 3.1. The process is initiated when a client meets with a salesperson. The client provides the salesperson with the drawings to identify the locations where windows and doors are to be installed. The salesperson then engages in discussion with the client to identify the client's preferences and requirements, and shows the client the company's product catalogue, outlining the various options available. Based on the client's input, the salesperson then sketches a preliminary window configuration. If the client is agreeable to this configuration, the salesperson then calculates a rough estimate of the cost and gives the client a preliminary quote (usually a price range rather than a specific price). If the client is not agreeable to the preliminary configuration, the salesperson modifies it based on the client's input. Once the client has agreed to the window configuration and corresponding quote provided by the salesperson, a quote number is issued in order to initiate the detailed design of the windows, the generating of a detailed BOM, and the forecasting of a delivery date. Based on the detailed design and BOM, an exact quote is then provided to the client to approve and sign.

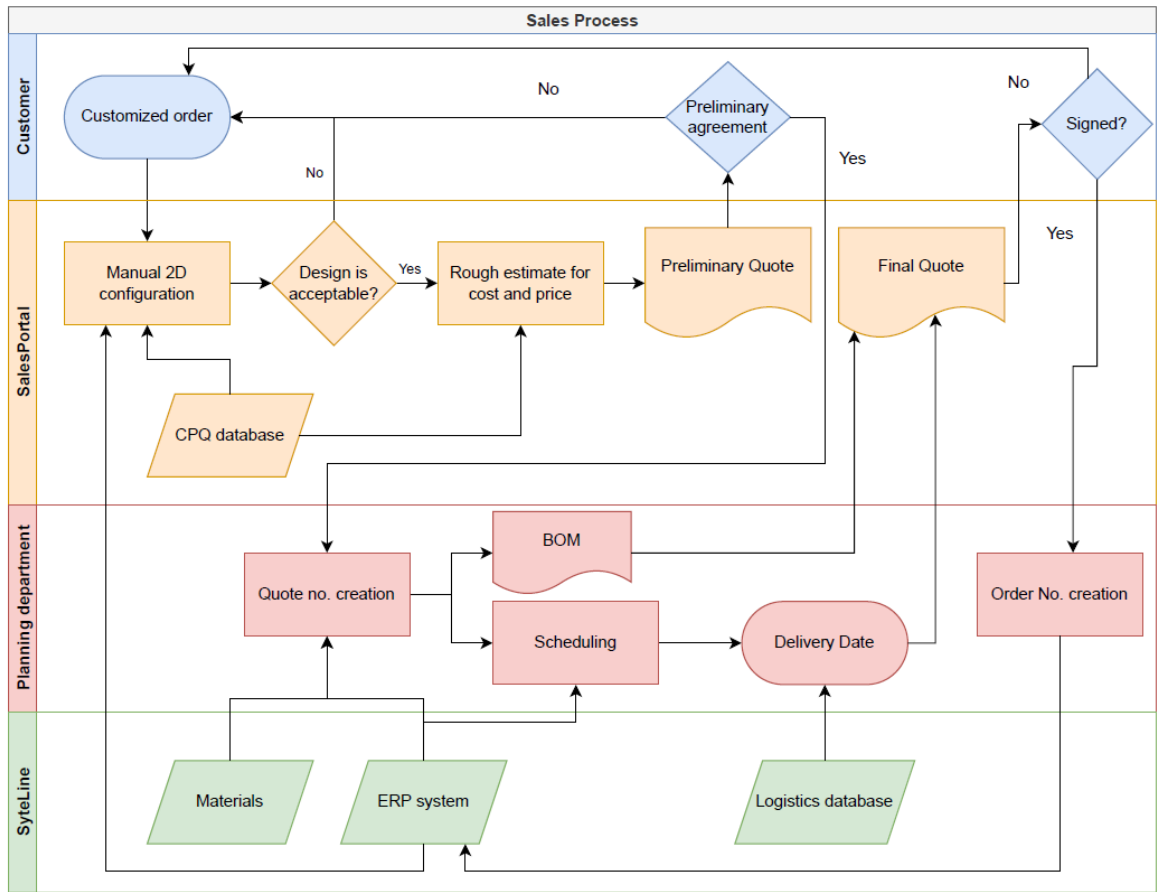


Figure 3.1: Sales current process.

The current state of the sales and design processes as described above are inherently inefficient. For instance, the client must interact with the salesperson on two separate occasions, once before the exact quote is generated and second time after the exact quote has been generated, with the second meeting typically occurring 1 to 3 business days after the first meeting. Furthermore, the client can modify or refuse the order after the detailed quote, resulting in wasted effort. Regarding design, because the material and hardware used are the same for most windows and come in standard dimensions from the suppliers, conducting detailed design for each order can be considered a non-value-added activity. Finally, as shown in Figure 3.1, the internal information exchange is inefficient in that the sales and planning departments exchange information in two

directions. The sales department first transfers preliminary information to the planning department based on the initial consultation with the client. The planning department then responds by generating a detailed design and quote and sending them to the sales department to in turn present to the client.

This process can be improved through the introduction of a framework and rule-based functions to automate and govern the design and streamline communication between departments. Moreover, because visualization is facilitated by manual 2D drawings in the current process, a novel approach by which to automate the geometric representation of window sub-components based on parametric design can streamline the generating of assembly instructions for the shop floor and lay the groundwork for automated 3D drafting.

3.2 Overview of the framework

Figure 3.2 provides an overview of the framework developed to address the deficiencies in the current practice as described above. The inputs to the framework are the window types and client preferences, time study, and the available materials associated costs. The criteria to which the framework is subject, meanwhile, are the constraints that govern product customization, including the material specifications, available suppliers, relationship between the materials and hardware and the limits imposed by the production process itself. The main process begins with the window configuration being determined with the aid of a web interface. Using the user-friendly web interface, the salesperson consults with the client to select window types, materials, and colours. Then, in the parametric design, the sub-components that make up the window are identified, along with their parameters, where these parameters govern the design customization process according to rule-based functions developed to calculate the number of sub-components and compute their geometric locations. Based on the window configuration and parametric design, a BOM and

hardware locations are generated, and the material costs and labour hours are calculated. The outputs of the framework are the window design, BOM, and geometric representations of hardware (which are forwarded to the planning department), and the quote (which is presented to the client).

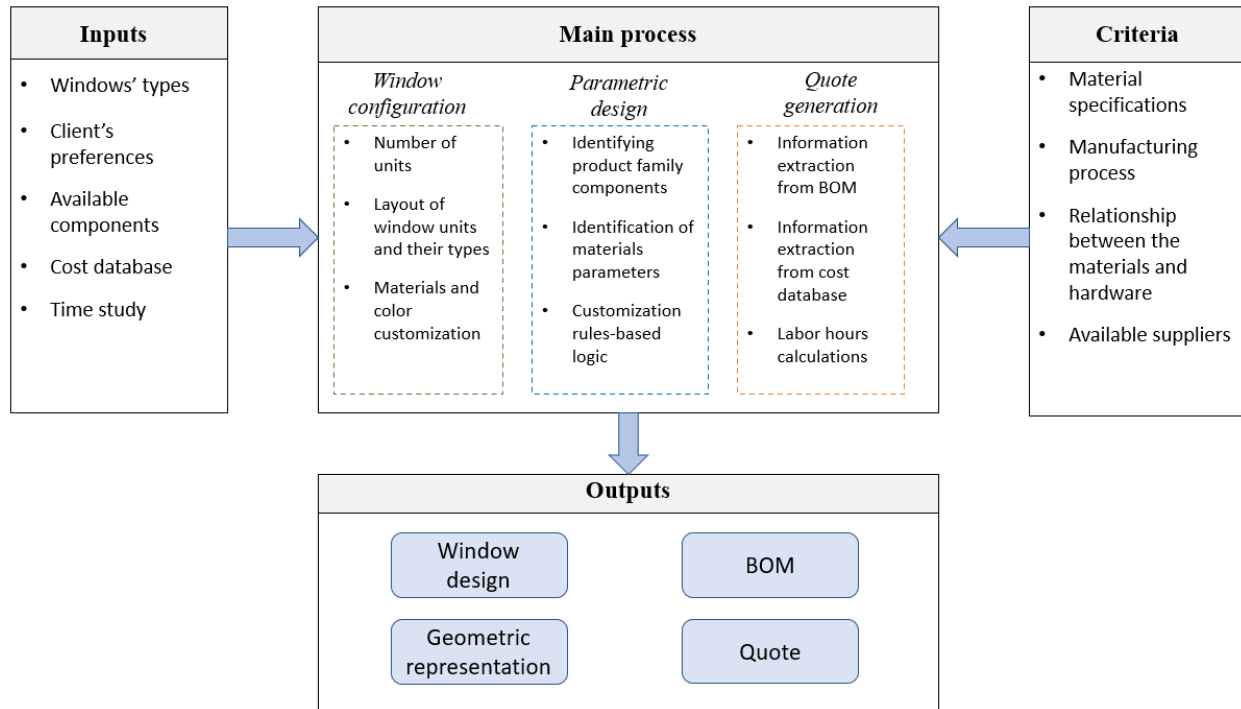


Figure 3.2: Overview of the framework

3.3 Types of windows

Company ABC operates production lines for several types of windows. The production line under study in the present research, in which products are customized, is referred to herein as Line XYZ. In Line XYZ, there are four different types of windows, as shown in Figure 3.3. These four windows differ from one another in terms of their basic design, and each type can be further customized. Because these four window designs share many of the same hardware elements and other components and are produced on the same production line, they are considered a product family.

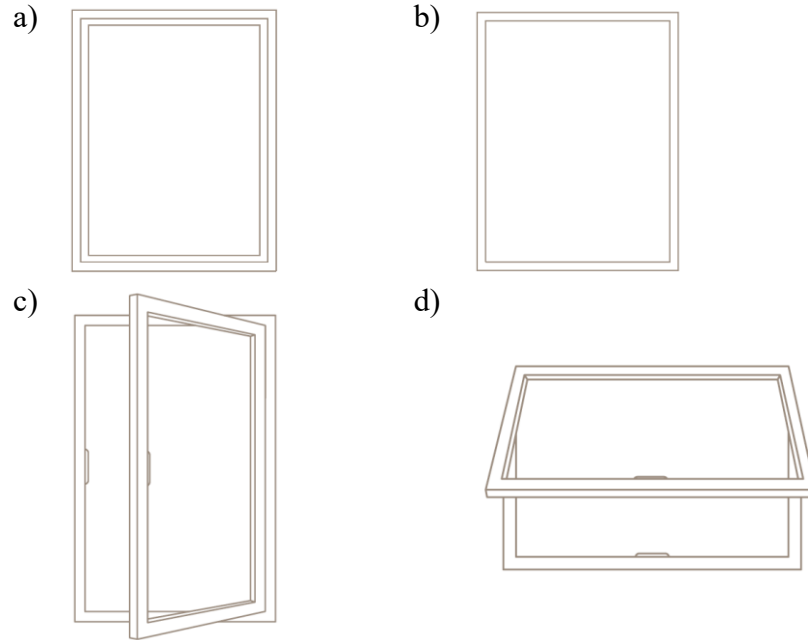


Figure 3.3: Types of windows: (a) fixed, (b) picture, (c) casement, and (d) awning (Note: the schemata above are drawn from Company ABC's 2017 product catalogue)

The first type is the fixed window (Figure 3.3a). Fixed windows are fixed in place (hence the name) and are not operable. The second type is the picture window (Figure 3.3b). The picture window is a type of fixed window with a large frame size. The third type of window manufactured on this line is the casement window (Figure 3.3c). Casement windows are operable and open outwards from a vertical hinge on either the left or right side of the window. The fourth type is the awning window (Figure 3.3d), which is an operable window that opens from the bottom outward, usually with a rotating operator. This type of window is effective at keeping out rain due to its orientation.

3.4 Production line

Line XYZ consists of two sub-production lines—the awning/casement (A/C) line and the picture/fixed (P/F) line—that converge into one line for final assembly and packaging, as shown in Figure 3.4. The awning/casement (A/C) sub-line consists of five workstations, while the

picture/fix (P/F) sub-line consists of four workstations. The combined portion of the line (after the two sub-lines converge) consists of three workstations.

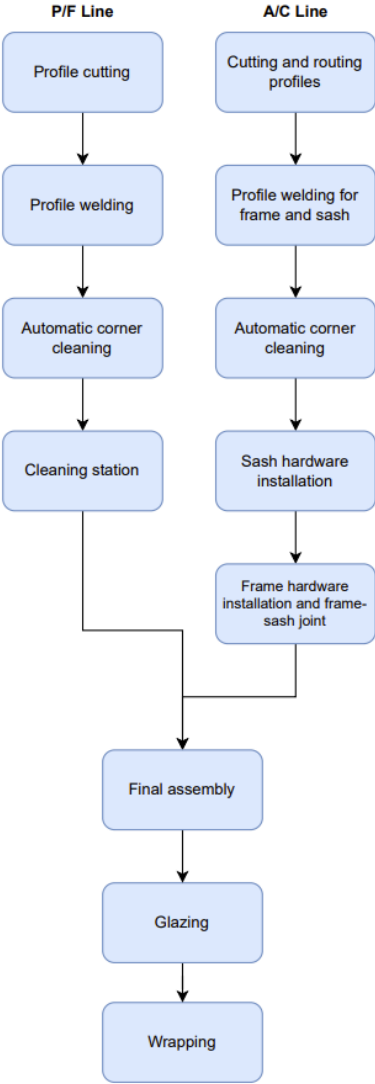


Figure 3.4: Overview of Line XYZ

The various workstations on Line XYZ are described in detail in the following subsections, while the various activities carried out at these workstations are summarized in Table 0.1, Table 0.2 and Table 0.3.

3.4.1 Profile cutting and routing station (A/C)

The cutting machine cuts in an automated manner the profiles for both frames and sashes at this station, as shown in Figure 3.5. The worker places the profile in the machine for cutting, and then, once it has been cut by the machine, delivers it to an adjacent table for routing and hardware assembly.



Figure 3.5: Cutting station for A/C windows

3.4.2 Profile welding station for frame and sash (A/C)

At this station, the worker places the profiles into a four-point welding machine that welds the four corners of the frame and sash, as shown in Figure 3.6.



Figure 3.6: Welding machine

3.4.3 Automatic corner cleaning station (A/C)

At this station, the welded frame or sash is inserted into the cleaning machine for automatic corner cleaning, as shown in Figure 3.7. Because it is a two-point cleaning machine, it cleans two corners at a time, and then the worker must rotate the frame or window in order for the other two corners to be cleaned.



Figure 3.7: Cleaning machine

3.4.4 Sash hardware installation station (A/C)

At this station, the corners of the A/C windows are manually cleaned to prepare the sash for hardware installation, and then the hardware is installed on the sash.

3.4.5 Frame hardware installation and sash–frame joining station (A/C)

At this station, hardware is installed on the window frame, and the sash is also installed on the frame. Further details regarding hardware installation are provided in Table 0.1.

3.4.6 Profile cutting station (P/F)

At this station, the cutting machine cuts the profiles for frames. The activity is done automatically in the same manner as in the A/C sub-line.

3.4.7 Profile welding station (P/F)

At this station, the worker places the profiles into a four-point welding machine that welds the four corners of the frame (as in the A/C sub-line).

3.4.8 Automatic corner cleaning station (P/F)

At this station, the welded frame is inserted into the two-point corner-cleaning machine for automatic corner cleaning (as in the A/C sub-line).

3.4.9 Cleaning station (P/F)

At this station, any residual material is manually cleaned from the welds, and the nailing fin is cut (depending on the design of the window).

3.4.10 Final assembly station

At this station, the jamb extension and brickmould are installed (on both P/F and A/C windows). Moreover, window units are joined together to form one large window (box-to-box), depending on the window design. Packaging is also installed at this station.

3.4.11 Glazing station

At this station, glass is installed into the frame. The window is then checked for quality.

3.4.12 Wrapping station

Finally, the finished window is wrapped and moved into the storage area, depending on the shipping address.

Table 0.1, Table 0.2, Table 0.3 summarize the various activities occurring at these workstations.

Table 0.1: Workstations and activities for A/C sub-line

No.	Workstation	Activities
1	Profile cutting and routing station	Cutting of profiles for frame and sash
2		Routing of cut-out for multi-lock handle
3		Routing of cut-out for operator mechanism
4		Punching of weep hole
5		Installing a weather strip

6	Profile welding station for frame and sash	Welding of frame and sash profiles
7	Automatic corner cleaning station	Automatic corner cleaning
8	Sash hardware installation station	Manual corner cleaning
9		Installation of tie-bar keeper
10		Installation of hinge arm
11		Installation of operator bracket
12		Installation of operator track
13		Installation of limit device
14	Frame hardware installation and sash-frame joining station	Cutting of nailing fin
15		Manual corner cleaning
16		Installation of hinge track
17		Installation of casement ramp
18		Installation of snubber
19		Installation of multi-lock handle and tie-bar connector
20		Installation of tie-bar and tie-bar guide
21		Installation of operator
22		Installation of limit device bracket
23		Sash-frame assembly

Table 0.2: Workstations and activities for P/F sub-line

No.	Workstation	Activities
1	Profile cutting station	Cutting of profiles
2		Punching of profiles
3	Profile welding station	Welding of profiles
4	Automatic corner cleaning station	Automatic corner cleaning
5	Cleaning station	Cutting of nailing fin
6		Manual corner cleaning

Table 0.3: Joint production line

No.	Workstation	Activities
1	Final assembly station	Installation of mullion cover
2		Box-to-box assembly
3		Installation of brickmould
4		Installation of jamb extension
5		Installation of cardboard and shipping block
6	Glazing station	Glazing unit assembly

7		Screen installation
8		Quality check
9	Wrapping station	Wrapping

3.5 Window sub-components

In order to automate the design, the sub-components that make up the windows are identified based on an analysis of the four types of windows described above. The various sub-components can be broadly categorized as either profiles (Figure 3.8) or hardware (Figure 3.10). A typical window is made of two sets of profiles: one for the frame and one for the sash. Hardware is installed on each of these assemblies of profiles, where the types, quantities, and locations of hardware depend on the type of window and its dimensions.

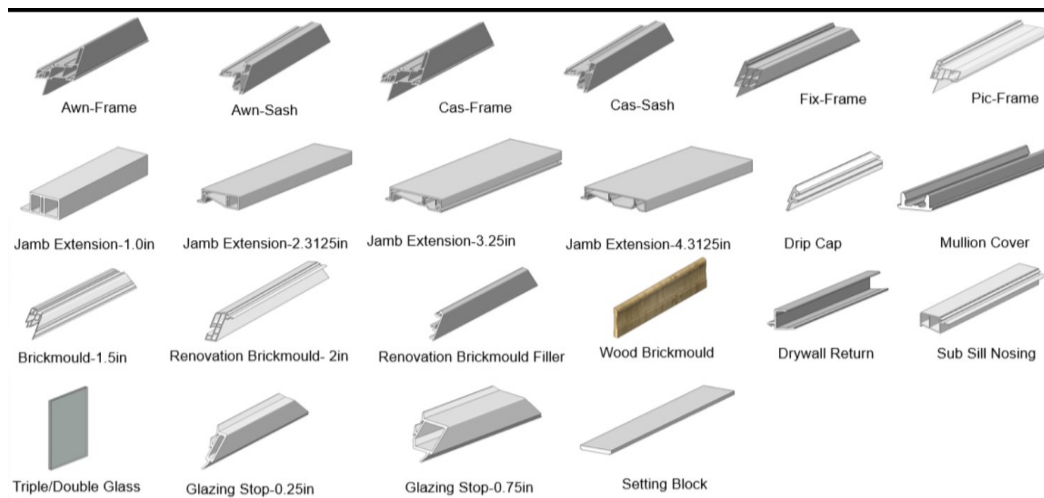


Figure 3.8: Profiles available at Company ABC



Figure 3.9: SDL and Grilles (product information drawn from Company ABC’s 2017 product catalogue)

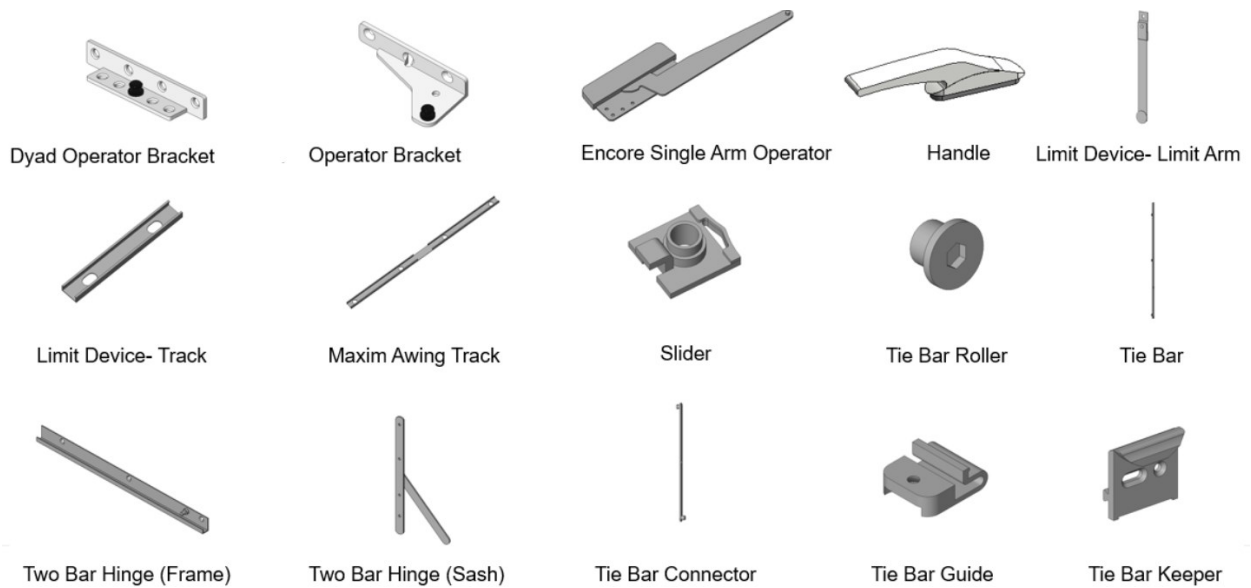


Figure 3.10: Hardware for the windows

3.6 Parametric design

According to Anderl and Mendgen (1995), parametric design is a common approach to product modelling in which engineering knowledge is incorporated with geometry and topology, and that is implemented by identifying the parameters that describe the material and product information. Monedero (2000) asserted that parametric design is one of the best approaches for describing the design of product families, where each product consists of various materials and components and

is linked to other components such that they can be parameterized and grouped to facilitate automated design. Monedero added that this is conducted by identifying the constraints and developing rule-based equations linking the components together. Moreover, Monedero (2000) noted that constraints are always present in parametric design in computer-aided design (CAD) systems. With rule-based functions, automation in product design can be realized. Hence, by changing the parameters of some of the components, other components' parameters will be updated.. According to Anderl and Mendgen (1995), meanwhile, these constraints can be broadly divided into two categories: engineering constraints (e.g., dimensions, material strength, capacity) and geometric constraints.

Nahm & Ishikawa (2006), meanwhile, defined parametric design as “the process of transforming a set of functional specifications and requirements into a complete description of a physical product or system (in design space) that meets those specifications and requirements (in performance space).”

Given its benefits as outlined above, parametric design is adopted in the present research to automate the window design process and is incorporated into the proposed framework. In reference to the discussion of Anderl and Mendgen (1995) above both engineering constraints (dimensions and capacity) and geometric constraints are taken into consideration in this research. First, when the dimensions of the window are changed, the dimensions of the hardware and their locations change accordingly to fit the customized window. Second, depending on the dimensions and the type of window selected, some hardware (e.g., the operator mechanism) will be changed due to strength and capacity considerations. Moreover, some hardware will be connected together in order to prevent clashes.

Moreover, the rule-based functions incorporated in the developed framework use a Cartesian system to provide a geometric visualization of the hardware. Thus, the type and quantity of material and hardware component are outputted, along with the location of each hardware component. The hardware locations are all linked to the bottom-left corner of the window (X, Y, Z) when facing the window from inside. After the calculation of each location, the locations are then transposed to the new reference point (X', Y', Z') , which is located at the bottom-left of the rough opening, as shown in Figure 3.11. As such, the final design outputs are all linked to the bottom-left corner of the rough opening.

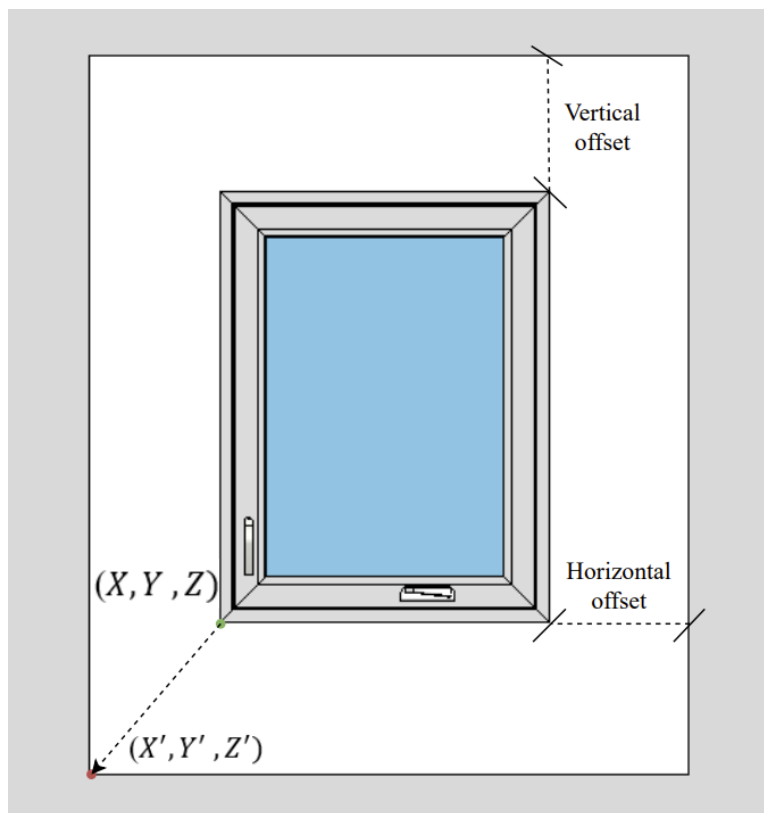


Figure 3.11: Reference points

Accordingly, in the developed framework three points in space are allocated for each hardware element. In turn, there are three equations corresponding to each hardware element describing the

X-, Y-, and Z-coordinates. In this respect, by using the Cartesian system, the benefits of parametric design can be leveraged to facilitate automatic drafting of windows in a CAD system.

Figure 3.12 illustrates format these equations follow. In these equations, α is the quantity of the given hardware element, where $A = \{1, \dots, \alpha\}$, and β is the quantity of screws, where $B = \{1, \dots, \beta\}$

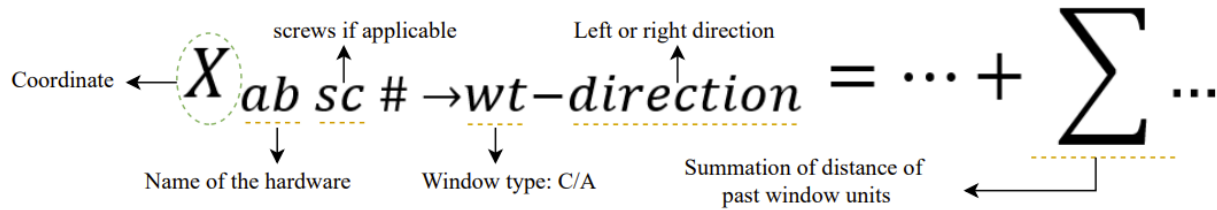


Figure 3.12: General format for the equations

It should be noted that the developed equations are generically applicable to other production lines and different product families of windows, and in fact this framework can be applied to other types of ATO products.

3.7 Time study

To support quote generation, a time study of the production line is undertaken to serve as the basis for labour-hour estimation, i.e., to determine the time it takes for each hardware element to be installed. Based on the labour hours, along with direct material costs, contingency, and markup, the CPQ tool can calculate an accurate cost of each customized window, thus providing an exact quote for the customer. The time study is conducted in two phases: collecting the activity times through observation on the shop floor, and using simulation to calculate the overall labour hours. For the first phase, it should be noted, each of the activities in the production line must first be identified, and how many in order to be able to workers are required for each activity. Table 0.4,

Table 0.5, and Table 0.6 show the labour requirements for each activity as determined based on observation of the shop floor.

Table 0.4: Labour required for the P/F sub-line

Station	Labour needed to complete the activities
Profile cutting station	1
Profile welding station	1
Automatic corner cleaning station	1
Manual cleaning station	1

Table 0.5: Labour required for the A/C sub-line

Station	Labour needed to complete the activities
Profile cutting station	1
Profile welding station for frame and sash	1
Automatic corner cleaning station	1
Sash hardware installation station	1
Frame hardware installation and sash–frame joining station	1

Table 0.6: Labour required for the joining section

Station	Labour needed to complete the activities
Final assembly station	2
Glazing station	2
Wrapping station	1 (2 for large windows)

The number of workers required for each activity having been determined, a time study for each activity is undertaken as shown in Table 0.7, Table 0.8, and Table 0.9. For each activity, it was recorded by a stop watch by observing the workers completing each activity. The equations developed by Paniquar De Souto (2020) in a time study of the same production line are used for this purpose (Equations 3-1 to 3-3). Whereas Paniquar De Souto’s time study was conducted as an input for simulation-based productivity analysis, in the present research these equations are used for calculating the labour hours as the basis for providing the client with an accurate quote.

Table 0.7: Time study for A/C sub-line

Activities	Time 1 (s)	Time 2 (s)	Time 3 (s)
Cutting of profiles for frame and sash	53.1	49.6	51.0
Routing of cut-out for multi-lock handle	17.3	17.5	18.0
Routing of cut-out for operator mechanism	17.0	15.0	16.2
Punching of weep hole	7.5	6.8	7.0
Installation of weather strip	24.0	31.5	26.8
Welding of frame and sash profiles	133.4	136.5	130.0
Automatic corner cleaning	71.0	77.0	79.5
Cutting of nailing fin	26.0	19.0	23.0
Manual corning cleaning for frame	36.0	36.7	37.0
Installation of hinge track (3 screws)	11.9	12.5	12.0
Installation of hinge track (4 screws)	12.5	12.3	12.8
Installation of casement ramp	6.0	7.0	5.5
Installation of snubber	16.0	16.7	16.5
Installation of multi-lock handle and tie-bar connector	16.5	16.9	18.0
Installation of tie-bar and tie-bar guide (Ng = 1)	15.2	16.0	15.8
Installation of tie-bar and tie-bar guide (Ng = 2)	18.3	18.0	18.5
Installation of tie-bar and tie-bar guide (Ng = 3)	22.5	23.0	22.5
Installation of tie-bar and tie-bar guide (Ng = 4)	26.7	26.0	26.0
Installation of tie-bar and tie-bar guide (Ng = 5)	29.0	28.5	26.7
Installation of operator	59.0	55.0	59.8
Manual corner cleaning on sash	38.0	36.0	36.8
Installation of tie-bar keeper	31.6	32.0	32.5
Installation of hinge arm	24.3	25.0	24.8
Installation of operator bracket	41.0	39.0	42.7
Installation of operator bracket (Dyad)	30.0	32.0	33.5
Installation of operator track	20.5	18.0	21.5
Installation of limit bracket	19.3	19.7	18.0
Installation of limit track	18.2	18.3	18.9
Frame-sash assembly	41.0	39.5	38.0

Table 0.8: Time study for P/F sub-line

Activities	Time 1 (s)	Time 2 (s)	Time 3 (s)
Cutting of profiles	96.0	95.6	93.8
Punching of weep hole	9.0	10.5	12.0

Welding of profiles	120.4	113.4	118.8
Automatic corner cleaning	72.0	98.0	73.8
Cutting of nailing fin	24.0	22.5	28.0
Manual cleaning of corners	48.6	44.4	45.0

Table 0.9: Time study for the combined line

Station	Time 1 (s)	Time 2 (s)	Time 3 (s)
Box-to-box assembly	98.0	85.0	82.4
Installation of mullion cover	29.5	70.8	35.0
Installation of brickmould	177.0	197.4	200.0
Installation of jamb extension	333.4	310.5	400.0
Installation of cardboard and shipping block	70.0	77.0	60.6
Glazing unit assembly	103.0	112.0	116.0
Screen installation	32.0	31.0	35.0
Quality check	24.5	22.0	29.0
Wrapping	108.0	101.0	110.0

$$\text{Mullion cover installation} = 0.017 \frac{\text{sec}}{\text{window height (mm)}} \times \text{window height (mm)} \quad (3-1)$$

$$\text{Jamb extension installation} = 0.049 \frac{\text{sec}}{\text{mm}} \times \text{Perimeter of the window (mm)} \quad (3-2)$$

$$\text{Cardboard and wood protection installation} = 0.008 \frac{\text{sec}}{\text{mm}} \times \text{Perimeter of the window (mm)} \quad (3-3)$$

For the simulation of overall labour hours, a discrete-event simulation (DES) model is developed in the Simphony environment to mimic the production line. DES is selected for this purpose given that the production line under study represents a series of distinct activities in which each activity is performed independently but is related to the other activities and is carried out using shared resources. Additionally, rather than calculating the average of the three readings of each activity, the simulation model can calculate the probability of each activity's duration using a triangular function, thus giving more accurate results while providing confidence intervals for the results.

The developed simulation model follows the logic, sequence, and activities of the simulation model developed and validated by Wang (2021) for the same production line, as shown in Figure 3.13, Figure 3.14 and Figure 3.15. The timing for the model from this research time study is inputted to the developed simulation model. The model developed for the present research is then verified using the results of Wang’s model.

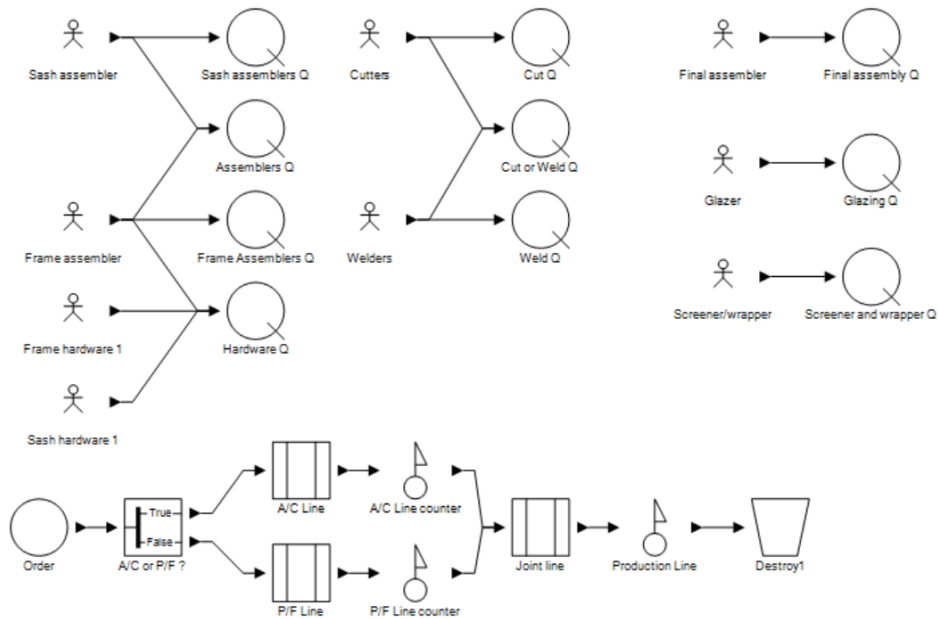


Figure 3.13: Overview of the simulation model

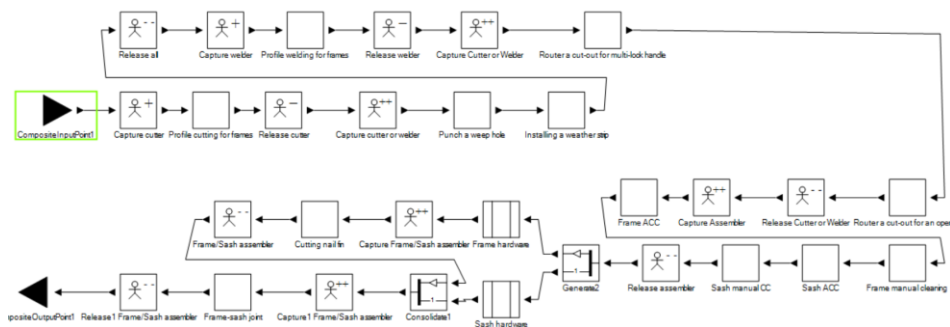


Figure 3.14: A/C sub-line

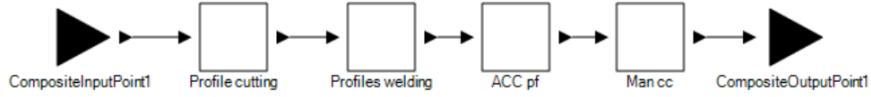


Figure 3.15: P/F sub-line

The simulation model is then run to forecast the total labour hours needed to produce a given window. Figure 3.16 show an example of the results of one run of the simulation model, where the time is given in seconds.

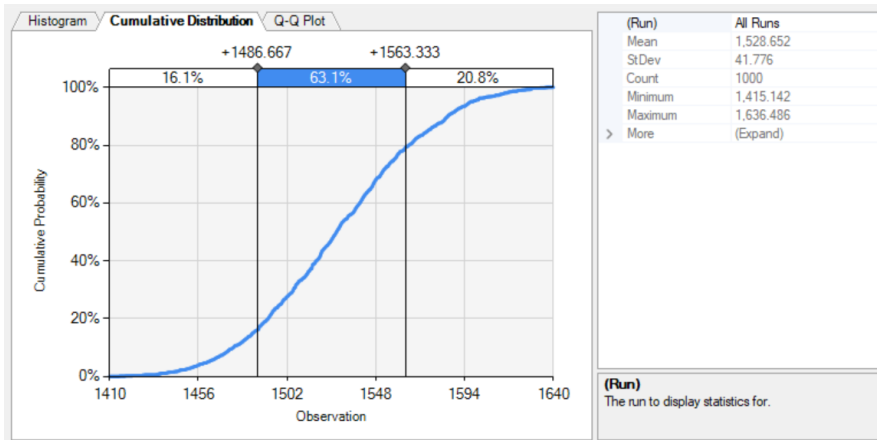


Figure 3.16: Total duration result with confidence interval.

Chapter 4: Implementation of the Proposed Methodology

4.1 Configuration logic

4.1.1 Dimensions and configuration

To extract important informant that will be employed in automating the configuration process, the product catalogue and customizations Company ABC offers, along with the profiles and hardware available from various suppliers, are carefully examined. Additionally, interviews are conducted with company personnel to gain further understanding of what customizations (e.g., colours, glass types, etc.) are available. Finally, the customization parameters are identified and incorporated into the interface's logic to facilitate the customization process for the client and salesperson, as shown in Figure 4.1.

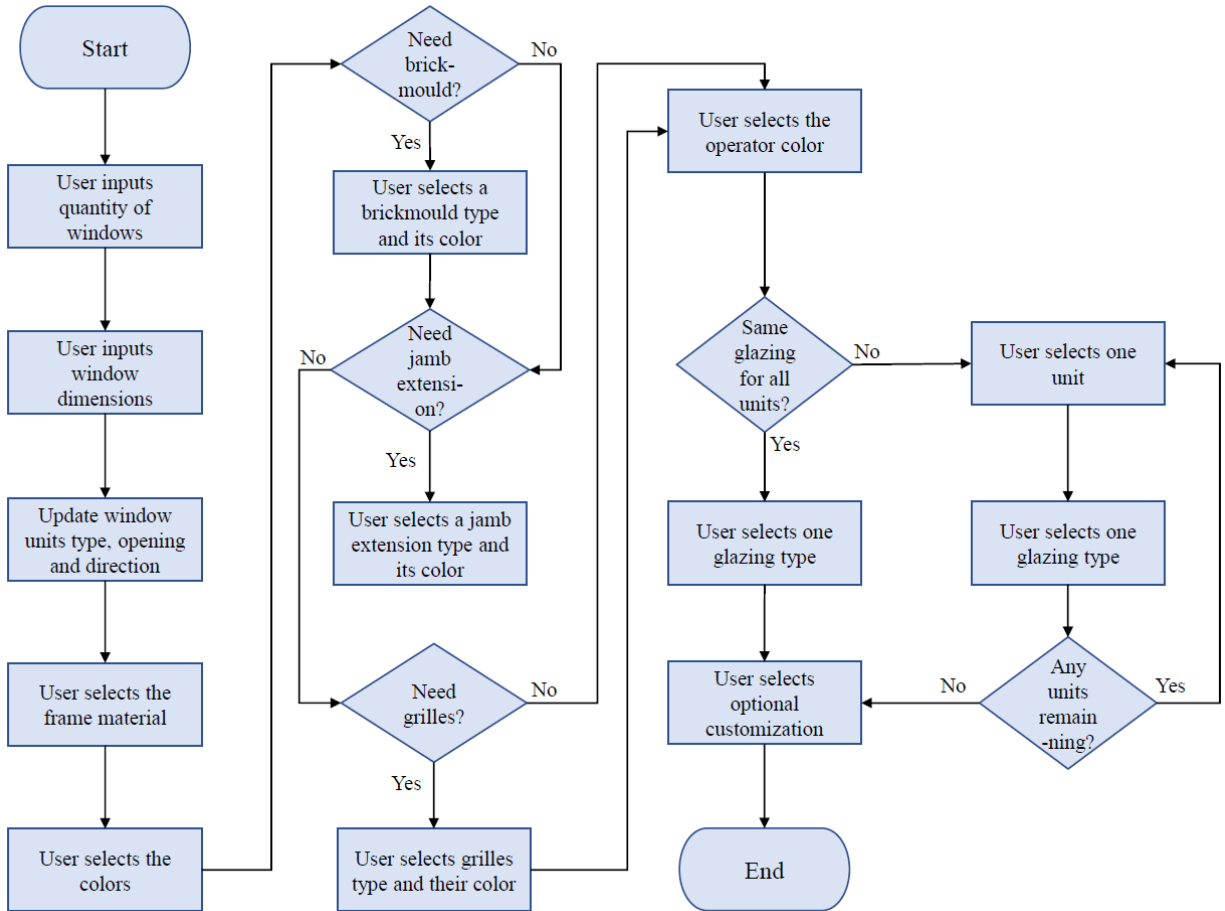


Figure 4.1: Configuration process overview

As noted above, to increase client engagement and achieve the desired state of the improved sales process, a web interface is developed, as shown in Figure 4.2

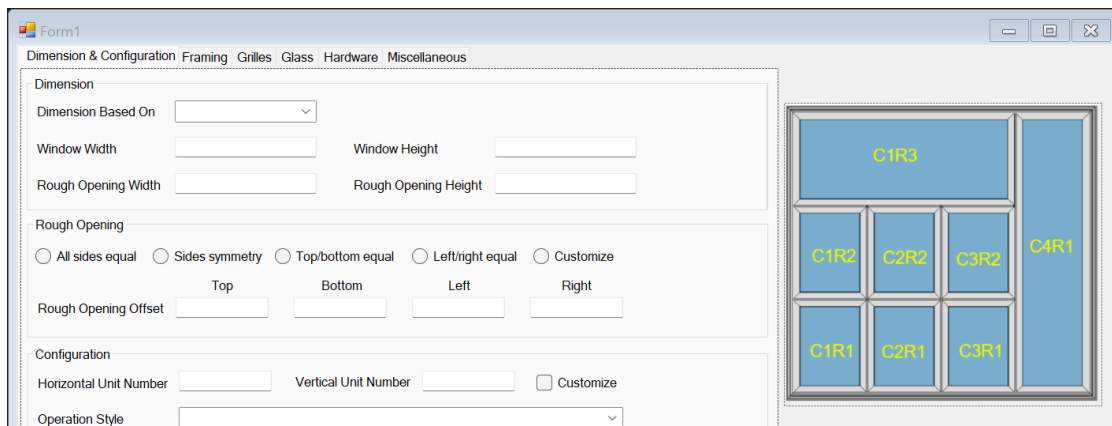


Figure 4.2: Web interface

In this interface, the user begins by specifying the dimensions of the window or of the rough opening. This is done by first choosing the desired calculation method from the “Dimension based on.” Once the user specifies the dimensions, the CPQ tool will capture these values and store them for subsequent calculations. Equations (4-1) and (4-2) govern the window dimensions, rough openings, and opening offsets.

$$W_w = W_{ro} - W_{osl} - W_{osr} \quad (4-1)$$

$$H_w = H_{ro} - H_{ost} - H_{osb} \quad (4-2)$$

where W_w and H_w are the width and height, respectively, of the window; W_{ro} and H_{ro} are the width and height, respectively, of the rough opening; W_{osl} and W_{osr} are the horizontal rough opening offsets on the left side and right side, respectively; and H_{ost} and H_{osb} are the vertical rough opening offsets on the top side and bottom side, respectively. It should be noted that the offsets can each be different depending on the client’s requirements, meaning that there are four offsets to be selected.

Once the dimensions and offsets have been selected, a 2D sketch of the window will appear on the right side of the web interface, and the window units will be assigned a unique ID that follows the form C1R1 (column 1, row 1) and that appears in the table at the bottom of the interface’s display, as shown in Figure 4.3.

Configuration

Horizontal Unit Number Vertical Unit Number Customize

Operation Style

Merge Units

	Merge #	Unit number	Unit number	Unit number	Unit number
*		<input type="text"/>	<input type="text"/>	<input type="text"/>	<input type="text"/>

Unit Information (Starting from Bottom Left Corner)

	Unit Number	Unit type	Opening direction	Width	Height
*		<input type="text"/>	<input type="text"/>	<input type="text"/>	<input type="text"/>

Figure 4.3: Web interface (merge and unit information table)

In this part of the interface, the user can select whether they want one window, or several smaller units assembled to form the required window (Company ABC refers to this customization as “box-to-box” installation). In the second table, under the unit number (C_iR_j), the user can customize the type of window from the four available options, and they can also select the direction of the opening (left or right) in the case of the casement window type. The width and height of each unit in the second table are automatically calculated based on default settings, but can be altered by the user. Equation (4-3) to Equation (4-6) govern the width and height.

Window unit size without user inputs:

$$W_{CiRj} = [W_w - M_{ci} \times (N_h - 1)]/N_h \quad (4-3)$$

$$H_{CiRj} = [H_w - M_{cj} * (N_v - 1)]/N_v \quad (4-4)$$

Window unit size with user input:

$$W_{CiRj} = [W_w - M_{ci} \times (N_h - 1) - \Sigma W_{CaRb}]/(N_h - k) \quad (4-5)$$

$$H_{CiRj} = [H_w - M_{cj} \times (N_v - 1) - \Sigma H_{CaRb}] / (N_v - k) \quad (4-6)$$

where W_{CiRj} , H_{CiRj} are the width and height, respectively, of the window unit C_iR_j , $i = \{1, 2, 3, 4, \dots\}$, $j = \{1, 2, 3, \dots\}$; W_w and H_w are the width and height, respectively, of the window; M_{ci} and M_{cj} are the horizontal gap width and vertical gap width, respectively, between window units, equal to 3 mm (1/8"); and N_h and N_v are, respectively, the horizontal and vertical maximum number of window units. With respect to the customized units only (i.e., the latter two equations), W_{CaRb} and H_{CaRb} are, respectively, the width and height of the window unit, and k is the number of customized units.

Figure 4.4 illustrates the process and logic the CPQ follows for merging window units, where U_k denotes the merging process. Figure 4.5 illustrates the configuration pattern, indicating what configurations are permitted in merging. Finally, Figure 4.6 summarizes the configuration parameters in the form of a decision tree.

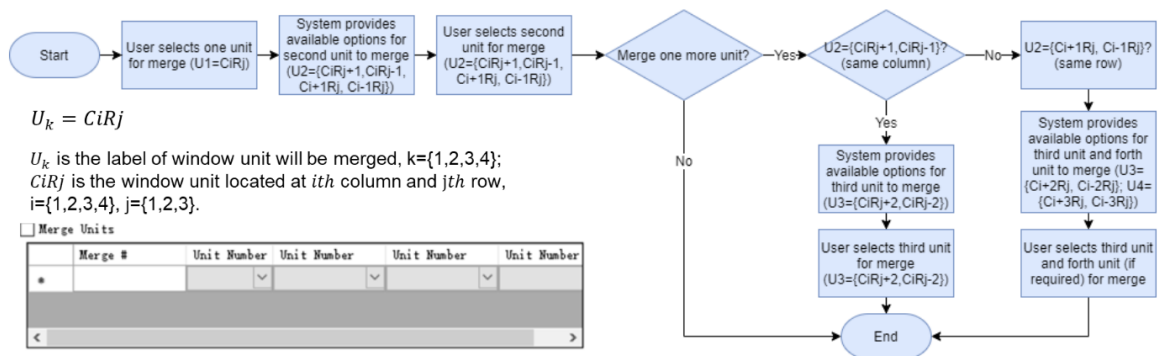


Figure 4.4: Window naming process

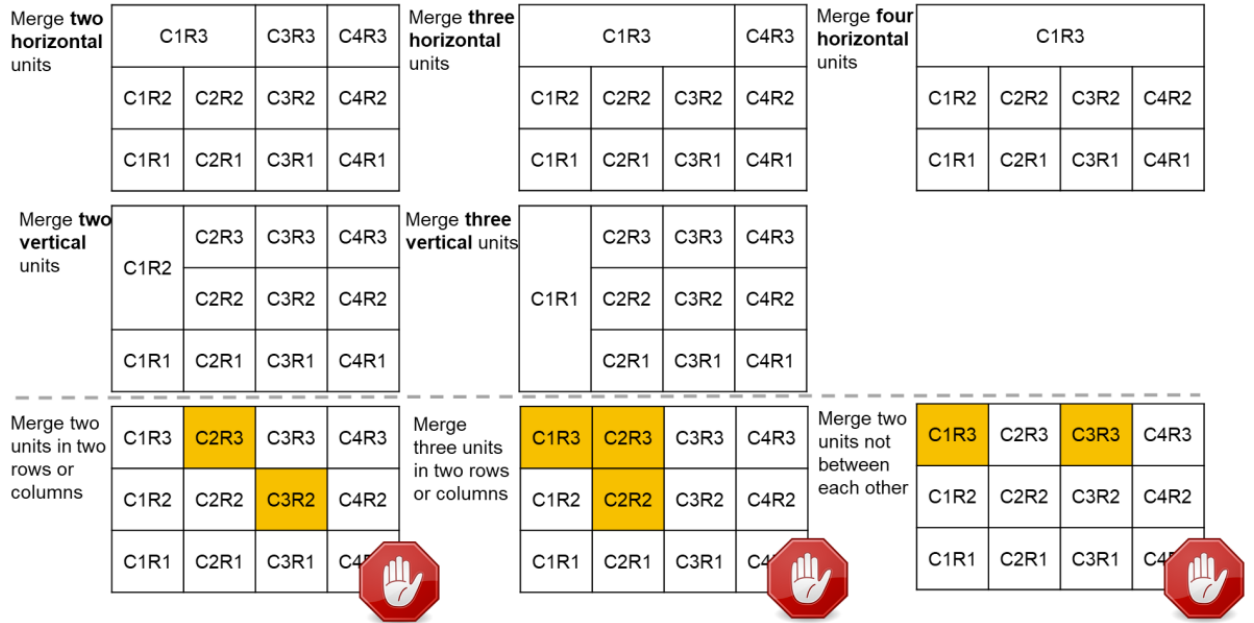


Figure 4.5: Configuration pattern

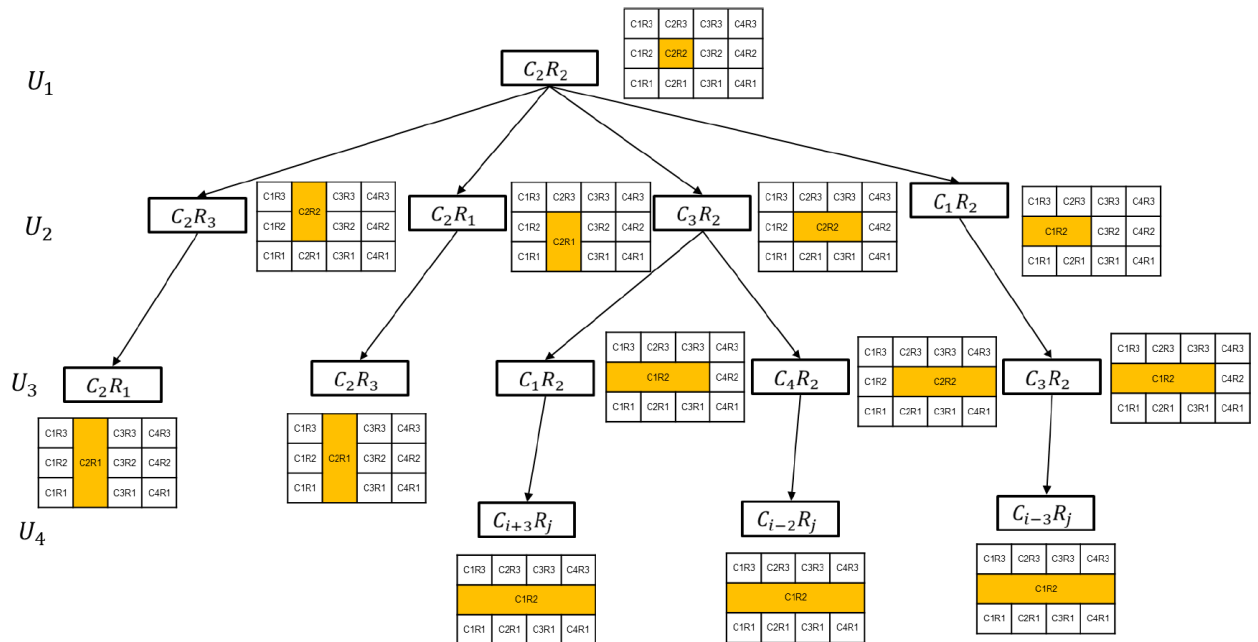


Figure 4.6: Window naming process (Decision Tree)

4.1.2 Window framing materials

As shown in Figure 4.7, Company ABC offers three different types of materials for window frames, PVC (which is the most common one), acrylic, and metal clad. Moreover, both the exterior and interior colours of the frames can be customized from a predefined set of colour combinations (see Figure 4.8). The user first selects the frame material, and then the exterior and interior colours, where both the frame materials available and the colour combinations available depend on the type of window selected earlier in the process.

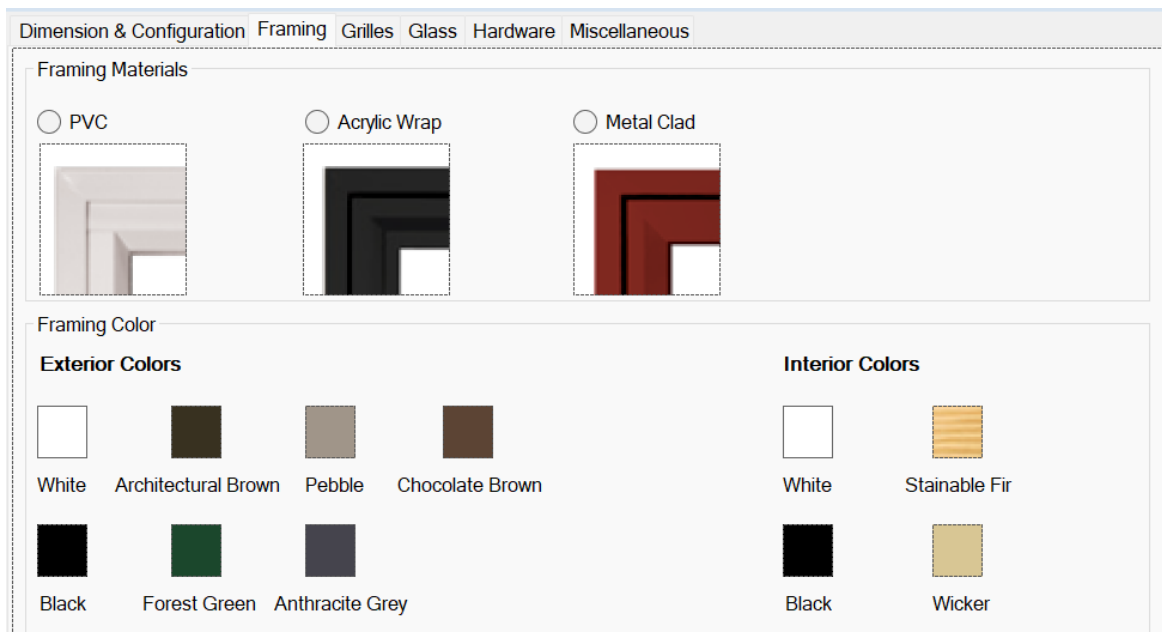


Figure 4.7: Framing materials and exterior colours

INTERIOR COLOURS	EXTERIOR COLOURS							
	White PVC	Wicker PVC	Black	Arch. Brown	Clear Anodized	Chocolate Brown	Anthracite Grey	Pebble
White PVC	•		•	•	•	•	•	•
Wicker PVC		•	•	•	•	•	•	•
Black	•		•	•			•	
Stainable Fir	•		•	•			•	

Figure 4.8: Colour combinations available (product information drawn from Company ABC’s 2017 product catalogue)

The next step under the “frame” tab in the interface is to select whether to add a brickmould and whether to add a jamb extension to the window, as shown in Figure 4.9. If opting to add a brickmould, the user can choose a dimension of either 1 ½” or 2”. Moreover, if opting to add a jamb extension, the user can choose a dimension of either ½” or ¾” (with drywall return clips attached).

Brickmould (optional)

1 1/2" BM 2" BM

Color:

White

Black

Architectural Brown

Pebble

Anthracite Grey

Chocolate Brown

Jamb Extension (optional)

Jamb Extension 1/2" Drywall Return Clip 3/4" Drywall Return Clip

Color:

White

Black

Stainable Fir

Wicker

Figure 4.9: Brickmould and Jamb extension (framing tab)

4.1.3 Grilles

In the “grille” tab of the interface, the user selects the grille and simulated divided lite (SDL) patterns. An SDL pattern, it should be noted, is installed on the exterior of the glass surface to simulate the look of divided panes of glass. Internal “grilles”, meanwhile, are installed between panes of glass, leaving the glass surfaces smooth and easy to clean. The user can either have the same grille pattern for all window units, or they can choose different grille patterns, sizes, and colours for each unit. The available patterns, shown in Figure 4.10, are ladder, double-ladder, rectangular, rectangular, perimeter, and double-perimeter.

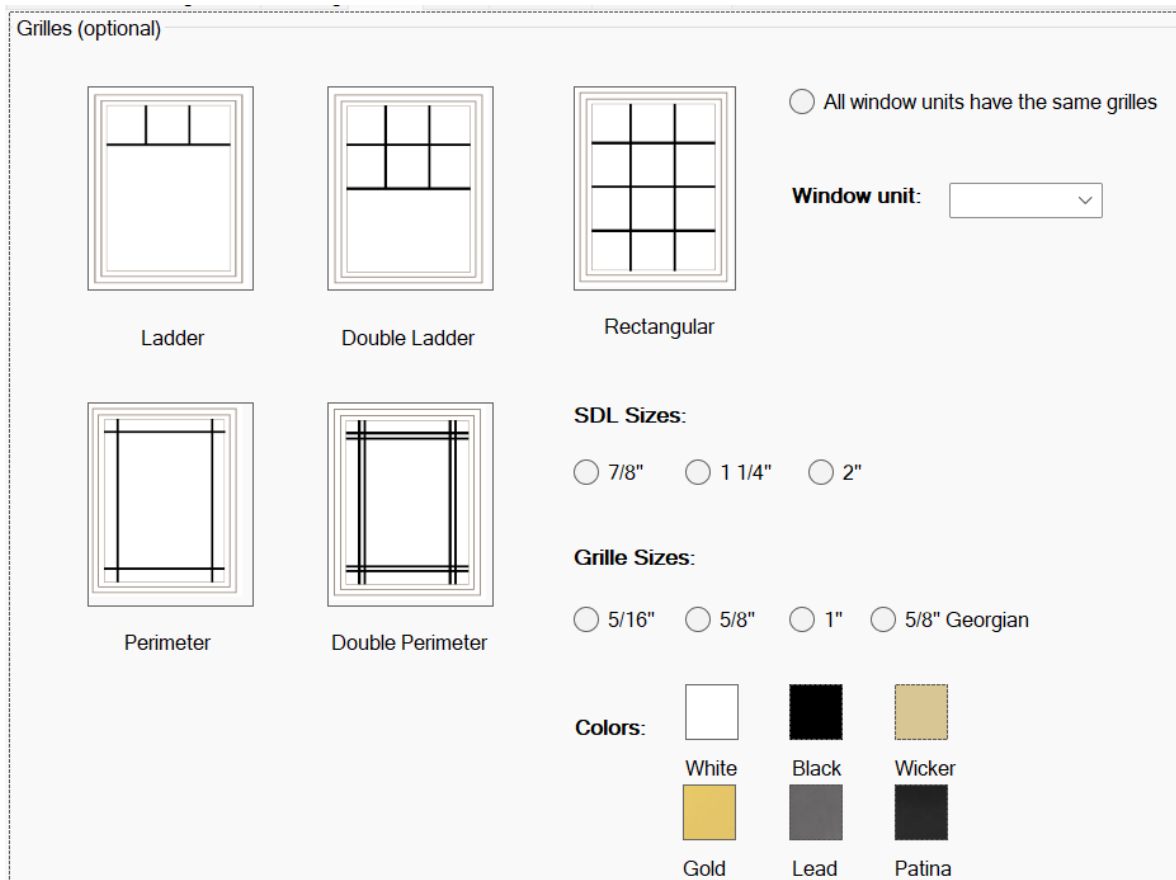


Figure 4.10: Grille patterns

4.1.4 Glazing

In the “glazing” tab of the interface, the user is presented with a table of available options of glass that the company offers. As illustrated in Figure 4.11, the table includes all the glass characteristics and specifications to facilitate the user selections. As with the grille patterns, the user can opt for the glass to be the same for all windows or they can customize it for individual window units.

Glass Types

Same for all units
 Customize: select unit

Choose type:

Glass Name	Heat System	Description	METRIC*		IMPERIAL*			Visible Light	Ultraviolet Block
			U-Value	R-Value	U-Value	R-Value	SHGC		
Clear	Dual	Dual pane, clear glass, no coatings	2.725	0.367	0.480	2.083	0.760	81%	42%
	Tri	Triple pane, clear glass, no coatings	1.760	0.568	0.310	3.226	0.685	74%	52%
Low-E	HS1-C180	Dual pane, one Low-E coating, Argon	1.476	0.678	0.260	3.846	0.685	79%	71%
	HS2-C180	Triple pane, one Low-E coating, Argon	1.045	0.957	0.184	5.435	0.615	73%	76%
	HS3-C180	Triple pane, two Low-E coatings, Argon	0.755	1.325	0.133	7.519	0.560	70%	87%
Sunstop	HS4-C270	Dual pane, one SunStop coating, Argon	1.408	0.710	0.248	4.032	0.367	70%	86%
	HS5-C270	Triple pane, one SunStop coating, Argon	1.056	0.947	0.186	5.376	0.338	63%	88%
	HS6-C270	Triple pane, two SunStop coatings, Argon	0.704	1.420	0.124	8.065	0.310	54%	96%
System V	HS1V-C180/i89	Dual pane, two Low-E coatings, Argon	1.187	0.843	0.209	4.785	0.623	77%	73%
	HS4V-C270/i89	Dual pane, one Low-E & one SunStop coating, Argon	1.136	0.881	0.200	5.000	0.361	69%	86%

R-Value: A measurement of the resistance of heat transfer through glass. The higher the R-Value, the better the window insulates against heat.

Solar Heat Gain (SHGC): The amount of the sun's heat that transfers through glass from the exterior to the interior side. The higher the solar heat gain, the more a window allows heat to pass through into a home.

U-Value: A measure of the rate of nonsolar heat flow through a material or assembly. The lower the U-Value, the greater a window's resistance to heat flow and the better its insulating value.

Figure 4.11: Glazing tab

4.1.5 Hardware colour

The “hardware colour” tab in the web interface allows the user to choose the colours of the window operators. Once again, they can choose to either apply the same colour choice to all units or to customize the operator colour for individual units (see Figure 4.12).

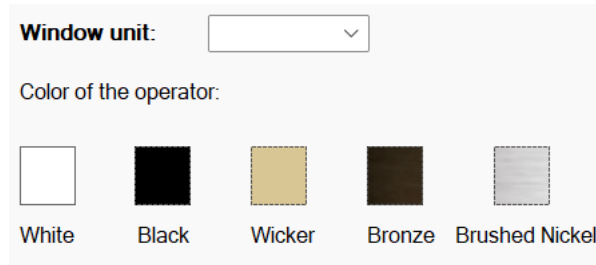


Figure 4.12: Operator colour

4.1.6 Miscellaneous

In this last tab of the interface, the user can choose whether to include a limit device, whether to include a screen, whether to include a subsill, and whether to include a nailing fin, as shown in Figure 4.13.

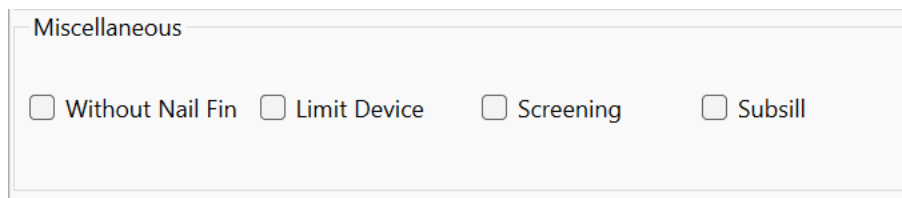


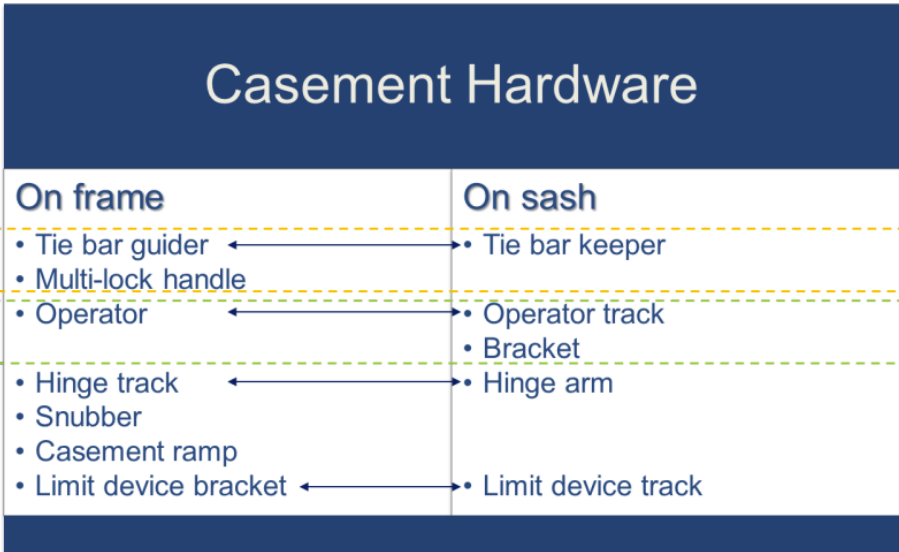
Figure 4.13: Miscellaneous tab in the interface

4.2 Window design

The client experience can be enhanced by offering them the option to customize their order, as discussed in the literature, as this allows the client to fulfil their needs and preferences. To ensure both client satisfaction and production efficiency, though, it is critical that these preferences and requirements be translated into ready designs and configurations for the shop floor. As discussed in the literature, having a clear linkage between design options and manufacturing parameters in the form of rule-based functions allows for the client to be able to customize their order based on their preferences within the constraints of what is feasible on the shop floor. Moreover, having rule-based functions that govern the hardware configuration and window design benefits the manufacturer in three ways. First, it allows the CPQ tool to calculate the hardware locations for a

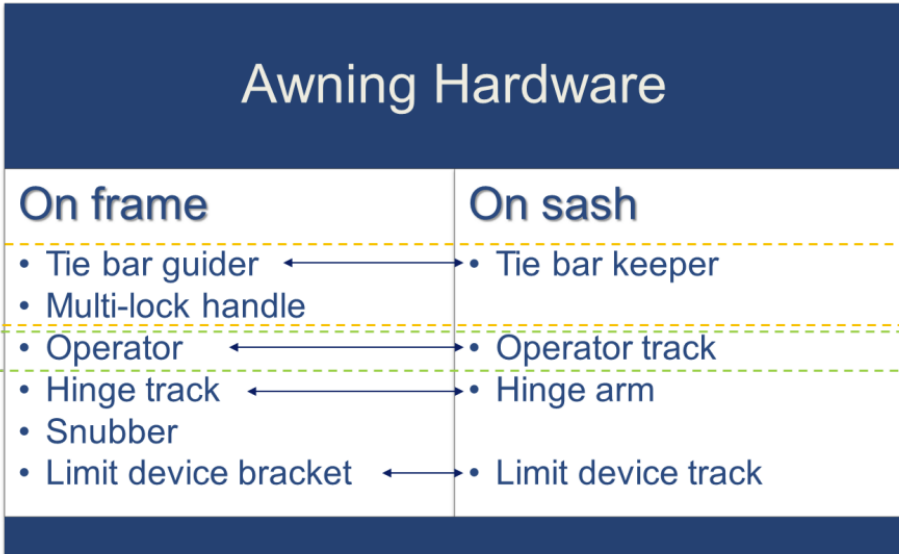
geometric representation and automated window design. Second, it allows for a bill of materials (BOM) to be generated instantaneously that can be used to calculate the cost of production in order to provide the client with an accurate quote. Third, it provides the shop floor with detailed information and instructions regarding the quantities and locations of hardware and screws such that the hardware assembly process can be standardized. To exemplify how these rule-based functions are applied, the following sub-sections illustrate some of the functions governing the hardware configuration for a casement window. (The functions for casement window configuration not described in this chapter can be found in Appendix A, while the functions governing the design of the awning window can be found in Appendix B.). For simplicity, picture and fixed windows are out of the scope of this implementation regarding their hardware configurations.

As explained in the previous chapter, a window structure typically consists of two main components (the frame and the sash) that are joined together in the combined portion of the production line. These components undergo profile cutting, welding, and hardware installation separately before being joined together at the joining station. Figure 4.14 and Figure 4.15 show the hardware used in manufacturing the two types of operable windows (i.e., casement and awning, respectively).



- ↔ Involved in one set of hardware
- ⌞ Connect together for locking window
- ⌞ Connect together for opening window

Figure 4.14: Hardware for casement windows



- ↔ Involved in one set of hardware
- ⌞ Connect together for locking window
- ⌞ Connect together for opening window

Figure 4.15: Hardware for awning windows

To inform the development of the equations underlying the rule-based functions, interviews are conducted with personnel from Company ABC's production engineering and planning departments in order to identify the various types of hardware used. The drawings, specifications, dimensions, and installation locations of the hardware are also obtained from the company, and AutoCAD drawings and illustrations of the hardware are developed to aid understanding. The developed equations for tie-bars, tie-bar guides, tie-bar rollers, and tie-bar keepers are adapted from the equations proposed by Wang (2021), Wang's equations having been developed to serve as inputs to a simulation model for productivity analysis, whereas the equations developed for the present research are intended for automating the design and quotation processes. To ensure the generic applicability of the rule-based functions for all types of windows in this production line, variables are assigned to each description, as shown in Figure 4.16. The variables shown in Figure 4.16 are kept constant when applying these functions to Line XYZ, but the developed functions can be applied to another window production line at Company ABC's production facility or to another window manufacturer altogether by simply adjusting the variables to calibrate the functions to the given context.

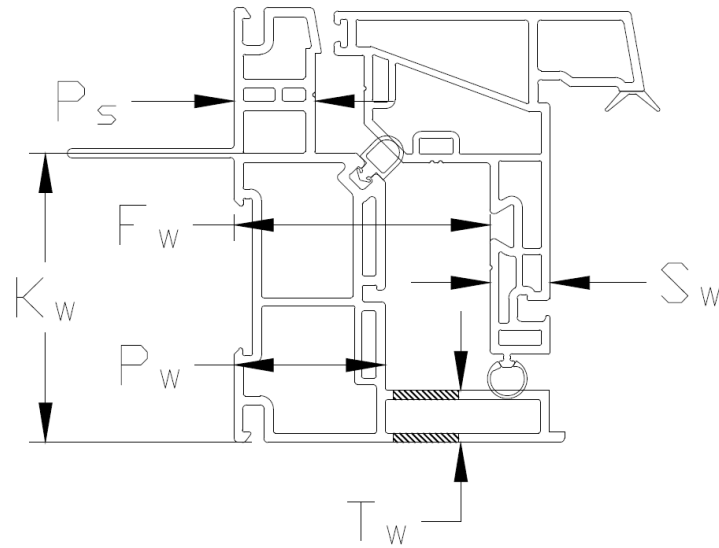


Figure 4.16: CAD details of a frame/sash cross-section

For implementation of the parametric design, two assumptions are made. First, the Z-coordinates are assumed to be constants. Second, the geometric locations are calculated only for the hardware, as these locations vary depending on a number of factors.

4.2.1 Locations of multi-lock handle cut-out and screws along frame (casement)

Each casement window has a multi-lock handle on the side of the window, where the location of this hardware depends on the orientation of the window's opening. The vertical profile on which the multi-lock handle is to be installed is routed at the designed location of the multi-lock handle, as shown in **Error! Reference source not found.**

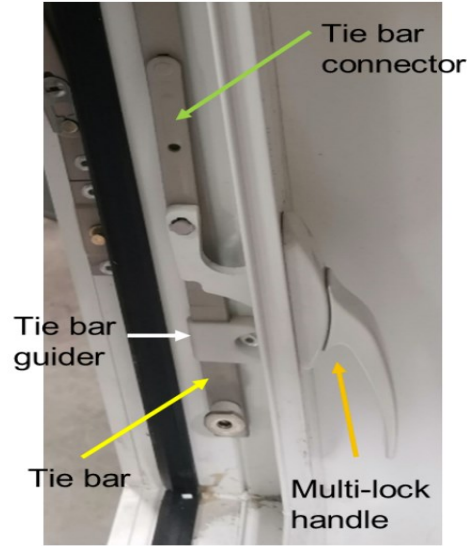


Figure 4.17: Multi-lock handle

The locations of the handle and screws along the X -axis satisfy the following equations:

$$X_{hco \rightarrow C-RH} = W_w - P_w - d_{cof} - \frac{d_{lco}}{2} + \sum_{i=1}^{n-1} W_{w,CiRj} + M_{ci} \quad (4-7)$$

$$X_{hco \rightarrow C-LH} = P_w + d_{cof} + \frac{d_{lco}}{2} + \sum_{i=1}^{n-1} W_{w,CiRj} + M_{ci} \quad (4-8)$$

$$X_{hcosc1 \rightarrow C-RH} = X_{hcosc2 \rightarrow C-LH} = W_w - P_w - d_{cof} - \frac{d_{lco}}{2} + \sum_{i=1}^{n-1} W_{w,CiRj} + M_{ci} \quad (4-9)$$

$$X_{hcosc1 \rightarrow C-LH} = X_{hcosc2 \rightarrow C-RH} = P_w + d_{cof} + \frac{d_{lco}}{2} + \sum_{i=1}^{n-1} W_{w,CiRj} + M_{ci} \quad (4-10)$$

The locations along the Y -axis satisfy the following equations:

$$Y_{hco} = d_{hco} + \frac{d_{out}}{2} + \sum_{j=1}^{n-1} H_{w,CiRj} + M_{cj} \quad (4-11)$$

$$Y_{hcosc1} = Y_{hco} - \frac{d_{out}}{2} - \delta_{ot} \quad (4-12)$$

$$Y_{hcosc2} = Y_{hco} + \frac{d_{out}}{2} + \delta_{ot} \quad (4-13)$$

The locations along the Z -axis satisfy the following equations:

$$X_{hco} = 0 \quad (4-14)$$

$$Z_{hcosc1} = Z_{hcosc2} = 10 \quad (4-15)$$

The variables used in the equations above are defined in Table 0.1 and illustrated in Figure 4.18.

Table 0.1: Symbols for the multi-lock handle equations

Symbol	Description	Constant used in case study
d_{hco}	Vertical distance from the bottom of the frame to the bottom of the handle cutout	155.0
d_{out}	Vertical length of the cut-out of the casement multi-lock handle	74.4
δ_{ot}	Vertical distance between the lock handle screw to the edge of the cut-out center	41.2
d_{lco}	Width of the cut-out	12.4
d_{cof}	Offset after P_w	1.5

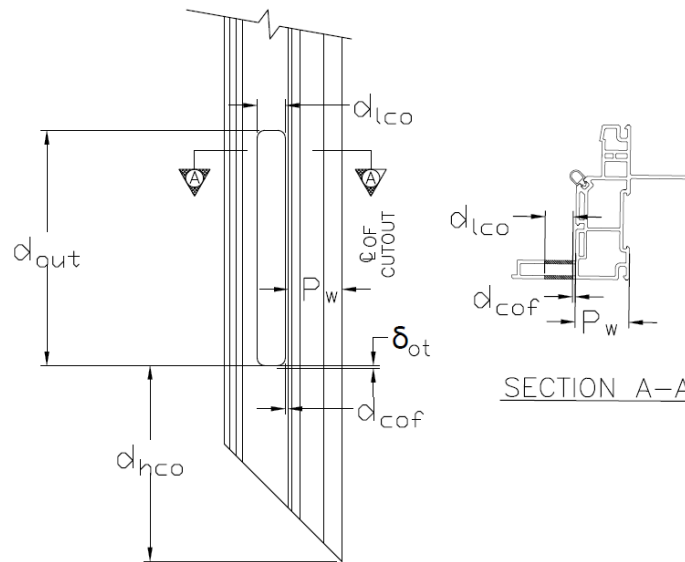


Figure 4.18: Multi-lock handle cut-out details in RH casement window

4.2.2 Operator selection and location (casement)

Company ABC uses three different operator mechanisms (Figure 4.19) depending on the capacity requirement (which in turn is a function of the window width). The appropriate operator to select is determined based on Equation (4-16).

$$\text{Operator type} = \begin{cases} \text{Reversed Dyad Operator, } 350 \leq W_w < 500 \\ \text{Single Arm Operator, } 500 \leq W_w < 600 \\ \text{Dual Arm Operator, } 600 \leq W_w \leq 950 \end{cases} \quad (4-16)$$



Figure 4.19: Different types of operators

4.2.3 Operator location on frame (casement)

The location of the operator (and, accordingly, the location of the cut-out in the profile to accommodate it) along the X -axis satisfies the following equations:

$$X_{co \rightarrow C-LH} = \begin{cases} d_{co1} + \sum_{i=1}^{n-1} W_{w,CiRj} + M_{ci}, & 350 \leq W_w < 500 \cup \text{Egress} \\ d_{co2} + \sum_{i=1}^{n-1} W_{w,CiRj} + M_{ci}, & 500 \leq W_w < 600 \\ d_{co3} + \sum_{i=1}^{n-1} W_{w,CiRj} + M_{ci}, & 600 \leq W_w \leq 950 \end{cases} \quad (4-17)$$

$$X_{co \rightarrow C-RH} = \begin{cases} W_w - d_{co1} + \sum_{i=1}^{n-1} W_{w,CiRj} + M_{ci}, & 350 \leq W_w < 500 \cup \text{Egress} \\ W_w - d_{co2} + \sum_{i=1}^{n-1} W_{w,CiRj} + M_{ci}, & 500 \leq W_w < 600 \\ W_w - d_{co3} + \sum_{i=1}^{n-1} W_{w,CiRj} + M_{ci}, & 600 \leq W_w \leq 950 \end{cases} \quad (4-18)$$

The location of the operator along the Y -axis satisfies the following equation:

$$Y_{co \rightarrow C-LH} = Y_{co \rightarrow C-RH} = P_w + d_{opy} + \sum_{j=1}^{n-1} H_{w,CiRj} + M_{cj} \quad (4-19)$$

The location of the operator along the Z -axis satisfies the following equation:

$$Z_{co} = 0 \quad (4-20)$$

As expressed in the preceding equations, the location of the casement window operator is determined based on the type and the capacity of the operator. Table 4.2 and Figure 4.20 define the variables appearing in the preceding equations.

Table 0.2: Symbols for the location of casement operators' equations

Symbol	Description	Constant used in case study
d_{co1}	Distance between the center of the casement operator cut-out location and the outer edge of the window frame (reverse and egress)	158
d_{co2}	Distance between the center of the casement operator cut-out location and the outer edge of the window frame (standard single arm)	208
d_{co3}	Distance between the center of the casement operator cut-out location and the outer edge of the window frame (dual-arm operator)	273
d_{opy}	Width of the cut-out of the casement operator	15

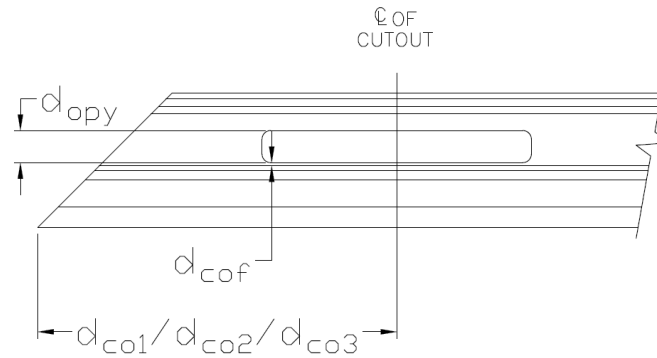


Figure 4.20: Casement operator cut-out details

4.2.4 Operator track (casement)

The operator track is available from the supplier in two lengths, 289 mm and 368.3 mm, where the length depends on the type of operator, which in turn is a function of the window width. (Windows with a width between 350 mm and 500 mm use the reverse operator, which does not require a track.) The track selection thus satisfies the following equation.

$$L_{cot} = \begin{cases} N/A, & 350 \leq w_w < 500 \\ 289, & 500 \leq w_w < 600 \\ 368.3, & 600 \leq w_w < 950 \end{cases} \quad (4-21)$$

As noted in the previous chapter, hardware that is described by length is described in terms of the locations of the start- and end-points of the hardware to display its location and direction instead of its center.

The locations of the track and its screws along the X -axis satisfy the following equations:

$$X_{ots \rightarrow C-LH} = \begin{cases} W_w - F_w - d_{cot1} + \sum_{i=1}^{n-1} W_{w,CiRj} + M_{ci}, & \text{Egress} \\ W_w - F_w - d_{cot2} + \sum_{i=1}^{n-1} W_{w,CiRj} + M_{ci}, & 500 \leq w_w < 600 \\ W_w - F_w - d_{cot3} + \sum_{i=1}^{n-1} W_{w,CiRj} + M_{ci}, & 600 \leq w_w \leq 950 \end{cases} \quad (4-22)$$

$$X_{otf \rightarrow C-LH} = X_{ots \rightarrow C-LH} - L_{cot} \quad (4-23)$$

$$X_{ots \rightarrow C-RH} = f(F_w) = \begin{cases} F_w + d_{cot1} + \sum_{i=1}^{n-1} W_{w,CiRj} + M_{ci}, & \text{Egress} \\ F_w + d_{cot2} + \sum_{i=1}^{n-1} W_{w,CiRj} + M_{ci}, & 500 \leq w_w < 600 \\ F_w + d_{cot3} + \sum_{i=1}^{n-1} W_{w,CiRj} + M_{ci}, & 600 \leq w_w \leq 950 \end{cases} \quad (4-24)$$

$$X_{otf \rightarrow C-RH} = X_{ots \rightarrow C-RH} + L_{cot} \quad (4-25)$$

For the screws:

$$X_{otsc1 \rightarrow C-LH} = X_{ots \rightarrow C-LH} - \delta_{cott} + \sum_{i=1}^{n-1} W_{w,CiRj} + M_{ci} \quad (4-26)$$

$$X_{otsc2 \rightarrow C-LH} = X_{ots \rightarrow C-LH} - \frac{L_{cot} - 2 \times \delta_{cott}}{2} + \sum_{i=1}^{n-1} W_{w,CiRj} + M_{ci} \quad (4-27)$$

$$X_{otsc3 \rightarrow C-LH} = X_{ots \rightarrow C-LH} - (L_{cot} - 2 \times \delta_{cott}) + \sum_{i=1}^{n-1} W_{w,CiRj} + M_{ci} \quad (4-28)$$

$$X_{otsc1 \rightarrow C-RH} = X_{ots \rightarrow C-RH} + \delta_{cott} + \sum_{i=1}^{n-1} W_{w,CiRj} + M_{ci} \quad (4-29)$$

$$X_{otsc2 \rightarrow C-RH} = X_{ots \rightarrow C-RH} + \frac{L_{cot} - 2 \times \delta_{cott}}{2} + \sum_{i=1}^{n-1} W_{w,CiRj} + M_{ci} \quad (4-30)$$

$$X_{otsc3 \rightarrow C-RH} = X_{ots \rightarrow C-LH} + (L_{cot} - 2 \times \delta_{cott}) + \sum_{i=1}^{n-1} W_{w,CiRj} + M_{ci} \quad (4-31)$$

The locations of the track and its screws along the Y -axis satisfy the following equations:

$$Y_{ot \rightarrow C} = \begin{cases} \delta_{cosy1} + \sum_{j=1}^{n-1} H_{w,CiRj} + M_{cj}, & \text{Egress} \\ \delta_{cosy1} + \sum_{j=1}^{n-1} H_{w,CiRj} + M_{cj}, & 500 \leq W_w < 600 \\ \delta_{cosy2} + \sum_{j=1}^{n-1} H_{w,CiRj} + M_{cj}, & 600 \leq W_w \leq 950 \end{cases} \quad (4-32)$$

$$Y_{otsc\beta \rightarrow C} | \forall \alpha \in A, Y_{otsc\beta \rightarrow C} = \begin{cases} \delta_{cosy1} + \sum_{j=1}^{n-1} H_{w,CiRj} + M_{cj}, & \text{Egress} \\ \delta_{cosy1} + \sum_{j=1}^{n-1} H_{w,CiRj} + M_{cj}, & 500 \leq W_w < 600 \\ \delta_{cosy2} + \sum_{j=1}^{n-1} H_{w,CiRj} + M_{cj}, & 600 \leq W_w \leq 950 \end{cases} \quad (4-33)$$

The locations of the track and its screws along the Y -axis satisfy the following equations:

$$Z_{ot \rightarrow C} = Z_{otsc\alpha \rightarrow C} = 42.1 \quad (4-34)$$

$$Z_{otsca \rightarrow C} | \forall \alpha \in A, Z_{otsca \rightarrow C} = 50.7 \quad (4-35)$$

As shown in Table 0.3, the track's location is a function of the operator type, which in turn is governed by the window's width. Because the track's screws are symmetrically distributed (as shown in Figure 4.21 and Figure 4.22), other screw locations can be calculated accordingly by simply identifying the first screw's location from the track's edge. Table 4.3 defines the variables appearing in the preceding equations.

Table 0.3: Symbols for operator track equations (casement)

Symbol	Description	Constant used in case study
d_{cot1}	Distance between the start of the operator track and the outside edge of the sash (egress operator)	37.1
d_{cot2}	Distance between the start of the operator track and the outside edge of the sash (standard single arm operator)	87.1
d_{cot3}	Distance between the start of the operator track and the outside edge of the sash (dual-arm operator)	124.6
δ_{cosy1}	Vertical distance between the casement operator's track screws and the outer edge of the frame (single, reverse and egress operators)	24.7
δ_{cosy2}	Vertical distance between the casement operator's track screws and the outer edge of the frame (dual-arm operator)	26.6
δ_{cott}	Space between the edge screw of the operator track and the nearest track's edge	19.0

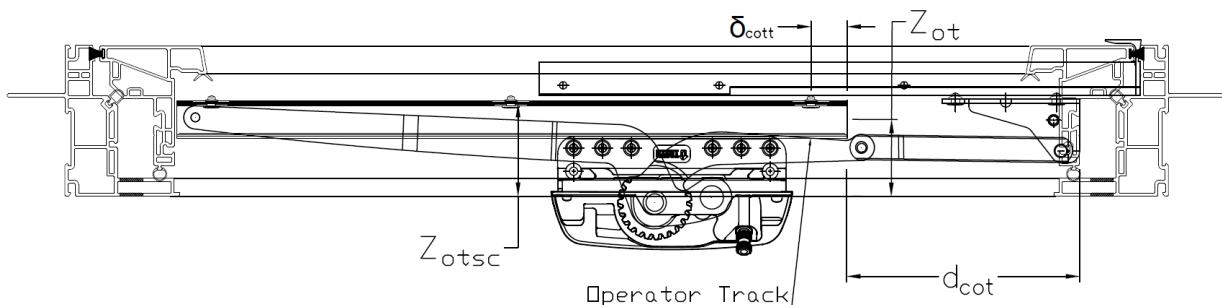


Figure 4.21: CAD details for dual-arm operator track

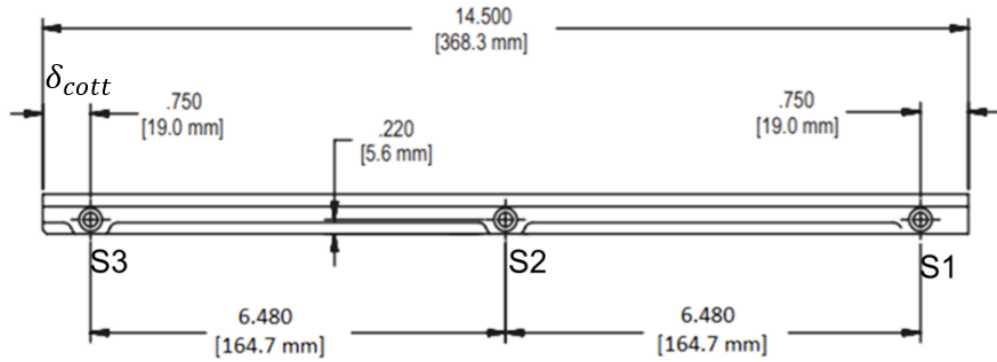


Figure 4.22: Dual-arm operator track specifications

4.2.5 Hinge arm and screws on sash (casement)

The hinge arm is an arm installed on the sash and connected to the hinge track. Hinge arms are installed on the top and bottom of casement windows, as shown in Figure 4.23 and Figure 4.24. The hinge arm secures the sash in place and connects it to the frame with the hinge track, and both of the arms determine the movement of the window opening.

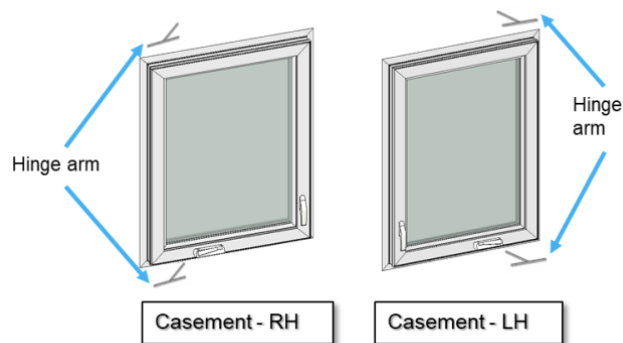


Figure 4.23: Hinge arm locations

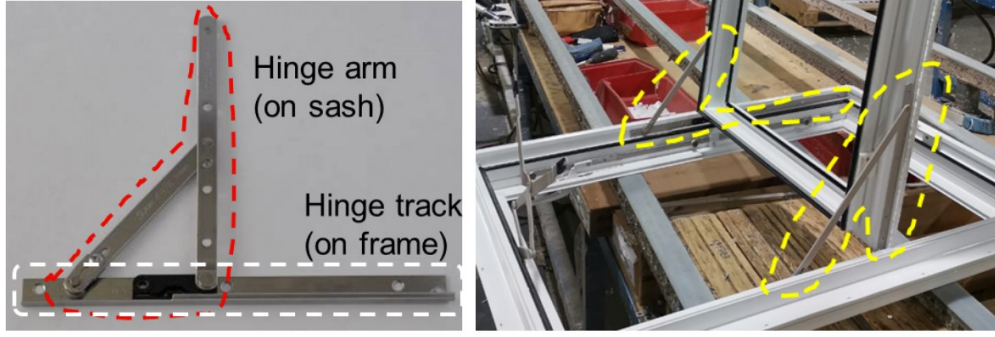


Figure 4.24: Hinge arm and track

The length of the hinge arm satisfies the following equation:

$$L_a = \begin{cases} 184, & 350 \leq w_w < 600 \\ 177.8, & 600 \leq w_w < 950 \end{cases} \quad (4-36)$$

The locations of the hinge arm and its screws on the sash along the X -axis satisfy the following equations:

$$X_{has \rightarrow C-RH} = P_w + A + \frac{d_{sc}}{2} + \sum_{i=1}^{n-1} W_{w,CiRj} + M_{ci} \quad (4-37)$$

$$X_{haf \rightarrow C-RH} = P_w + A + \frac{d_{sc}}{2} + L_a + \sum_{i=1}^{n-1} W_{w,CiRj} + M_{ci} \quad (4-38)$$

$$X_{has \rightarrow C-LH} = W_w - P_w - A - \frac{d_{sc}}{2} + \sum_{i=1}^{n-1} W_{w,CiRj} + M_{ci} \quad (4-39)$$

$$X_{haf \rightarrow C-LH} = W_w - P_w - A - \frac{d_{sc}}{2} - L_a + \sum_{i=1}^{n-1} W_{w,CiRj} + M_{ci} \quad (4-40)$$

For the screws along the X -axis:

$$X_{hasc1 \rightarrow C-RH} = P_w + A + \delta_{a1} + \sum_{i=1}^{n-1} W_{w,CiRj} + M_{ci} \quad (4-41)$$

$$X_{hasc2 \rightarrow C-RH} = P_w + A + \delta_{a2} + \sum_{i=1}^{n-1} W_{w,CiRj} + M_{ci} \quad (4-42)$$

$$X_{hasc3 \rightarrow C-RH} = P_w + A + \delta_{a3} + \sum_{i=1}^{n-1} W_{w,CiRj} + M_{ci} \quad (4-43)$$

$$X_{hasc4 \rightarrow C-RH} = P_w + A + \delta_{a4} + \sum_{i=1}^{n-1} W_{w,CiRj} + M_{ci} \quad (4-44)$$

$$X_{hasc1 \rightarrow C-LH} = W_w - P_w - A - \delta_{a1} + \sum_{i=1}^{n-1} W_{w,CiRj} + M_{ci} \quad (4-45)$$

$$X_{hasc2 \rightarrow C-LH} = W_w - P_w - A - \delta_{a2} + \sum_{i=1}^{n-1} W_{w,CiRj} + M_{ci} \quad (4-46)$$

$$X_{hasc3 \rightarrow C-LH} = W_w - P_w - A - \delta_{a3} + \sum_{i=1}^{n-1} W_{w,CiRj} + M_{ci} \quad (4-47)$$

$$X_{hasc4 \rightarrow C-LH} = W_w - P_w - A - \delta_{a4} + \sum_{i=1}^{n-1} W_{w,CiRj} + M_{ci} \quad (4-48)$$

The locations of the hinge arm and its screws on the sash along the Y -axis satisfy the following equations:

$$Y_{hts \rightarrow C-RH} = Y_{hts \rightarrow C-LH} = P_w + \sum_{j=1}^{n-1} H_{w,CiRj} + M_{cj} \quad (4-49)$$

For the screws along the Y -axis:

$$Y_{hasc\beta \rightarrow C} | \forall \beta \in A, Y_{hasc\beta \rightarrow C} = P_w + \sum_{i=1}^{n-1} H_{w,CiRj} + M_{ci} \quad (4-50)$$

The location of the hinge arm on the sash along the Z -axis satisfies the following equations:

$$Z_{ha} = 54 \quad (4-51)$$

It should be noted that “ A ” in the preceding equations describes the distance between the hinge arm's edge and the hinge track's nearest edge, as shown in Figure 4.25, Figure 4.26, and Figure 4.27. In this case study, A is a function of the hinge track length, thus making it a function of the window width (as described above). Table 4.4 defines the variables appearing in the preceding equations.

$$A = \begin{cases} 140.5, & 350 \leq w_w < 600 \\ 57.9, & \text{Egress} \\ 166.8, & 600 \leq w_w < 950 \end{cases} \quad (4-52)$$

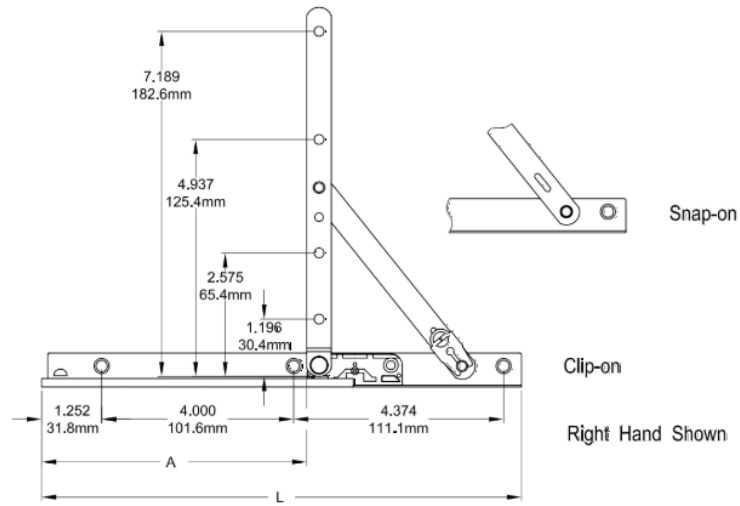


Figure 4.25: Standard 10" hinge

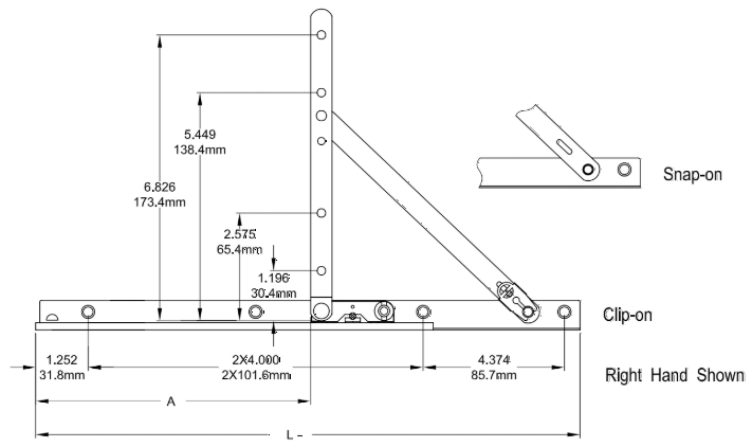


Figure 4.26: Standard 13" hinge

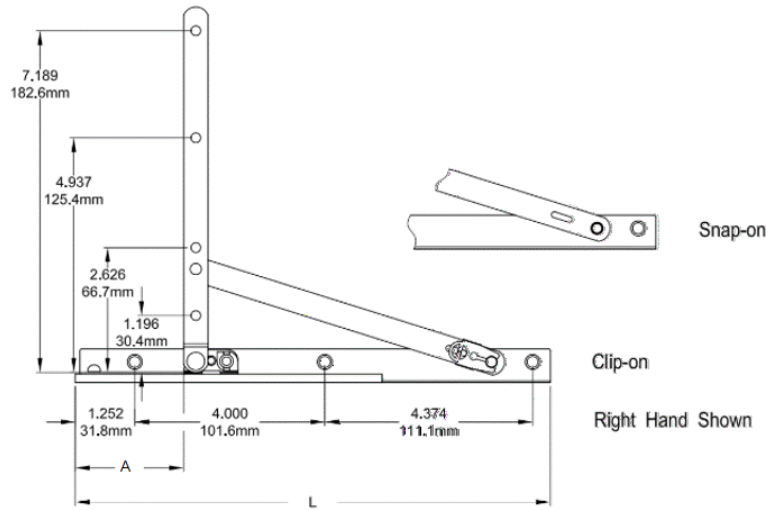


Figure 4.27: 10" egress standard hinge

Table 0.4: Symbols for casement hinge arm equations

Symbol	Description	Constant used in case study
d_{sc}	Diameter of the screw hole on the hinge arm	2.9
δ_{a1}	Distance between the first screw of the hinge arm and the hinge arm's initial point	30.4
δ_{a2}	Distance between the second screw of the hinge arm and the hinge arm's initial point	65.4
δ_{a3}	Distance between the third screw of the hinge arm and the hinge arm initial point (10" track)	125.4
	Distance between the third screw of the hinge arm and the hinge arm initial point (13" track)	138.4
δ_{a4}	Distance between the fourth screw of the hinge arm and the hinge arm initial point (10" track)	182.6
	Distance between the third screw of the hinge arm and the hinge arm initial point (13" track)	173.4

4.3 Case study

The framework developed in this research is a configure-price-quote (CPQ) tool. Company ABC's is to present an estimated preliminary quote to the client before initiating the detailed design, and to provide a final quote only after detailed design. To streamline this approach and enable mass customization (MC), the design and pricing processes must be automated. The automation of design is achieved by developing equations to govern the selection of hardware and

determination of geometric locations, along with an interface for configuring and visualizing the windows, as discussed above.

To implement the framework, a prototype CPQ tool is programmed using the Python programming language. The developed prototype allows the user to fully customize a casement window, including selecting the opening direction, determining the dimensions, selecting the frame materials, and determining whether to add a brickmould and a jamb extension. To illustrate the prototype's functionality, a window is customized in a case study, as shown in Figure 4.28. The window considered is a left-side casement window with a width of 700 mm and a height of 1,000 mm.

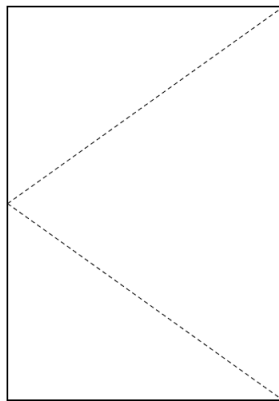


Figure 4.28: Left side casement window

The dimensions of the window are determined by specifying the rough opening dimensions ($W_{ro} = 750, H_{ro} = 1,050$) and the offsets (i.e., 25 mm in all directions). After the CPQ tool receives the user's configuration inputs through the interface, it determines the hardware types and quantities, then calculates the hardware locations using the developed functions. The developed CPQ tool based on the developed framework provides three outputs: (1) the window design and the hardware geometric locations, (2) the BOM, and (3) the final quote that is to be presented to the client for signature.

4.3.1 Design and hardware geometric locations

The first output specifies the window design by providing the types and geometric locations of hardware. In the case study, this output results in a total of 73 hardware items and locations. An excerpt of this output is provided in Table 0.5.

Table 0.5: Sample of the design output

Hardware	X-axis	Y-axis	Z-axis
Dual-arm Operator screw number 1	509.0	55.6	26.4
Dual-arm Operator screw number 2	493.1	55.6	26.4
Dual-arm Operator screw number 3	477.2	55.6	26.4
Dual-arm Operator screw number 4	432.7	55.6	26.4
Dual-arm Operator screw number 5	416.9	55.6	26.4
Dual-arm Operator screw number 6	401.0	55.6	26.4
Operator track (368.3) start-point	551.6	55.6	49.5
Operator track (368.3) end-point	183.3	55.6	49.5
Operator track screw number 1	521.6	55.6	49.5
Operator track screw number 2	367.5	55.6	49.5
Operator track screw number 3	213.3	55.6	49.5
Operator bracket	662.0	55.6	41.6
Operator bracket screw number 1	663.5	55.6	52.3
Operator bracket screw number 2	608.0	55.6	52.3
Start-point of tie-bar	53.8	139.0	16.5
End-point of tie-bar	53.8	969.0	16.5
Tie-bar roller number 1	53.8	159.0	16.5
Tie-bar roller number 2	53.8	554.0	16.5
Tie-bar roller number 3	53.8	889.0	16.5

As shown in the previous table, the CPQ calculates the geometric locations of each item of hardware and its screws, where the coordinates of each item are determined in reference to the bottom-left corner of the rough opening. In this way, the CPQ supports visualization of the hardware locations in the design space. Moreover, this output can be used to prepare production specifications for the shop floor complete with hardware installation locations.

4.3.2 Bill of materials (BOM)

Once the window design and hardware locations have been determined, a BOM is generated. The BOM specifies all of the profiles, hardware, and other materials needed to manufacture the customized window. Table 0.6 shows a sample BOM generated by the CPQ prototype.

Table 0.6: Sample BOM

Material item	Quantity of materials
Tie-bar	1
Tie-bar rollers	3
Tie-bar guides	3
Screws for tie-bar guides	3
Tie-bar keepers	3
Screws for tie-bar keepers	9
Multi-lock handle	1
Screws for multi-lock handle	2
Dual-arm operator	1
Screws for dual-arm operator	6
Operator track (368.3)	1
Screws for operator track (368.3)	3
Hinge track (13" standard hinge)	2
Screws for hinge track (13" standard hinge)	8
Hinge arm (177.8)	2
Screws for hinge arm (177.8)	8
Snubber	1

The BOM output is essential, as it provides the procurement department with the required quantities of materials, thereby helping them to manage inventory more efficiently. Additionally, the BOM is used in conjunction with the time study data to generate the third output, i.e., the quote.

4.3.3 Quote

After generating the BOM, the CPQ tool extracts the cost data and production line activity time associated with each item in the BOM in order to calculate (1) the direct cost of the required

Chapter 5: Conclusion

Due to the rapid changes and technological development seen within the manufacturing industry in recent decades, manufacturers can offer clients more choice with respect to product variability and design flexibility. In this respect, manufacturers that can offer customized products at a similar price and turnaround time to standardized products will gain a significant competitive advantage, especially within the off-site construction (OSC) domain, where tailoring the project to the client's requirements while achieving efficient production poses a significant technical challenge.

This research enhances the current practice of window manufacture in OSC by developing a framework to enable window manufacturers to produce customized windows (i.e., ATO products) at a price point and lead time comparable to those of standardized products. This framework aids the configuration tool—i.e., a configure-price-quote (CPQ) tool—in automating the design process and quotation generation. Additionally, it serves as a cornerstone for automating the drafting process by calculating the geometric location of each hardware component. This is achieved by first analyzing the production line, current design and sales practices, materials and hardware used, and the customizations offered. Based on this analysis, a product family of customized windows is established accordingly. Rule-based functions are then developed to govern the hardware configuration. Finally, a time study is conducted in order to calculate the direct labour cost of each activity in the production process based on the given design/configuration.

The framework outputs a bill of material (BOM) that includes all hardware components, along with their quantities and locations, in addition to an accurate quote for the client, as shown in Figure 5.1. In this manner, the framework enhances the design process and facilitates the process of generating design sheets for manufacturing purposes.

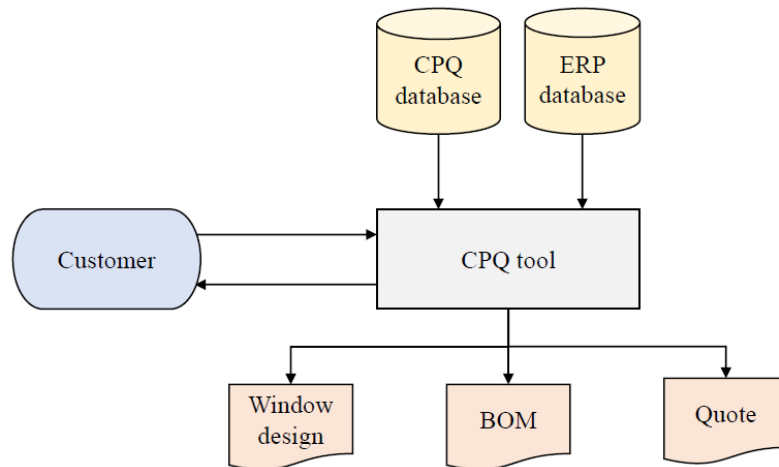


Figure 5.1: Future state of window design by a CPQ tool

As shown in Figure 5.1, the client can interact with the CPQ tool in order to configure a window order and receives an instant and accurate quote. In this way, the framework eliminates the need for extensive exchange of information between the sales and planning departments prior to issuing a quote (which usually takes one to three business days in the case company's current practice). Moreover, the framework automates the design process, enabling the client to explore various configurations of window components without the need for manual redesign for each configuration. Furthermore, if the client does not make an order, there will be no non-value-added activities, (i.e., given that the client can change their mind during or after the design phase, thereby rendering the process of developing the original design a non-value-added activity). It should be noted that while window manufacture is considered as a case study to demonstrate the implementation of the developed framework, it could be implemented in the design and manufacture of other ATO products in OSC.

5.1 Research Contributions

This research presented a framework that establishes a product family for windows and identifies the sub-components. In this way, it aids the CPQ tool in enabling the client or salesperson to

customize windows in an efficient manner. Manufacturers can use this tool to offer various customized products based on the configuration of the selected sub-components (which is determined by the tool). Moreover, the framework provides an accurate quote and BOM for each custom window order, making it implementable on any window production line. As noted above, this framework can also be extended to other ATO products in OSC.

Specific contributions of this research are as follows:

- developed a framework for automating the design and quote generation for custom windows, including developing functions and logic to govern the design and configuration processes; (this framework serves as a cornerstone for automated drafting of windows by calculating the geometric location of hardware in the design space; moreover, it can be extended to other ATO products in OSC);
- introduced geometric representations to a CPQ tool;
- pioneered the use of a CPQ tool for a construction product; and
- improved the sales process in window production by reducing non-value-adding activities in the sales and design stages and streamlining communication and the flow of information;

5.2 Research limitations

The following points are the limitations of this study:

- the framework was developed on one production line only, while this can be applied to other production lines or products, the framework must be adjusted accordingly; and
- the cost calculation was done by calculating labor hours and cost of material, disregarding shipping addresses and packaging options; and
- The time study collected was based on the assumption of no machine breakdown or absence of workers.

5.3 Recommendations for future studies

Recommendations for future work can be summarized as follows:

- incorporate the hardware coordinates into the path planning of a robotic arm for automation in hardware assembly; and
- incorporate delivery date estimation into the framework by linking the CPQ with the current status of the production line; and
- program the parametric design functions in a BIM software add-on on for automated 3D drafting.

References

- Alazzaz, F., & Whyte, A. (2014). Uptake of off-site construction: Benefit and future application. *International Journal of Civil, Architectural, Structural and Construction Engineering*, 8(12).
- Anderl, R., & Mendgen, R. (1995). Parametric design and its impact on solid modeling applications. *Proceedings of the Third ACM Symposium on Solid Modeling and Applications* (pp. 1–12).
- Arif, M., Goulding, J., & Rahimian, F. P. (2012). Promoting off-site construction: Future challenges and opportunities. *Journal of Architectural Engineering*, 18(2), 75–78. [https://doi.org/10.1061/\(asce\)ae.1943-5568.0000081](https://doi.org/10.1061/(asce)ae.1943-5568.0000081)
- Atan, Z., Ahmadi, T., Stegehuis, C., de Kok, T., & Adan, I. (2017). Assemble-to-order systems: A review. *European Journal of Operational Research*, 261(3), 866–879. <https://doi.org/10.1016/j.ejor.2017.02.029>
- Baranauskas, G., Raišienė, A. G., & Korsakienė, R. (2020). Mapping the scientific research on mass customization domain: A critical review and bibliometric analysis. *Journal of Risk and Financial Management*, 13(9), 220. <https://doi.org/10.3390/jrfm13090220>
- Batchelor, J., Land, J., & Limited, R. (2012). Bridging the product configuration gap between PLM and ERP-An automotive case study. In *19th International Product Development Management Conference, Manchester, UK* (pp. 17-19). <https://www.researchgate.net/publication/270587184>
- Blismas, N. G., Pendlebury, M., Gibb, A., & Pasquire, C. (2005). Constraints to the use of off-site production on construction projects. *Architectural Engineering and Design Management*, 1(3), 153–162. <https://doi.org/10.1080/17452007.2005.9684590>
- Bonev, M., Hvam, L., Clarkson, J., & Maier, A. (2015). Formal computer-aided product family architecture design for mass customization. *Computers in Industry*, 74, 58–70. <https://doi.org/10.1016/j.compind.2015.07.006>
- Cao, J., Bucher, D. F., Hall, D. M., & Lessing, J. (2021). Cross-phase product configurator for modular buildings using kit-of-parts. *Automation in Construction*, 123. <https://doi.org/10.1016/j.autcon.2020.103437>
- Choi, K. C., & Jarboe, T. B. (1996). Mass customization in power plant design and construction. *Power Engineering*, 100(1), 33+. <https://link.gale.com/apps/doc/A18024523/AONE?u=anon~c352c53a&sid=googleScholar&xid=8b49ba8f>
- Davis, S. M. (1987). *Future perfect*. Addison-Wesley Publ. Co.
- Elfving, J., Tommelein, I., and Ballard, G. (2002). Reducing lead time for electrical switchgear. In *Proceedings of the 10th Annual Conference of the International Group for Lean Construction (IGLC 10), Gramado, Brazil 6–8*.

- Elnaas, H., Gidado, K., & Ashton, P. (2014). Factors and drivers effecting the decision of using off-site manufacturing (OSM) systems in house building industry. *Journal of Engineering, Project, and Production Management*, 4(1), 51-58.
- Farr, E. R. P., Piroozfar, P. A. E., & Robinson, D. (2014). BIM as a generic configurator for facilitation of customisation in the AEC industry. *Automation in Construction*, 45, 119–125. <https://doi.org/10.1016/j.autcon.2014.05.012>
- Fogliatto, F. S., da Silveira, G. J. C., & Borenstein, D. (2012). The mass customization decade: An updated review of the literature. *International Journal of Production Economics*, 138(1), 14–25. <https://doi.org/10.1016/j.ijpe.2012.03.002>
- Gao, S., Jin, R., & Lu, W. (2020). Design for manufacture and assembly in construction: A review. *Building Research and Information*, 48(5), 538–550. <https://doi.org/10.1080/09613218.2019.1660608>
- Gibb, A. (1999). *Off-site fabrication: Prefabrication, pre-assembly and modularisation*. John Wiley & Sons.
- Gibb, A. G. F. (2001). Pre-assembly in construction: A review of recent and current industry and research initiatives on pre-assembly in construction. *CRISP Report, 00/19, Construction Research & Innovation Strategy Panel*.
- Gibb, A. G. F., & Isack, F. (2003). Re-engineering through pre-assembly: Client expectations and drivers. *Building Research and Information*, 31(2), 146–160. <https://doi.org/10.1080/09613210302000>
- Goodier, C., Gibb, A., Mancini, M., Turck, C., Gjepali, O., & Daniels, E. (2019). Modularisation and off-site in engineering construction: An early decision-support tool. *Proceedings of the Institution of Civil Engineers: Civil Engineering*, 172(6), 3–14. <https://doi.org/10.1680/jcien.19.00015>
- Gosling, J., Pero, M., Schoenwitz, M., Towill, D., & Cigolini, R. (2016). *Defining and categorizing modules in building projects: An international perspective*. *Journal of Construction Engineering and Management*, 142(11), 04016062. [https://doi.org/10.1061/\(ASCE\)CO.1943-7862](https://doi.org/10.1061/(ASCE)CO.1943-7862)
- Guo, L., Chen, S., Allen, J. K., & Mistree, F. (2021). A framework for designing the customer-order decoupling point to facilitate mass customization. *Journal of Mechanical Design, Transactions of the ASME*, 143(2). <https://doi.org/10.1115/1.4047684>
- Guo, S., Choi, T. M., Shen, B., & Jung, S. (2019). Inventory management in mass customization operations: A review. *IEEE Transactions on Engineering Management*, 66(3), 412–428. <https://doi.org/10.1109/TEM.2018.2839616>
- Hosseini, M. R., Martek, I., Zavadskas, E. K., Aibinu, A. A., Arashpour, M., & Chileshe, N. (2018). Critical evaluation of off-site construction research: A scientometric analysis. *Automation in Construction*, 87, 235–247. <https://doi.org/10.1016/j.autcon.2017.12.002>

- Hu, S. J. (2013). Evolving paradigms of manufacturing: From mass production to mass customization and personalization. *Procedia CIRP*, 7, 3–8. <https://doi.org/10.1016/j.procir.2013.05.002>
- Hu, X., Chong, H. Y., & Wang, X. (2019). Sustainability perceptions of off-site manufacturing stakeholders in Australia. *Journal of Cleaner Production*, 227, 346–354. <https://doi.org/10.1016/j.jclepro.2019.03.258>
- James, C. D., & Mondal, S. (2021). Optimization of decoupling point position using metaheuristic evolutionary algorithms for smart mass customization manufacturing. *Neural Computing and Applications*, 33(17), 11125–11155. <https://doi.org/10.1007/s00521-020-05657-1>
- Jang, J., Ahn, S., Cha, S. H., Cho, K., Koo, C., & Kim, T. W. (2021). Toward productivity in future construction: Mapping knowledge and finding insights for achieving successful off-site construction projects. *Journal of Computational Design and Engineering*, 8(1). Oxford University Press. <https://doi.org/10.1093/jcde/qwaa071>
- Jensen, P., Lidelöw, H., & Olofsson, T. (2015). Product configuration in construction. *International Journal of Mass Customisation*, 5(1), 73. <https://doi.org/10.1504/ijmassc.2015.069601>
- Jordan, M., Auth, G., Jokisch, O., & Kühn, J.-U. (2020). Knowledge-based systems for the configure price quote (CPQ) process-A case study in the IT solution business. *Online Journal of Applied Knowledge Management A Publication of the International Institute for Applied Knowledge Management*, 8(2).
- Kaplan, A., Haenlein, M. (2006). Toward a parsimonious definition of traditional and electronic mass customization. *Journal of Product Innovation Management* 23(2), 168–182.
- Kristianto, Y., Helo, P., & Jiao, R. J. (2015). A system level product configurator for engineer-to-order supply chains. *Computers in Industry*, 72, 82–91. <https://doi.org/10.1016/j.compind.2015.04.004>
- Larsen, M. S., Lindhard, S. M., Brunoe, T. D., Nielsen, K., & Larsen, J. K. (2019). Mass customization in the house building industry: Literature review and research directions. *Frontiers in Built Environment*, 5. <https://doi.org/10.3389/fbuil.2019.00115>
- Lim, E. C., & Alum, J. (1995). Construction productivity: issues encountered by contractors in Singapore. *International Journal of Project Management*, 13(1).
- MacCarthy, B., Brabazon, P., Bramham, J., (2003). Fundamental modes of operation for mass customization. *International Journal of Production Economics*, 85(3), 289–304.
- McCarthy, I. P. (2004). Special issue editorial: The what, why and how of mass customization. *Production Planning and Control*, 15(4), 347–351. <https://doi.org/10.1080/0953728042000238854>
- McKinsey Global Institute. (2017). *Reinventing Construction: A route to higher productivity*.

- Mello, M. H., Strandhagen, J. O., & Alfnes, E. (2015). Analyzing the factors affecting coordination in engineer-to-order supply chain. *International Journal of Operations and Production Management*, 35(7), 1005–1031. <https://doi.org/10.1108/IJOPM-12-2013-0545>
- Monedero, J. (2000). Parametric design: a review and some experiences. *Automation in construction*, 9(4), 369-377.
- Monizza, G. P., & Matt, D. T. (2022). Mass customization as the convergent vision for the digital transformation of the manufacturing and the building industry. In *Rethinking Building Skins* (pp. 453–474). Woodhead Publishing. <https://doi.org/10.1016/b978-0-12-822477-9.00006-1>
- Mourlas, C., & Germanakos, P. (2009). *Mass customization for personalized communication environments: Integrating human factors*. IGI Global.
- Näsi, A. (2020). *Enhancing sales & product management with CPQ systems*.
- Nahm, Y. E., & Ishikawa, H. (2006). A new 3D-CAD system for set-based parametric design. *The International Journal of Advanced Manufacturing Technology*, 29(1), 137-150.
- Noergaard, K., Pero, M., Nielsen, K., & Brunoe, T. D. (2020). Applying and developing mass customization in construction industries – A multi case study. *International Journal of Construction Supply Chain Management*, 10(3), 141–171. <https://doi.org/10.14424/ijscsm100320-141-171>
- Olhager, J. (2010). The role of the customer order decoupling point in production and supply chain management. *Computers in Industry*, 61(9), 863–868. <https://doi.org/10.1016/j.compind.2010.07.011>
- Paniquar De Souto, A. (2020). *Simulation-based approach to improving Overall Equipment Effectiveness analysis in construction manufacturing*. [Master's thesis, University of Alberta]. <https://doi.org/10.7939/r3-zte9-xj59>
- Piller, F. T. (2007). Observations on the present and future of mass customization. *International Journal of Flexible Manufacturing Systems*, 19(4), 630–636. <https://doi.org/10.1007/s10696-008-9042-z>
- Poot, L. P., Wehlin, C., Tarkian, M., & Ölvander, J. (2020). Integrating sales and design: applying CAD configurators in the product development process. *Proceedings of the Design Society: DESIGN Conference* (Vol. 1, pp. 345–354). Cambridge University Press.
- Popovic, D. (2018). *Off-site manufacturing systems development in timber house building: Towards mass customization-oriented manufacturing* [Doctoral dissertation, Jönköping University, School of Engineering].
- Roberts, M (2003). *Internet marketing: Integrating online and offline strategies*. McGraw-Hill/Irwin.
- Rudberg, M., & Wikner, J. (2004). Mass customization in terms of the customer order decoupling point. *Production Planning and Control*, 15(4), 445–458. <https://doi.org/10.1080/0953728042000238764>

- Schoenwitz, M., Naim, M., & Potter, A. (2012). The nature of choice in mass customized house building. *Construction Management and Economics*, 30(3), 203–219. <https://doi.org/10.1080/01446193.2012.664277>
- Sorokovaia, E. (2019). *Efficient application of configuration and pricing technologies to industrial service products at Valmet Technologies Oy* [Bachelor's thesis, JAMK University of Applied Sciences Jyväskylä].
- Sorri, K., Kumpulainen, M., Seppänen, M., Dunne, M., & Huittinen, K. (2017). *Prospects of CPQ: Evolving toward industry platforms*. In *IWSECO* (pp. 3-15).
- Suzić, N., Forza, C., Trentin, A., & Anišić, Z. (2018). Implementation guidelines for mass customization: Current characteristics and suggestions for improvement. *Production Planning and Control*, 29(10), 856–871. <https://doi.org/10.1080/09537287.2018.1485983>
- Trentin, A., Perin, E., & Forza, C. (2014). Increasing the consumer-perceived benefits of a mass-customization experience through sales-configurator capabilities. *Computers in Industry*, 65(4), 693–705. <https://doi.org/10.1016/j.compind.2014.02.004>
- Tseng, M. M., & Jiao, J. (1996). *Design for Mass Customization*. *CIRP annals*, 45(1), 153-156. [https://doi.org/10.1016/S0007-8506\(07\)63036-4](https://doi.org/10.1016/S0007-8506(07)63036-4)
- Vesänen, J. (2005). *What is personalization? A literature review and framework*.
- Viana, D. D., Tommelein, I. D., & Formoso, C. T. (2017). Using modularity to reduce complexity of industrialized building systems for mass customization. *Energies*, 10(10). <https://doi.org/10.3390/en10101622>
- Wang, M. (2021). *Windows Hardware Installation Production Line Improvement* [Master's Thesis, University of Alberta].
- Wang, M., Wang, C. C., Sepasgozar, S., & Zlatanova, S. (2020). A systematic review of digital technology adoption in off-site construction: Current status and future direction towards industry 4.0. *Buildings*, 10(11) 204. <https://doi.org/10.3390/buildings10110204>
- Wehlin, C., Vidner, O., Poot, L., & Tarkian, M. (2021). Integrating sales, design and production: A configuration system for automation in mass customization. In *International Design Engineering Technical Conferences and Computers and Information in Engineering Conference*. <https://doi.org/10.1115/DETC2021-68426>
- Wortmann, J. C. (1983). A classification scheme for master production scheduling. *Efficiency of Manufacturing Systems*, 101–109. https://doi.org/10.1007/978-1-4684-4475-9_10
- Xia, S. S., & Wang, L. Y. (2008). Customer requirements mapping method based on association rule mining for mass customization. *Journal of Shanghai Jiaotong University (Science)*, 13 (3), 291–296. <https://doi.org/10.1007/s12204-008-0291-5>
- Xu, X. G. (2007). Position of customer order decoupling point in mass customization. In *2007 International Conference on Machine Learning and Cybernetics 1*, 302-307. IEEE.

<https://doi.org/10.1109/ICMLC.2007.4370159> Yan, Y., Gupta, S., Schoefer, K., & Licsandru, T. (2020). A review of e-mass customization as a branding strategy. *Corporate Reputation Review*, 23(3), 215–223. <https://doi.org/10.1057/s41299-019-00087-9> Zhang, C., Chen, D., Tao, F., & Liu, A. (2019). Data driven smart customization. *Procedia CIRP*, 81, 564–569. <https://doi.org/10.1016/j.procir.2019.03.156>

Appendix A: Hardware design for casement windows

1. Tie-bar

Tie-bars are placed on the sides of the window. Its purpose is to help secure locking the window from opening along with tie-bar rollers and keepers, as shown in Figure A.1: Tie-bar rollers and guides CAD details. Its length depends on the height of the window as it must follow the following equation.

$$l_{tb} = \begin{cases} 230 + \sum_{j=1}^{n-1} H_{w,CiRj} + M_{cj}, & 350 \leq H_w < 500 \\ [H_w - 400] + 230 + \sum_{j=1}^{n-1} H_{w,CiRj} + M_{cj}, & H_w \geq 500 \end{cases} \quad (\text{A.1-1})$$

Tie-bar location along the X -axis:

$$X_{ts \rightarrow LH} = X_{tf} = f(P_w) = P_w + \sum_{i=1}^{n-1} W_{w,CiRj} + M_{ci} \quad (\text{A.1-2})$$

$$X_{ts \rightarrow RH} = X_{tf \rightarrow RH} = f(W_w, P_w) = W_w - P_w + \sum_{i=1}^{n-1} W_{w,CiRj} + M_{ci} \quad (\text{A.1-3})$$

Tie-bar location along the Y -axis:

$$Y_{ts \rightarrow LH} = Y_{ts \rightarrow RH} = f(T_s) = T_s + \sum_{j=1}^{n-1} H_{w,CiRj} + M_{cj} \quad (\text{A.1-4})$$

$$Y_{tf \rightarrow LH} = Y_{ts \rightarrow LH} + l_{tb} \quad (\text{A.1-5})$$

$$Y_{tf \rightarrow RH} = Y_{ts \rightarrow RH} + l_{tb} \quad (\text{A.1-6})$$

Tie-bar location along the Z -axis:

$$Z_{tl} = 16.5 \quad (\text{A.1-7})$$

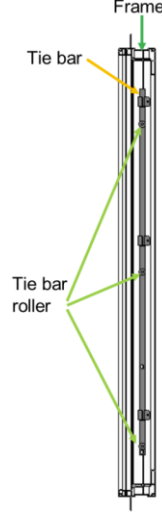


Figure A.1: Tie-bar rollers and guides CAD details

1.1 Tie-bar rollers

The quantity of tie-bar rollers is determined based on the height of the window and satisfies the following equation:

$$N_r = \begin{cases} 1, & H_w < 500 \\ 2, & 500 \leq H_w < 900 \\ 3, & 900 \leq H_w < 1,200 \\ 4, & 1,200 \leq H_w < 1,700 \\ 5, & 1,700 \leq H_w < 2,100 \end{cases} \quad (\text{A.1-8})$$

The locations of the tie-bar rollers along the X -axis satisfy:

$$A = \{1, 2, \dots, \alpha\}$$

$$X_{r\alpha \rightarrow LH} | \forall \alpha \in A, X_{r\alpha \rightarrow LH} = P_w + \sum_{i=1}^{n-1} W_{w,CiRj} + M_{ci} \quad (\text{A.1-9})$$

$$X_{r\alpha \rightarrow RH} | \forall \alpha \in A, X_{r\alpha \rightarrow RH} = W_w - P_w + \sum_{i=1}^{n-1} W_{w,CiRj} + M_{ci} \quad (\text{A.1-10})$$

The locations of the tie-bar rollers along the Y -axis satisfy:

$$Y_{r1 \rightarrow LH} = T_s + r_{ts} + \sum_{j=1}^{n-1} H_{w,CiRj} + M_{cj} \quad (\text{A.1-11})$$

$$Y_{r2 \rightarrow LH} = \begin{cases} l_{tb} - r_{tf} + T_s + \sum_{j=1}^{n-1} H_{w,CiRj} + M_{cj}, & N_r = 2 \\ \frac{l_{tb}}{N_r - 1} + T_s + \sum_{j=1}^{n-1} H_{w,CiRj} + M_{cj}, & N_r = 3 \cup N_r = 4 \\ \frac{l_{tb} - (r_{ts} + r_{tf})}{N_r - 1} + T_s + r_{ts} + \sum_{j=1}^{n-1} H_{w,CiRj} + M_{cj}, & N_r = 5 \end{cases} \quad (\text{A.1-12})$$

$$Y_{r3 \rightarrow LH} = \begin{cases} l_t - r_{tf} + T_s + \sum_{j=1}^{n-1} H_{w,CiRj} + M_{cj}, N_r = 3 \\ \frac{l_t}{N_r-1} \times 2 + T_s + \sum_{j=1}^{n-1} H_{w,CiRj} + M_{cj}, N_r = 4 \\ \frac{l_t - (r_{ts} + r_{tf})}{N_r-1} \times 2 + T_s + r_{ts} + \sum_{j=1}^{n-1} H_{w,CiRj} + M_{cj}, N_r = 5 \end{cases} \quad (\text{A.1-13})$$

$$Y_{r4 \rightarrow LH} = \begin{cases} l_t - r_{tf} + T_s + \sum_{j=1}^{n-1} H_{w,CiRj} + M_{cj}, N_r = 4 \\ \frac{l_{tb} - (r_{ts} + r_{tf})}{N_r-1} \times 3 + T_s + r_{ts} + \sum_{j=1}^{n-1} H_{w,CiRj} + M_{cj}, N_r = 5 \end{cases} \quad (\text{A.1-14})$$

$$Y_{r5 \rightarrow LH} = l_t - r_{tf} + T_s + \sum_{j=1}^{n-1} H_{w,CiRj} + M_{cj}, N_r = 5 \quad (\text{A.1-15})$$

$$Y_{r\alpha \rightarrow RH} | \forall \alpha \in A, Y_{r\alpha \rightarrow RH} = Y_{r\alpha \rightarrow LH} \quad (\text{A.1-16})$$

The locations of the tie-bar rollers along the Z -axis satisfy:

$$Z_{rr\alpha} | \forall \alpha \in A, Z_{rr\alpha} = 16.5 \quad (\text{A.1-17})$$

1.2 Tie-bar guides

The tie-bar guide serves the function of securing the tie-bar to the frame. Figure 24 shows the tie-bar guide.

The quantity of tie-bar guides used is governed by the following equation:

$$N_g = N_r = f(H_w) = \begin{cases} 1, H_w < 500 \\ 2, 500 \leq H_w < 900 \\ 3, 900 \leq H_w < 1,200 \\ 4, 1,200 \leq H_w < 1,700 \\ 5, 1,700 \leq H_w < 2,100 \end{cases} \quad (\text{A.1-18})$$

$$A = \{1, 2, \dots, \alpha\}$$

The locations of the tie-bar guides along the X -axis satisfy:

$$X_{g\alpha \rightarrow LH} | \forall \alpha \in A, X_{g\alpha \rightarrow LH} = P_w + \sum_{i=1}^{n-1} W_{w,CiRj} + M_{ci} \quad (\text{A.1-19})$$

$$X_{g\alpha \rightarrow RH} | \forall \alpha \in A, X_{g\alpha \rightarrow RH} = f(W_w, P_w) = W_w - P_w + \sum_{i=1}^{n-1} W_{w,CiRj} + M_{ci} \quad (\text{A.1-20})$$

The locations of the tie-bar guides along the Y -axis satisfy:

$$Y_{g\alpha \rightarrow LH} = \begin{cases} Y_{r\alpha} + d_{rg1} + \sum_{j=1}^{n-1} H_{w,CiRj} + M_{cj}, \alpha < N_g \cup N_g = 1 \\ Y_{r\alpha} + d_{rg2} + \sum_{j=1}^{n-1} H_{w,CiRj} + M_{cj}, \alpha = N_g \cap N_g > 1 \end{cases} \quad (\text{A.1-21})$$

$$Y_{g\alpha \rightarrow RH} | \forall \alpha \in A, Y_{g\alpha \rightarrow RH} = Y_{g\alpha \rightarrow LH} \quad (\text{A.1-22})$$

The locations of the tie-bar guides along the Z-axis satisfy:

$$Z_{gr\alpha} | \forall \alpha \in A, Z_{gr\alpha} = 20.1 \quad (\text{A.1-23})$$

The details of the equations and the link between the rollers and the guides are illustrated in Figure A.2

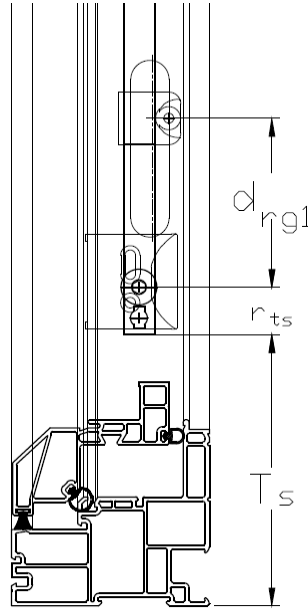


Figure A.2: Tie-bar rollers and guides CAD details

1.3 Tie-bar keepers

The tie-bar keepers are used to lock the window along with the tie-bar. The quantity of tie-bar keepers is determined using the following equation:

$$N_k = N_r = \begin{cases} 1, & H_w < 500 \\ 2, & 500 \leq H_w < 900 \\ 3, & 900 \leq H_w < 1,200 \\ 4, & 1,200 \leq H_w < 1,700 \\ 5, & 1,700 \leq H_w < 2,100 \end{cases} \quad (\text{A.1-24})$$

Moreover, like the locations of the guides, the locations of the keepers are governed by the locations of the tie-bar rollers, where the tie-bar keeper locations along the X-axis satisfy the following equations:

$$A = \{1, 2, \dots, \alpha\}$$

$$X_{k\alpha \rightarrow LH} | \forall \alpha \in A, X_{k\alpha \rightarrow LH} = F_w + \sum_{i=1}^{n-1} W_{w,CiRj} + M_{ci} \quad (\text{A.1-25})$$

$$X_{k\alpha \rightarrow RH} | \forall \alpha \in A, X_{k\alpha \rightarrow RH} = W_w - F_w + \sum_{i=1}^{n-1} W_{w,CiRj} + M_{ci} \quad (\text{A.1-26})$$

Tie-bar keeper locations along the Y -axis satisfy the following equations:

$$Y_{k1 \rightarrow LH} = T_s + r_{ts} + d_k + \sum_{j=1}^{n-1} H_{w,CiRj} + M_{cj} \quad (\text{A.1-27})$$

$$Y_{k2 \rightarrow LH} = \begin{cases} l_{tb} - r_{tf} + T_s + d_k + \sum_{j=1}^{n-1} H_{w,CiRj} + M_{cj}, N_r = 2 \\ \frac{l_{tb}}{N_r-1} + T_s + d_k + \sum_{j=1}^{n-1} H_{w,CiRj} + M_{cj}, N_r = 3 \cup N_r = 4 \\ \frac{l_{tb} - (r_{ts} + r_{tf})}{N_r-1} + T_s + d_k + r_{ts} + \sum_{j=1}^{n-1} H_{w,CiRj} + M_{cj}, N_r = 5 \end{cases} \quad (\text{A.1-28})$$

$$Y_{k3 \rightarrow LH} = \begin{cases} l_t - r_{tf} + T_s + d_k + \sum_{j=1}^{n-1} H_{w,CiRj} + M_{cj}, N_r = 3 \\ \frac{l_t}{N_r-1} \times 2 + T_s + d_k + \sum_{j=1}^{n-1} H_{w,CiRj} + M_{cj}, N_r = 4 \\ \frac{l_t - (r_{ts} + r_{tf})}{N_r-1} \times 2 + T_s + d_k + r_{ts} + \sum_{j=1}^{n-1} H_{w,CiRj} + M_{cj}, N_r = 5 \end{cases} \quad (\text{A.1-29})$$

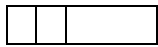
$$Y_{k4 \rightarrow LH} = \begin{cases} l_t - r_{tf} + T_s + d_k + \sum_{j=1}^{n-1} H_{w,CiRj} + M_{cj}, N_r = 4 \\ \frac{l_{tb} - (r_{ts} + r_{tf})}{N_r-1} \times 3 + T_s + d_k + r_{ts} + \sum_{j=1}^{n-1} H_{w,CiRj} + M_{cj}, N_r = 5 \end{cases} \quad (\text{A.1-30})$$

$$Y_{k5 \rightarrow LH} = l_{tb} - r_{tf} + T_s + d_k + \sum_{j=1}^{n-1} H_{w,CiRj} + M_{cj}, N_r = 5 \quad (\text{A.1-31})$$

$$Y_{k\alpha \rightarrow RH} | \forall \alpha \in A, Y_{k\alpha \rightarrow RH} = Y_{k\alpha \rightarrow LH} \quad (\text{A.1-32})$$

Tie-bar keeper locations along the Z -axis satisfy the following equations:

$$Z_{k\alpha} | \forall \alpha \in A, Z_{k\alpha} = 23.2 \quad (\text{A.1-33})$$



Locations of tie-bar keeper screws along the X -axis satisfy the following equations:

$$B = \{1, 2, \dots, \beta\}$$

$$X_{k\beta \rightarrow LH} | \forall \beta \in B, X_{k\beta \rightarrow LH} = F_w + \sum_{i=1}^{n-1} W_{w,CiRj} + M_{ci} \quad (\text{A.1-34})$$

$$X_{k\beta \rightarrow RH} | \forall \beta \in B, X_{k\beta \rightarrow RH} = W_w - F_w + \sum_{i=1}^{n-1} W_{w,CiRj} + M_{ci} \quad (\text{A.1-35})$$

Tie-bar keeper screw locations along the Y -axis satisfy the following equations:

$$Y_{ksc1 \rightarrow LH} = Y_{kl\alpha} - \delta_{kl1} \quad (\text{A.1-36})$$

$$Y_{ksc2 \rightarrow LH} = Y_{kl\alpha} + \delta_{kl2} \quad (\text{A.1-37})$$

$$Y_{ksc3 \rightarrow LH} = Y_{kl\alpha} + \delta_{kl3} \quad (\text{A.1-38})$$

$$Y_{ksc\beta \rightarrow RH} | \forall \beta \in A, Y_{ksc\beta \rightarrow RH} = Y_{ksc\beta \rightarrow LH} \quad (\text{A.1-39})$$

Tie-bar keeper screw locations along the Z -axis satisfy the following equations:

$$Z_{ksc\beta} | \forall \alpha \in A, Z_{ksc\beta} = 23.2 \quad (\text{A.1-40})$$

2. Hinge selection

2.1. Hinge track and screw locations

The selection of the hinge track depends on the width of the window and satisfies the following equation:

$$\text{Hinge Type } (L) = \begin{cases} 10" \text{ standard hinge, } 350 \leq W_w < 600 \\ 13" \text{ standard hinge, } 600 \leq W_w \leq 950 \\ 10" \text{ egress hinge, Egress} \end{cases} \quad (\text{A.2-1})$$

2.2. Hinge track and screw locations

Hinge track location along the X -axis satisfies the following equations:

$$X_{hts \rightarrow C-RH} = P_w + \sum_{i=1}^{n-1} W_{w,CiRj} + M_{ci} \quad (\text{A.2-2})$$

$$X_{htf \rightarrow C-RH} = P_w + L + \sum_{i=1}^{n-1} W_{w,CiRj} + M_{ci} \quad (\text{A.2-3})$$

$$X_{hts \rightarrow C-LH} = W_w - P_w + \sum_{i=1}^{n-1} W_{w,CiRj} + M_{ci} \quad (\text{A.2-4})$$

$$X_{htf \rightarrow C-LH} = W_w - P_w - L + \sum_{i=1}^{n-1} W_{w,CiRj} + M_{ci} \quad (\text{A.2-5})$$

Hinge track location along the Y -axis satisfies the following equations:

$$Y_{hts \rightarrow C-RH} = P_w + \sum_{j=1}^{n-1} H_{w,CiRj} + M_{cj} \quad (\text{A.2-6})$$

$$Y_{htf \rightarrow C-RH} = Y_{hts \rightarrow C-RH} \quad (\text{A.2-7})$$

$$Y_{hts \rightarrow C-LH} = P_w + \sum_{j=1}^{n-1} H_{w,CiRj} + M_{cj} \quad (\text{A.2-8})$$

$$Y_{htf \rightarrow C-LH} = Y_{hts \rightarrow C-RH} \quad (\text{A.2-9})$$

Hinge track location along the Z -axis satisfies the following equations:

$$Z_{ht} = 54 \quad (\text{A.2-10})$$

RH hinge track screw locations along the X -axis satisfy the following equations:

$$B = \{1, 2, \dots, \beta\}$$

$$X_{htsc1 \rightarrow C-RH} = P_w + \delta_{t1} \sum_{i=1}^{n-1} W_{w,CiRj} + M_{ci} \quad (\text{A.2-11})$$

$$X_{htsc2 \rightarrow C-RH} = \delta_{t1} + \delta_{t2} + P_w + \sum_{i=1}^{n-1} W_{w,CiRj} + M_{ci} \quad (\text{A.2-12})$$

$$X_{htsc3 \rightarrow C-RH} = \begin{cases} P_w + \delta_{t1} + \delta_{t3s10} + \sum_{i=1}^{n-1} W_{w,CiRj} + M_{ci}, & 350 \leq W_w < 600 \\ P_w + \delta_{t1} + \delta_{t3s13} + \sum_{i=1}^{n-1} W_{w,CiRj} + M_{ci}, & 600 \leq W_w \leq 950 \\ P_w + \delta_{t1} + \delta_{t3e} + \sum_{i=1}^{n-1} W_{w,CiRj} + M_{ci}, & 10'' \text{ egress hinge} \end{cases} \quad (\text{A.2-13})$$

$$X_{htsc4 \rightarrow C-RH} = P_w + \delta_{t1} + \delta_{t3} + \sum_{i=1}^{n-1} W_{w,CiRj} + M_{ci}, \quad 600 \leq W_w \leq 950 \quad (\text{A.2-14})$$

LH hinge track screw locations along the X -axis satisfy the following equations:

$$X_{htsc1 \rightarrow C-LH} = W_w - P_w - \delta_{t1} \sum_{i=1}^{n-1} W_{w,CiRj} + M_{ci} \quad (\text{A.2-15})$$

$$X_{htsc2 \rightarrow C-LH} = W_w - P_w - \delta_{t1} - \delta_{t2} + \sum_{i=1}^{n-1} W_{w,CiRj} + M_{ci} \quad (\text{A.2-16})$$

$$X_{htsc3 \rightarrow C-LH} = \begin{cases} W_w - P_w - \delta_{t1} - \delta_{t3s10} + \sum_{i=1}^{n-1} W_{w,CiRj} + M_{ci}, & 350 \leq W_w < 600 \\ W_w - P_w - \delta_{t1} - \delta_{t3s13} + \sum_{i=1}^{n-1} W_{w,CiRj} + M_{ci}, & 600 \leq W_w \leq 950 \\ W_w - P_w - \delta_{t1} - \delta_{t3e} + \sum_{i=1}^{n-1} W_{w,CiRj} + M_{ci}, & 10'' \text{ egress hinge} \end{cases} \quad (\text{A.2-17})$$

$$X_{htsc4 \rightarrow C-LH} = W_w - P_w - \delta_{t1} - \delta_{t3} + \sum_{i=1}^{n-1} W_{w,CiRj} + M_{ci}, \quad 600 \leq W_w \leq 950 \quad (\text{A.2-18})$$

Hinge track screw locations along the Y -axis satisfy the following equations:

$$Y_{htsc\beta \rightarrow C} | \forall \beta \in B, Y_{htsc\beta \rightarrow C} = P_w + \sum_{i=1}^{n-1} W_{w,CiRj} + M_{ci} \quad (\text{A.2-19})$$

Hinge track screw locations along the Z -axis satisfy the following equations:

$$Z_{htsc} = 54 \quad (\text{A.2-20})$$

3. Operator screws

Location of operator screws along the X -axis satisfies the following equations:

$$X_{osc1 \rightarrow C-RH} = f(x) = \begin{cases} \delta_{cosc1}, & 350 \leq W_w < 500 \cup Egress \\ \delta_{cosc2}, & 500 \leq W_w < 600 \\ \delta_{cosc3}, & 600 \leq W_w \leq 950 \end{cases} \quad (A.3-1)$$

$$X_{osc2 \rightarrow C-RH} = X_{osc1 \rightarrow C-RH} + \delta_{cos1} + \sum_{i=1}^{n-1} W_{w,CiRj} + M_{ci} \quad (A.3-2)$$

$$X_{osc3 \rightarrow C-RH} = X_{osc1 \rightarrow C-RH} + \delta_{cos2} + \sum_{i=1}^{n-1} W_{w,CiRj} + M_{ci} \quad (A.3-3)$$

$$X_{osc4 \rightarrow C-RH} = X_{osc1 \rightarrow C-RH} + \delta_{cos3} + \sum_{i=1}^{n-1} W_{w,CiRj} + M_{ci} \quad (A.3-4)$$

$$X_{osc5 \rightarrow C-RH} = X_{osc1 \rightarrow C-RH} + \delta_{cos4} + \sum_{i=1}^{n-1} W_{w,CiRj} + M_{ci} \quad (A.3-5)$$

$$X_{osc6 \rightarrow C-RH} = X_{osc1 \rightarrow C-RH} + \delta_{cos5} + \sum_{i=1}^{n-1} W_{w,CiRj} + M_{ci} \quad (A.3-6)$$

$$X_{osc1 \rightarrow C-LH} = \begin{cases} W_w - \delta_{cosc1}, & 350 \leq W_w < 500 \cup Egress \\ W_w - \delta_{cosc2}, & 500 \leq W_w < 600 \\ W_w - \delta_{cosc3}, & 600 \leq W_w \leq 950 \end{cases} \quad (A.3-7)$$

$$X_{osc2 \rightarrow C-LH} = X_{osc1 \rightarrow C-LH} - \delta_{cos1} + \sum_{i=1}^{n-1} W_{w,CiRj} + M_{ci} \quad (A.3-8)$$

$$X_{osc3 \rightarrow C-LH} = X_{osc1 \rightarrow C-LH} - \delta_{cos2} + \sum_{i=1}^{n-1} W_{w,CiRj} + M_{ci} \quad (A.3-9)$$

$$X_{osc4 \rightarrow C-LH} = X_{osc1 \rightarrow C-LH} - \delta_{cos3} + \sum_{i=1}^{n-1} W_{w,CiRj} + M_{ci} \quad (A.3-10)$$

$$X_{osc5 \rightarrow C-LH} = X_{osc1 \rightarrow C-LH} - \delta_{cos4} + \sum_{i=1}^{n-1} W_{w,CiRj} + M_{ci} \quad (A.3-11)$$

$$X_{osc6 \rightarrow C-LH} = X_{osc1 \rightarrow C-LH} - \delta_{cos5} + \sum_{i=1}^{n-1} W_{w,CiRj} + M_{ci} \quad (A.3-12)$$

Location of operator screws along the Y -axis satisfies the following equations:

$$Y_{osc\beta \rightarrow C-LH} = Y_{osc\beta \rightarrow C-RH} = \begin{cases} \delta_{cosy1} + \sum_{j=1}^{n-1} H_{w,CiRj} + M_{cj}, & 350 \leq W_w < 600 \\ \delta_{cosy2} + \sum_{j=1}^{n-1} H_{w,CiRj} + M_{cj}, & 600 \leq W_w \leq 950 \end{cases} \quad (A.3-13)$$

Location of operator screws along the Z -axis satisfies the following equations:

$$Z_{osc\beta \rightarrow C} = 26.4 \quad (A.3-14)$$

4. Operator bracket

The selection of the operator's bracket is a function of the width of the window

$$Bracket\ type = \begin{cases} \text{Dyad Operator Bracket, } 350 \leq W_w < 500 \\ N/A, 500 \leq W_w < 600 \\ \text{Operator Bracket, } 600 \leq W_w \leq 950 \end{cases} \quad (A.4-1)$$

The location of the selected bracket along the X -axis satisfies the following equations:

$$X_{br \rightarrow C-LH} = \begin{cases} P_w + d_{cdb} + \sum_{i=1}^{n-1} W_{w,CiRj} + M_{ci}, & 350 \leq W_w < 500 \\ W_w - F_w - d_{cob} + \sum_{i=1}^{n-1} W_{w,CiRj} + M_{ci}, & 600 \leq W_w \leq 950 \end{cases} \quad (A.4-2)$$

$$X_{br \rightarrow C-RH} = \begin{cases} W_w - P_w - d_{cdb} + \sum_{i=1}^{n-1} W_{w,CiRj} + M_{ci}, & 350 \leq W_w < 500 \\ F_w + d_{cob} + \sum_{i=1}^{n-1} W_{w,CiRj} + M_{ci}, & 600 \leq W_w \leq 950 \end{cases} \quad (A.4-3)$$

The location of the selected bracket along the Y -axis satisfies the following equations:

$$Y_{br \rightarrow C-LH} = Y_{br \rightarrow C-RH} = \begin{cases} \delta_{cosy1} + \sum_{j=1}^{n-1} H_{w,CiRj} + M_{cj}, & 350 \leq W_w < 600 \\ \delta_{cosy2} + \sum_{j=1}^{n-1} H_{w,CiRj} + M_{cj}, & 600 \leq W_w \leq 950 \end{cases} \quad (A.4-4)$$

The location of the selected bracket along the Z -axis satisfies the following equations:

$$Z_{br \rightarrow C} = \begin{cases} 42.3, & 350 \leq W_w < 600 \\ 41.6, & 600 \leq W_w \leq 950 \end{cases} \quad (A.4-5)$$

Location of the casement operator bracket screws along the X -axis satisfies the following equations:

$$X_{brsc1 \rightarrow C-LH} = \begin{cases} P_w + d_{cdb} - 2 \times \delta_{cbcs} + \sum_{i=1}^{n-1} W_{w,CiRj} + M_{ci}, & 350 \leq W_w < 500 \\ W_w - F_w - d_{cob} + \delta_{u1} + \sum_{i=1}^{n-1} W_{w,CiRj} + M_{ci}, & 600 \leq W_w \leq 950 \end{cases} \quad (A.4-6)$$

$$X_{brsc2 \rightarrow C-LH} = \begin{cases} P_w + d_{cdb} - \delta_{cbcs} + \sum_{i=1}^{n-1} W_{w,CiRj} + M_{ci}, & 350 \leq W_w < 500 \\ W_w - F_w - d_{cob} - \delta_{u2} + \sum_{i=1}^{n-1} W_{w,CiRj} + M_{ci}, & 600 \leq W_w \leq 950 \end{cases} \quad (A.4-7)$$

$$X_{brsc3 \rightarrow C-LH} = P_w + d_{cdb} + \delta_{cbcs} + \sum_{i=1}^{n-1} W_{w,CiRj} + M_{ci}, \quad 350 \leq W_w < 500 \quad (A.4-8)$$

$$X_{brsc4 \rightarrow C-LH} = P_w + d_{cdb} + 2 \times \delta_{cbcs} + \sum_{i=1}^{n-1} W_{w,CiRj} + M_{ci}, \quad 350 \leq W_w < 500 \quad (A.4-9)$$

$$X_{brsc1 \rightarrow C-RH} = \begin{cases} W_w - (P_w + d_{cdb} - 2 \times \delta_{cbsc}) + \sum_{i=1}^{n-1} W_{w,CiRj} + M_{ci}, & 350 \leq W_w < 500 \\ F_w + d_{cob} - \delta_{u1} + \sum_{i=1}^{n-1} W_{w,CiRj} + M_{ci}, & 600 \leq W_w \leq 950 \end{cases} \quad (\text{A.4-10})$$

$$X_{brsc2 \rightarrow C-RH} = \begin{cases} W_w - (P_w + d_{cdb} - \delta_{cbsc}) + \sum_{i=1}^{n-1} W_{w,CiRj} + M_{ci}, & 350 \leq W_w < 500 \\ F_w + d_{cob} + \delta_{u2} + \sum_{i=1}^{n-1} W_{w,CiRj} + M_{ci}, & 600 \leq W_w \leq 950 \end{cases} \quad (\text{A.4-11})$$

$$X_{brsc3 \rightarrow C-RH} = W_w - (P_w + d_{cdb} + \delta_{cbsc}) + \sum_{i=1}^{n-1} W_{w,CiRj} + M_{ci}, \quad 350 \leq W_w < 500 \quad (\text{A.4-12})$$

$$X_{brsc4 \rightarrow C-RH} = W_w - (P_w + d_{cdb} + 2 \times \delta_{cbsc}) + \sum_{i=1}^{n-1} W_{w,CiRj} + M_{ci}, \quad 350 \leq W_w < 500 \quad (\text{A.4-13})$$

Location of the casement operator bracket screws along the Y -axis satisfies the following equations:

$$Y_{brsc\beta \rightarrow C-LH} = Y_{brsc\beta \rightarrow C-RH} = \begin{cases} \delta_{cosy1} + \sum_{j=1}^{n-1} H_{w,CiRj} + M_{cj}, & 350 \leq W_w < 600 \\ \delta_{cosy2} + \sum_{j=1}^{n-1} H_{w,CiRj} + M_{cj}, & 600 \leq W_w \leq 950 \end{cases} \quad (\text{A.4-14})$$

Location of the casement operator bracket screws along the Z -axis satisfies the following equations:

$$Z_{brsc\beta \rightarrow C} | \forall \beta \in B, Z_{brsc\beta \rightarrow C} = \begin{cases} 51.7, & 350 \leq W_w < 600 \\ 52.3, & 600 \leq W_w \leq 950 \end{cases} \quad (\text{A.4-15})$$

5. Snubber quantity and locations on frame

The quantity of snubbers used is a function of the window's height, since the snubber's purpose is to prevent bowing of tall casement windows.

$$N_s = \begin{cases} 1, & 400 \leq H_w < 1,200 \\ 2, & 1,200 \leq H_w \leq 1,900 \\ 3, & H_w > 1,900 \end{cases} \quad (\text{A.5-1})$$

The snubber locations along the X -axis satisfy the following equations:

$$A = \{1, 2, \dots, \alpha\}$$

$$X_{s\alpha \rightarrow C-LH} | \forall \alpha \in A, X_{s\alpha \rightarrow C-LH} = P_s + \sum_{i=1}^{n-1} W_{w,CiRj} + M_{ci} \quad (\text{A.5-2})$$

$$X_{s\alpha \rightarrow C-RH} | \forall \alpha \in A, X_{s\alpha \rightarrow C-RH} = f(d_s) = W_w - P_s + \sum_{i=1}^{n-1} W_{w,CiRj} + M_{ci} \quad (\text{A.5-3})$$

The snubber locations along the Y-axis satisfy the following equations:

$$Y_{s1 \rightarrow C-LH} = (H_w - d_s \times 2) / (N_s + 1) + d_s + \sum_{j=1}^{n-1} H_{w,CiRj} + M_{cj} \quad (\text{A.5-4})$$

$$Y_{s2 \rightarrow C-LH} = 2 \times (H_w - d_s \times 2) / (N_s + 1) + d_s + \sum_{j=1}^{n-1} H_{w,CiRj} + M_{cj} \quad (\text{A.5-5})$$

$$Y_{s3 \rightarrow C-LH} = 3 \times (H_w - d_s \times 2) / (N_s + 1) + d_s + \sum_{j=1}^{n-1} H_{w,CiRj} + M_{cj} \quad (\text{A.5-6})$$

$$Y_{s1 \rightarrow C-RH} = (H_w - d_s \times 2) / (N_s + 1) + P_s + \sum_{j=1}^{n-1} H_{w,CiRj} + M_{cj} \quad (\text{A.5-7})$$

$$Y_{s2 \rightarrow C-RH} = 2 \times (H_w - d_s \times 2) / (N_s + 1) + P_s + \sum_{j=1}^{n-1} H_{w,CiRj} + M_{cj} \quad (\text{A.5-8})$$

$$Y_{s3 \rightarrow C-RH} = 3 \times (H_w - d_s \times 2) / (N_s + 1) + P_s + \sum_{j=1}^{n-1} H_{w,CiRj} + M_{cj} \quad (\text{A.5-9})$$

The snubber locations along the Z-axis satisfy the following equations:

$$Z_s = K_w + d_{sn} \quad (\text{A.5-10})$$

The locations of the screws for the snubbers satisfy the following equations:

$$B = \{1, 2, \dots, \beta\}$$

$$X_{ss\alpha\beta \rightarrow C} | \forall \beta \in B, X_{ss\alpha\beta \rightarrow C-RH} = X_{s\alpha \rightarrow C} \quad (\text{A.5-11})$$

$$Y_{ss\alpha\beta \rightarrow C} = \begin{cases} Y_{s\alpha \rightarrow C} - \delta_{s1}, & \beta = 1 \\ Y_{s\alpha \rightarrow C} + \delta_{s2}, & \beta = 2 \end{cases} \quad (\text{A.5-12})$$

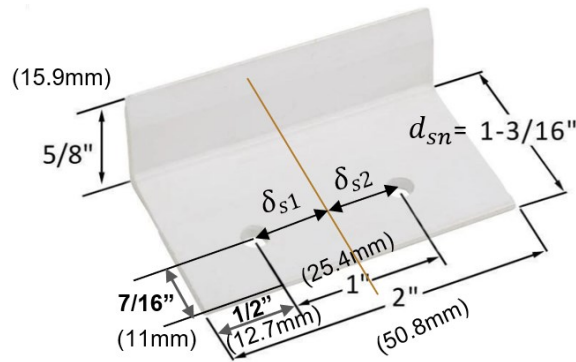


Figure A.3: Snubber details



Figure A.4: Snubber locations

6. Casement ramp on frame

Only one casement ramp for each casement window. This part is only designed for the casement window, and it is used to let sash go up when close window and to support the weight of the sash. The distance from the lock side frame inside to the casement ramp is roughly 4 in (101.6 mm) as shown in Figure A.5 and its details are in Figure A.6.

Casement ramp location along the X -axis satisfies the following equations:

$$X_{cr \rightarrow C-RH} = P_w + d_{cr} + \sum_{i=1}^{n-1} W_{w,CiRj} + M_{ci} \quad (\text{A.6-1})$$

$$X_{cr \rightarrow C-LH} = W_w - P_w - d_{cr} + \sum_{i=1}^{n-1} W_{w,CiRj} + M_{ci} \quad (\text{A.6-2})$$

Casement ramp location along the Y -axis satisfies the following equations:

$$Y_{cr \rightarrow C-RH} = Y_{cr \rightarrow C-LH} = P_w + \sum_{j=1}^{n-1} H_{w,CiRj} + M_{cj} \quad (\text{A.6-3})$$

Casement ramp location along the Z -axis satisfies the following equations:

$$Z_{cr} = 40 \quad (\text{A.6-4})$$

And $d_{cr} = 101.6$

where d_{cr} is the distance from casement ramp center (screw location) to side frame inner edge



Figure A.5: Location of the casement ramp

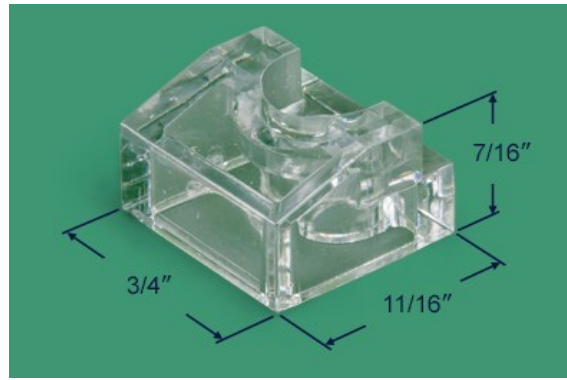


Figure A.6: Casement ramp details

7. Limit device

The limit device consists of three elements. First is the limit bracket, second is the limit arm and finally the limit track as shown in Figure A.7. The function of the limit device is to limit the opening of the window as shown in Figure A.8. The limit device is only installed for special cases.

Normally, there is no limit device on a window. The minimum window height is 500 mm.

The limit bracket's length is $L_{lb} = 58$ and its location along the X -axis satisfies the following equations:

$$X_{lb \rightarrow C-LH} = P_w + d_{lb}/2 + \sum_{i=1}^{n-1} W_{w,CiRj} + M_{ci} \quad (\text{A.7-1})$$

$$X_{lb \rightarrow C-RH} = W_w - P_w - d_{lb}/2 + \sum_{i=1}^{n-1} W_{w,CiRj} + M_{ci} \quad (\text{A.7-2})$$

For the limit bracket screws:

$$X_{lb\beta \rightarrow C} = f(\delta_{lb}) = \begin{cases} X_{lb \rightarrow C} - \delta_{lb}/2, & \beta = 1 \\ X_{lb \rightarrow C} + \delta_{lb}/2, & \beta = 2 \end{cases} \quad (\text{A.7-3})$$

Location of the limit bracket along the Y -axis satisfies the following equations:

$$Y_{lb \rightarrow C-LH} = Y_{lb \rightarrow C-RH} = f(P_w) = P_w + \sum_{j=1}^{n-1} H_{w,CiRj} + M_{cj} \quad (\text{A.7-4})$$

For the screws:

$$Y_{lb\beta \rightarrow C} = P_w + \sum_{j=1}^{n-1} H_{w,CiRj} + M_{cj} \quad (\text{A.7-5})$$

Location of the limit bracket along the Z -axis satisfies the following equations:

$$Z_{lb} = 57.7 \quad (\text{A.7-6})$$

The limit track is installed on the sash and its length is $L_{lt} = 114.3$ and the following equations determine its location on the X -axis:

$$X_{lts \rightarrow C-LH} = P_w + \sum_{i=1}^{n-1} W_{w,CiRj} + M_{ci} \quad (\text{A.7-7})$$

$$X_{ltf \rightarrow C-LH} = P_w + L_{lt} + \sum_{i=1}^{n-1} W_{w,CiRj} + M_{ci} \quad (\text{A.7-8})$$

$$X_{lts \rightarrow C-RH} = W_w - P_w + \sum_{i=1}^{n-1} W_{w,CiRj} + M_{ci} \quad (\text{A.7-9})$$

$$X_{ltf \rightarrow C-RH} = W_w - P_w - L_{lt} + \sum_{i=1}^{n-1} W_{w,CiRj} + M_{ci} \quad (\text{A.7-10})$$

For the locations of the limit track screws

$$X_{ltsc1 \rightarrow C-LH} = P_w + \frac{L_{lt} - \delta_{lt}}{2} + \sum_{i=1}^{n-1} W_{w,CiRj} + M_{ci} \quad (\text{A.7-11})$$

$$X_{ltsc2 \rightarrow C-LH} = P_w + \frac{L_{lt} - \delta_{lt}}{2} + \delta_{lt} + \sum_{i=1}^{n-1} W_{w,CiRj} + M_{ci} \quad (\text{A.7-12})$$

$$X_{ltsc1 \rightarrow C-RH} = W_w - P_w - \frac{L_{lt} - \delta_{lt}}{2} + \sum_{i=1}^{n-1} W_{w,CiRj} + M_{ci} \quad (\text{A.7-13})$$

$$X_{ltsc2 \rightarrow C-RH} = W_w - P_w - \frac{L_{lt} - \delta_{lt}}{2} - \delta_{lt} + \sum_{i=1}^{n-1} W_{w,CiRj} + M_{ci} \quad (\text{A.7-14})$$

Location of the limit track along the Y -axis satisfies the following equations.

$$Y_{lt \rightarrow C-LH} = Y_{lt \rightarrow C-RH} = P_w + \sum_{j=1}^{n-1} H_{w,CiRj} + M_{cj} \quad (\text{A.7-15})$$

For the screws

$$Y_{ltsc\beta \rightarrow C-LH} = Y_{ltsc\beta \rightarrow C-RH} = f(P_w) = P_w + \sum_{j=1}^{n-1} H_{w,CiRj} + M_{cj} \quad (A.7-16)$$

Location of the limit track and its screws along the Z-axis satisfies the following equations.

$$Z_{lt \rightarrow C} = Z_{ltsc \rightarrow C} = 57.7 \quad (A.7-17)$$

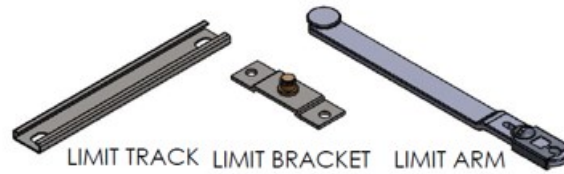


Figure A.7: Limit device

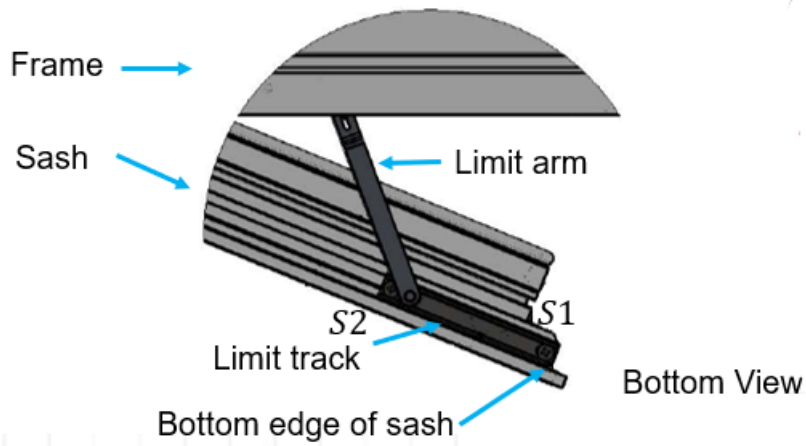


Figure A.8: Limit track

Appendix B: Hardware design for Awning windows

1. Awning operator selection

There are two types of operators for awning windows, and the selection between these two is determined based on the required operator capacity (which in turn is governed by the width of the window).

$$\text{Operator type} = \begin{cases} \text{Encore Narrow Awning Operator, } 490 \leq W_w < 510 \\ \text{Encore Awning Operator, } 510 \leq W_w < 1,500 \end{cases} \quad (\text{B.1-1})$$



Figure B.1: Awning operators

1.1 Operator cut-out location on frame

The operator for awning windows is always located in the middle of the window. Therefore, making it a function of the width of the awning window

$$X_{co \rightarrow A} = f(W_w) = W_w/2 \quad (\text{B.1-2})$$

$$Y_{co \rightarrow A} = f(W_w) = P_w + d_{aof} + d_{aco} \quad (\text{B.1-3})$$

$$Z_{co \rightarrow A} = 0 \quad (\text{B.1-4})$$

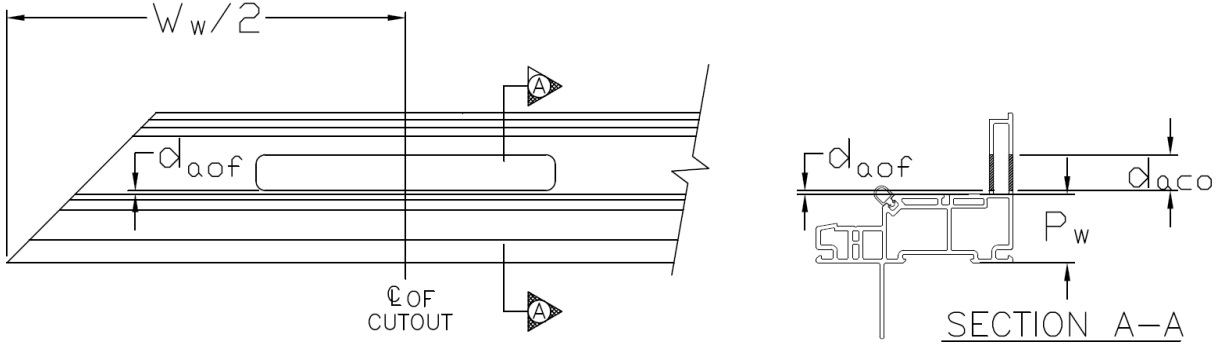


Figure B.2: Location of awning operator and its cut-out

1.2 Operator screw location

Locations of the operator screws along the X -axis satisfy the following equations:

$$X_{osc1 \rightarrow A} = \frac{W_w}{2} - \frac{L_{coa}}{2} + \delta_{osc1} + \sum_{i=1}^{n-1} W_{w,CiRj} + M_{ci} \quad (\text{B.1-5})$$

$$X_{osc2 \rightarrow A} = \frac{W_w}{2} - \frac{L_{coa}}{2} + \delta_{osc1} + \delta_{osc2} + \sum_{i=1}^{n-1} W_{w,CiRj} + M_{ci} \quad (\text{B.1-6})$$

$$X_{osc3 \rightarrow A} = \frac{W_w}{2} - \frac{L_{coa}}{2} + \delta_{osc1} + \delta_{osc3} + \sum_{i=1}^{n-1} W_{w,CiRj} + M_{ci} \quad (\text{B.1-7})$$

$$X_{osc4 \rightarrow A} = \frac{W_w}{2} - \frac{L_{coa}}{2} + \delta_{osc1} + \delta_{osc4} + \sum_{i=1}^{n-1} W_{w,CiRj} + M_{ci} \quad (\text{B.1-8})$$

$$X_{osc5 \rightarrow A} = \frac{W_w}{2} - \frac{L_{coa}}{2} + \delta_{osc1} + \delta_{osc5} + \sum_{i=1}^{n-1} W_{w,CiRj} + M_{ci} \quad (\text{B.1-9})$$

$$X_{osc6 \rightarrow A} = \frac{W_w}{2} - \frac{L_{coa}}{2} + \delta_{osc1} + \delta_{osc6} + \sum_{i=1}^{n-1} W_{w,CiRj} + M_{ci} \quad (\text{B.1-10})$$

Locations of the operator screws along the Y -axis satisfy the following equations:

$$B = \{1, 2, \dots, \beta\}$$

$$Y_{osc\beta \rightarrow A} | \forall \beta \in B, Y_{osc\beta \rightarrow A} = d_{oscy} + \sum_{j=1}^{n-1} H_{w,CiRj} + M_{cj} \quad (\text{B.1-11})$$

Locations of the operator screws along the Z -axis satisfy the following equations:

$$Z_{osc\beta \rightarrow A} | \forall \beta \in B, Z_{osc\beta \rightarrow A} = 23.8 \quad (\text{B.1-12})$$

1.3 Operator track

The selection of the operator track depends on the type of the selected operator. Thus, making it a function of the width.

$$f(W_w) = \begin{cases} N/A, & 490 \leq W_w < 0 \\ \text{Maxim Awning Operator Track}, & 510 \leq W_w < 1,500 \end{cases} \quad (\text{B.1-13})$$

The location of the operator's track along the X -axis satisfies the following equations:

$$X_{ots \rightarrow A} = \frac{W_w - 2 \times P_w}{2} - \frac{L_{aot}}{2} - d_{aot} + \sum_{i=1}^{n-1} W_{w,CiRj} + M_{ci} \quad (\text{B.1-14})$$

$$X_{otf \rightarrow A} = \frac{W_w - 2 \times P_w}{2} - \frac{L_{aot}}{2} - d_{aot} + L_{aot} + \sum_{i=1}^{n-1} W_{w,CiRj} + M_{ci} \quad (\text{B.1-15})$$

The location of the operator's track along the Y -axis satisfies the following equations:

$$Y_{ots \rightarrow A} = Y_{otf \rightarrow A} = P_w + \sum_{j=1}^{n-1} H_{w,CiRj} + M_{cj} \quad (\text{B.1-16})$$

The location of the operator's track along the Z -axis satisfies the following equations:

$$Z_{ot \rightarrow A} = 32.6 \quad (\text{B.1-17})$$

The location of the operator's track screws along the X -axis satisfies the following equations:

$$X_{otsc1 \rightarrow A} = \frac{W_w}{2} - d_{aot} - \frac{L_{aot}}{2} + \delta_{otsc1} + \sum_{i=1}^{n-1} W_{w,CiRj} + M_{ci} \quad (\text{B.1-18})$$

$$X_{otsc2 \rightarrow A} = \frac{W_w}{2} - d_{aot} - \delta_{otsc2} \quad (\text{B.1-19})$$

$$X_{otsc3 \rightarrow A} = \frac{W_w}{2} - d_{aot} + \delta_{otsc2} \quad (\text{B.1-20})$$

$$X_{otsc4 \rightarrow A} = \frac{W_w}{2} - d_{aot} + \frac{L_{aot}}{2} - \delta_{otsc1} \quad (\text{B.1-21})$$

The location of the operator's track screws along the Y -axis satisfies the following equations:

$$Y_{otsc\beta \rightarrow A} = \delta_{otscy} + \sum_{j=1}^{n-1} H_{w,CiRj} + M_{cj} \quad (\text{B.1-22})$$

The location of the operator's track screws along the Z -axis satisfies the following equations:

$$Z_{otsc\beta \rightarrow A} = 32.6 \quad (\text{B.1-23})$$

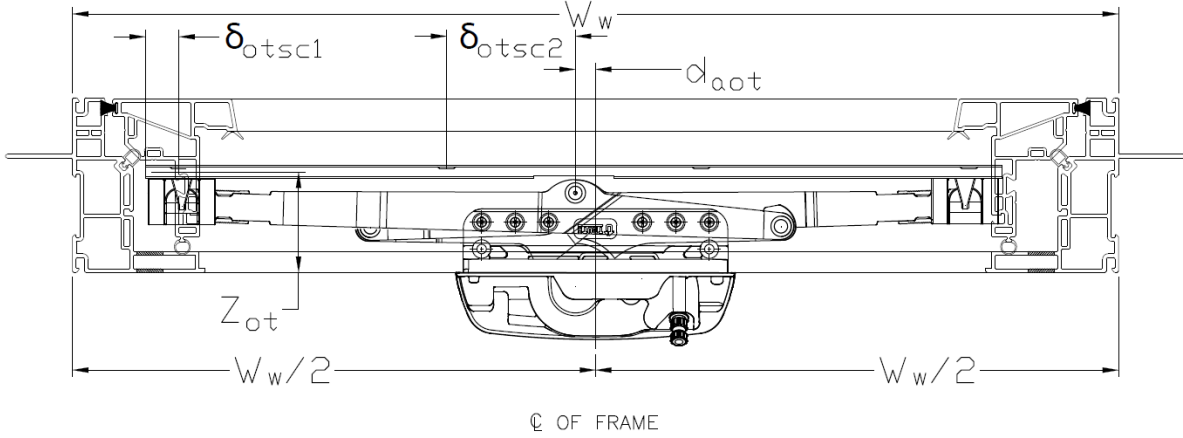


Figure B.3: Awning operator track CAD details

2. Awning operator bracket

$$\text{Operator bracket} = \begin{cases} \text{Bracket for awning operator, } 490 \leq W_w < 510 \\ \text{N/A, } 510 \leq W_w < 1,500 \end{cases} \quad (\text{B.2-1})$$

The location of the operator bracket along the X -axis satisfies the following equations:

$$X_{ob \rightarrow A} = \frac{W_w}{2} - \frac{d_{aob}}{2} + \sum_{i=1}^{n-1} W_{w,CiRj} + M_{ci} \quad (\text{B.2-2})$$

For the screws:

$$X_{obsc1 \rightarrow A} = X_{ob \rightarrow A} - \delta_{xb} + \sum_{i=1}^{n-1} W_{w,CiRj} + M_{ci} \quad (\text{B.2-3})$$

$$X_{obsc2 \rightarrow A} = X_{ob \rightarrow A} + \delta_{xb} + \sum_{i=1}^{n-1} W_{w,CiRj} + M_{ci} \quad (\text{B.2-4})$$

The location of the operator bracket along the Y -axis satisfies the following equations:

$$Y_{ob \rightarrow A} = d_{aoby} + \sum_{j=1}^{n-1} H_{w,CiRj} + M_{cj} \quad (\text{B.2-5})$$

For the screws:

$$Y_{obsc1 \rightarrow A} = Y_{obsc2 \rightarrow A} = d_{aoby} + \sum_{j=1}^{n-1} H_{w,CiRj} + M_{cj} \quad (\text{B.2-6})$$

The location of the operator bracket along the Z -axis satisfies the following equations:

$$Z_{ob \rightarrow A} = 42.25 \quad (\text{B.2-7})$$

$$Y_{obsc\beta \rightarrow A} | \forall \beta \in B, Y_{obsc\beta \rightarrow A} = 51.74 \quad (\text{B.2-8})$$

3. Awning hinge track selection on frame

$$L_{Ah} = \begin{cases} 10'' \text{ awning hinge, } 365 \leq H_w \leq 553 \\ 14'' \text{ awning hinge, } 553 < H_w \leq 680 \\ 18'' \text{ awning hinge, } 680 < H_w \leq 800 \\ 22'' \text{ awning hinge, } 800 < H_w \leq 950 \\ 26'' \text{ awning hinge, } 950 < H_w \leq 1,200 \end{cases} \quad (\text{B.3-1})$$

For the awning window, there are two hinge tracks that are installed on the vertical profiles of the window.

The location of the hinge tracks along the X -axis satisfies the following equations:

$$X_{hts \rightarrow A-L} = P_w + \sum_{i=1}^{n-1} W_{w,CiRj} + M_{ci} \quad (\text{B.3-2})$$

$$X_{htf \rightarrow A-L} = P_w + \sum_{i=1}^{n-1} W_{w,CiRj} + M_{ci} \quad (\text{B.3-3})$$

$$X_{hts \rightarrow A-R} = W_w - P_w + \sum_{i=1}^{n-1} W_{w,CiRj} + M_{ci} \quad (\text{B.3-4})$$

$$X_{htf \rightarrow A-R} = W_w - P_w + \sum_{i=1}^{n-1} W_{w,CiRj} + M_{ci} \quad (\text{B.3-5})$$

The location of the hinge tracks along the Y -axis satisfies the following equations:

$$Y_{hts \rightarrow A-L} = Y_{hts \rightarrow A-R} = H_w - P_w + \sum_{j=1}^{n-1} H_{w,CiRj} + M_{cj} \quad (\text{B.3-6})$$

$$Y_{htf \rightarrow A-L} = Y_{htf \rightarrow A-R} = H_w - P_w - L_{Ah} + \sum_{j=1}^{n-1} H_{w,CiRj} + M_{cj} \quad (\text{B.3-7})$$

The location of the hinge tracks along the Z -axis satisfies the following equations:

$$Z_{ht \rightarrow A} = 41.5 \quad (\text{B.3-8})$$

The following function determines the number of screws in a hinge track.

$$N_{ht \rightarrow A} = \begin{cases} 3, 365 \leq H_w \leq 553 \\ 4, 553 < H_w \leq 680 \\ 5, 680 < H_w \leq 800 \\ 6, 800 < H_w \leq 950 \\ 7, 950 < H_w \leq 1,200 \end{cases} \quad (\text{B.3-9})$$

For the screws, the first screw is always at a fixed distance regardless of the length of the hinge track. Therefore, the screw locations along the X -axis satisfy the following equations:

$$X_{htsc\beta \rightarrow A-L} | \forall \beta \in B, X_{htsc\beta \rightarrow A-L} = P_w + \sum_{i=1}^{n-1} W_{w,CiRj} + M_{ci} \quad (B.3-10)$$

$$X_{htsc\beta \rightarrow A-R} | \forall \beta \in B, X_{htsc\beta \rightarrow A-R} = W_w - P_w + \sum_{i=1}^{n-1} W_{w,CiRj} + M_{ci} \quad (B.3-11)$$

The screw locations along the Y -axis satisfy the following equations:

$$Y_{htsc1 \rightarrow A-L} = H_w - P_w - \delta_{ht1} + \sum_{j=1}^{n-1} H_{w,CiRj} + M_{cj} \quad (B.3-12)$$

$$Y_{htsc2 \rightarrow A-L} = H_w - P_w - \delta_{ht1} - \delta_{ht2} + \sum_{j=1}^{n-1} H_{w,CiRj} + M_{cj} \quad (B.3-13)$$

$$Y_{htsc3 \rightarrow A-L} = \begin{cases} H_w - P_w - \delta_{ht1} - \delta_{ht2} + \sum_{j=1}^{n-1} H_{w,CiRj} + M_{cj}, & 365 \leq H_w \leq 553 \\ H_w - P_w - 2 \times \delta_{ht1} + \sum_{j=1}^{n-1} H_{w,CiRj} + M_{cj}, & 553 < H_w \leq 1,200 \end{cases} \quad (B.3-14)$$

$$Y_{htsc4 \rightarrow A-L} = \begin{cases} H_w - P_w - 2 \times \delta_{ht1} - \delta_{ht2} + \sum_{j=1}^{n-1} H_{w,CiRj} + M_{cj}, & 553 < H_w \leq 680 \\ H_w - P_w - 3 \times \delta_{ht1} + \sum_{j=1}^{n-1} H_{w,CiRj} + M_{cj}, & 680 < H_w \leq 1,200 \end{cases} \quad (B.3-15)$$

$$Y_{htsc5 \rightarrow A-L} = \begin{cases} H_w - P_w - 3 \times \delta_{ht1} - \delta_{ht2} + \sum_{j=1}^{n-1} H_{w,CiRj} + M_{cj}, & 680 < H_w \leq 800 \\ H_w - P_w - 4 \times \delta_{ht1} + \sum_{j=1}^{n-1} H_{w,CiRj} + M_{cj}, & 800 < H_w \leq 1,200 \end{cases} \quad (B.3-16)$$

$$Y_{htsc6 \rightarrow A-L} = \begin{cases} H_w - P_w - 4 \times \delta_{ht1} - \delta_{ht2} + \sum_{j=1}^{n-1} H_{w,CiRj} + M_{cj}, & 800 < H_w \leq 950 \\ H_w - P_w - 5 \times \delta_{ht1} + \sum_{j=1}^{n-1} H_{w,CiRj} + M_{cj}, & 950 < H_w \leq 1,200 \end{cases} \quad (B.3-17)$$

$$Y_{htsc7 \rightarrow A-L} = H_w - P_w - 5 \times \delta_{ht1} - \delta_{ht2} + \sum_{j=1}^{n-1} H_{w,CiRj} + M_{cj}, 950 < H_w \leq 1,200 \quad (B.3-18)$$

$$Y_{htsc\beta \rightarrow A-R} | \forall \beta \in B, Y_{htsc\beta \rightarrow A-R} = Y_{htsc\beta \rightarrow A-L} \quad (B.3-19)$$

4. Awning hinge arm on sash

The length of the hinge arm is selected based on the height of the window and satisfies the following function.

$$L_{aha} = f(H_w) = \begin{cases} 171.5, & 365 \leq H_w \leq 680 \\ 222.3, & 680 < H_w \leq 800 \\ 273.1, & 800 < H_w \leq 950 \\ 311.1, & 950 < H_w \leq 1,200 \end{cases} \quad (B.4-1)$$

The location of the hinge arm along the X -axis satisfies the following equations:

$$X_{has \rightarrow A-L} = F_w + \sum_{i=1}^{n-1} W_{w,CiRj} + M_{ci} \quad (B.4-2)$$

$$X_{haf \rightarrow A-L} = F_w + \sum_{i=1}^{n-1} W_{w,CiRj} + M_{ci} \quad (B.4-3)$$

$$X_{has \rightarrow A-R} = X_{haf \rightarrow A-R} = W_w - F_w + \sum_{i=1}^{n-1} W_{w,CiRj} + M_{ci} \quad (B.4-4)$$

The location of the hinge arm along the Y -axis satisfies the following equations:

$$Y_{has \rightarrow A-L} = H_w - F_w + \sum_{j=1}^{n-1} H_{w,CiRj} + M_{cj} \quad (B.4-5)$$

$$Y_{haf \rightarrow A-L} = H_w - F_w - d_{aha} - L_{aha} + \sum_{j=1}^{n-1} H_{w,CiRj} + M_{cj} \quad (B.4-6)$$

$$Y_{has \rightarrow A-R} = Y_{has \rightarrow A-L} \quad (B.4-7)$$

$$Y_{haf \rightarrow A-R} = Y_{haf \rightarrow A-L} \quad (B.4-8)$$

The location of the hinge arm along the Z -axis satisfies the following equations:

$$Z_{ha \rightarrow A-R} = Z_{ha \rightarrow A-L} = 41.5 \quad (B.4-9)$$

For the screws on the hinge arm, the number of screws is determined based on the height of the window.

$$N_{ha \rightarrow A} = f(H_w) = \begin{cases} 4, & 365 \leq H_w \leq 950 \\ 5, & 950 < H_w \leq 1,200 \end{cases} \quad (B.4-10)$$

The screw locations along the X -axis satisfy the following equations:

$$X_{hasc\beta \rightarrow A-L} | \forall \beta \in B, X_{hasc\beta \rightarrow A-L} = F_w + \sum_{i=1}^{n-1} W_{w,CiRj} + M_{ci} \quad (B.4-11)$$

$$X_{hasc\beta \rightarrow A-R} | \forall \beta \in B, X_{hasc\beta \rightarrow A-R} = W_w - F_w + \sum_{i=1}^{n-1} W_{w,CiRj} + M_{ci} \quad (B.4-12)$$

The screw locations along the Y -axis satisfy the following equations:

$$Y_{hasc1 \rightarrow A-L} = H_w - F_w - d_{aha} - \delta_{aha1} + \sum_{j=1}^{n-1} H_{w,CiRj} + M_{cj} \quad (B.4-13)$$

$$Y_{hasc2 \rightarrow A-L} = Y_{hasc1 \rightarrow A-L} - \delta_{aha2} + \sum_{j=1}^{n-1} H_{w,CiRj} + M_{cj} \quad (B.4-14)$$

$$Y_{hasc3 \rightarrow A-L} = \begin{cases} Y_{hasc1 \rightarrow A-L} - \delta_{aha31} + \sum_{j=1}^{n-1} H_{w,CiRj} + M_{cj}, & 365 \leq H_w \leq 680 \\ Y_{hasc1 \rightarrow A-L} - \delta_{aha32} + \sum_{j=1}^{n-1} H_{w,CiRj} + M_{cj}, & 680 < H_w \leq 950 \\ Y_{hasc1 \rightarrow A-L} - \delta_{aha33} + \sum_{j=1}^{n-1} H_{w,CiRj} + M_{cj}, & 950 < H_w \leq 1,200 \end{cases} \quad (B.4-15)$$

$$Y_{hasc4 \rightarrow A-L} = \begin{cases} Y_{hasc1 \rightarrow A-L} - \delta_{aha41} + \sum_{j=1}^{n-1} H_{w,CiRj} + M_{cj}, & 365 \leq H_w \leq 680 \\ Y_{hasc1 \rightarrow A-L} - \delta_{aha42} + \sum_{j=1}^{n-1} H_{w,CiRj} + M_{cj}, & 680 < H_w \leq 800 \\ Y_{hasc1 \rightarrow A-L} - \delta_{aha43} + \sum_{j=1}^{n-1} H_{w,CiRj} + M_{cj}, & 800 < H_w \leq 950 \\ Y_{hasc1 \rightarrow A-L} - \delta_{aha44} + \sum_{j=1}^{n-1} H_{w,CiRj} + M_{cj}, & 950 < H_w \leq 1,200 \end{cases} \quad (B.4-16)$$

$$Y_{hasc5 \rightarrow A-L} = Y_{hasc1 \rightarrow A-L} - \delta_{aha5} + \sum_{j=1}^{n-1} H_{w,CiRj} + M_{cj}, \quad 950 < H_w \leq 1,200 \quad (\text{B.4-17})$$

$$Y_{hasc\beta \rightarrow A-R} | \forall \beta \in B, Y_{hasc\beta \rightarrow A-R} = Y_{hasc\beta \rightarrow A-L} \quad (\text{B.4-18})$$

The screw locations along the Z-axis satisfy the following equations:

$$Z_{hasc\beta \rightarrow A-R} | \forall \beta \in B, Z_{hasc\beta \rightarrow A-R} = Z_{ha \rightarrow A-R} = Z_{ha \rightarrow A-L} = 41.5 \quad (\text{B.4-19})$$

5. Awning Snubber

The number of snubbers used is a function of the window's height, as the purpose of the snubber is to prevent bowing of tall casement windows.

$$N_s = \begin{cases} 1, & 490 \leq W_w < 1,200 \\ 2, & 1,200 \leq H_w \leq 1,500 \\ 3, & H_w > 1,500 \end{cases} \quad (\text{B.5-1})$$

$$A = \{1, 2, \dots, \alpha\}$$

The location of the snubbers along the X-axis satisfies the following equations:

$$X_{s1 \rightarrow A} = (W_w - d_s \times 2) / (N_s + 1) + d_s + \sum_{j=1}^{n-1} W_{w,CiRj} + M_{cj} \quad (\text{B.5-2})$$

$$X_{s2 \rightarrow A} = 2 \times (W_w - d_s \times 2) / (N_s + 1) + d_s + \sum_{j=1}^{n-1} W_{w,CiRj} + M_{cj} \quad (\text{B.5-3})$$

$$X_{s3 \rightarrow A} = 3 \times (W_w - d_s \times 2) / (N_s + 1) + d_s + \sum_{j=1}^{n-1} W_{w,CiRj} + M_{cj} \quad (\text{B.5-4})$$

The location of the snubbers along the Y-axis satisfies the following equations:

$$Y_{s\alpha \rightarrow A} | \forall \alpha \in A, Y_{s\alpha \rightarrow A} = H_w - d_s + \sum_{j=1}^{n-1} H_{w,CiRj} + M_{cj} \quad (\text{B.5-5})$$

The locations of the snubbers along the Z-axis satisfy the following equations:

$$Z_{s \rightarrow C} = K_w + d_{sn} \quad (\text{B.5-6})$$

The locations of the screws for the snubbers satisfy the following equations:

$$B = \{1, 2, \dots, \beta\}$$

$$Y_{SSc\alpha\beta \rightarrow A} | \forall \beta \in B, Y_{SSc\alpha\beta \rightarrow A-RH} = Y_{s\alpha \rightarrow C} \quad (\text{B.5-7})$$

$$X_{ss\alpha\beta\rightarrow A} = \begin{cases} X_{s\alpha\rightarrow C} - \delta_{s1}, & \beta = 1 \\ X_{s\alpha\rightarrow C} + \delta_{s2}, & \beta = 2 \end{cases} \quad (\text{B.5-8})$$

6. Awning limit device

For the limit bracket location along the X -axis:

$$X_{lb\rightarrow A-L} = P_w + \sum_{i=1}^{n-1} W_{w,CiRj} + M_{ci} \quad (\text{B.6-1})$$

$$X_{lb\rightarrow A-R} = f(P_w) = W_w - P_w + \sum_{i=1}^{n-1} W_{w,CiRj} + M_{ci} \quad (\text{B.6-2})$$

For the limit bracket screws:

$$X_{lb\beta\rightarrow C} = \begin{cases} X_{lb\rightarrow C} - \delta_{lb}/2, & \beta = 1 \\ X_{lb\rightarrow C} + \delta_{lb}/2, & \beta = 2 \end{cases} \quad (\text{B.6-3})$$

For the limit bracket location along the Y -axis:

$$Y_{lb\rightarrow A} = P_w + d_{ld} + L_{lb}/2 + \sum_{j=1}^{n-1} H_{w,CiRj} + M_{cj} \quad (\text{B.6-4})$$

$$X_{lb\beta\rightarrow C} = P_w + d_{ld} + L_{lb}/2 + \sum_{j=1}^{n-1} H_{w,CiRj} + M_{cj} \quad (\text{B.6-5})$$

$$L_{lb} = 58$$

The limit track is installed on the sash and the following equations determine its location along the

X -axis:

$$X_{lts\rightarrow A-L} = F_w + \sum_{i=1}^{n-1} W_{w,CiRj} + M_{ci} \quad (\text{B.6-6})$$

$$X_{lts\rightarrow A-R} = W_w - F_w + \sum_{i=1}^{n-1} W_{w,CiRj} + M_{ci} \quad (\text{B.6-7})$$

For the screws:

$$X_{lts\beta\rightarrow A-L} = X_{lts\beta\rightarrow A-R} = F_w + \sum_{i=1}^{n-1} W_{w,CiRj} + M_{ci} \quad (\text{B.6-8})$$

The limit track is installed on the sash and the following equations determine its location along the

Y -axis:

$$Y_{lts\rightarrow A} = F_w + \sum_{j=1}^{n-1} H_{w,CiRj} + M_{cj} \quad (\text{B.6-9})$$

$$Y_{lts\rightarrow A} = F_w + L_{lt} + \sum_{j=1}^{n-1} H_{w,CiRj} + M_{cj} \quad (\text{B.6-10})$$

For the screws:

$$Y_{ltsc1 \rightarrow A-L} = F_w + \frac{L_{lt} - \delta_{lt}}{2} + \sum_{j=1}^{n-1} H_{w,CiRj} + M_{cj} \quad (\text{B.6-11})$$

$$Y_{ltsc2 \rightarrow A-L} = F_w + \frac{L_{lt} - \delta_{lt}}{2} + \delta_{lt} + \sum_{j=1}^{n-1} H_{w,CiRj} + M_{cj} \quad (\text{B.6-12})$$

$$Y_{ltsc\beta \rightarrow A-R} | \forall \beta \in B, Y_{ltsc\beta \rightarrow A-R} = Y_{ltsc\beta \rightarrow A-L} \quad (\text{B.6-13})$$

The limit track's location and its screws along the Z-axis satisfy the following equations:

$$Z_{lt \rightarrow A-L} = Z_{lt \rightarrow A-R} = 57.7 \quad (\text{B.6-14})$$

$$Z_{ltsc\beta \rightarrow A-L} = Z_{ltsc\beta \rightarrow A-R} = 57.7 \quad (\text{B.6-15})$$